EXPERIMENTAL HIGH VELOCITY ACID JETTING IN LIMESTONE CARBONATES

A Thesis

by

CHRISTOPHER CHARLES HOLLAND

Submitted to the Office of Graduate and Professional Studies of
Texas A&M University
in partial fulfillment of the requirements for the degree of

MASTER OF SCIENCE

Chair of Committee,	Ding Zhu
Committee Members,	A. Daniel Hill
	Yuefeng Sun
Head of Department,	A. Daniel Hill

May 2014

Major Subject: Petroleum Engineering

ABSTRACT

Acid jetting is a well stimulation technique that is used in carbonate reservoirs. It typically involves injecting acid down hole at high flow rates through small orifices which cause high velocities of acid to strike the borehole wall. The combination of high kinetic energy and chemical reaction of the acid removes drilling mud filter cake from the borehole wall and produces long conductive channels, called wormholes, into the formation, therefore improving well performance.

Studies have shown that injecting fluid down hole at high velocities can mitigate damage to wellbore caused by drilling mud filter cake. Both water and acid have shown positive results in such cases. However, there are no laboratory results on how high velocity acid impacts the borehole wall and the formation of wormholes. The purpose of this study is to investigate how the high velocity acid affects the acidizing treatments. The experiments are conducted on 4" diameter by 16" length Indiana limestone cores with acid injected at the velocity of 106 ft/s, 150 ft/s, and 200 ft/s. The experiments are conducted with a constant pressure differential across the core. 15%wt Hydrochloric acid is injected at room temperature at various flux rates.

The results show that the higher the velocity of jetted acid, the further it penetrates into the formation. The 200 ft/s acid penetrates furthest into the core, thus potentially lowering the skin factor the greatest. A large cavity is formed into the core from the high velocity acid. This large cavity creates a pathway for acid to divert into the core to create wormholes. Acid jetting cannot be directly compared with matrix

acidizing because of the formation of these large cavities. The Buijse-Glasbergen model that is used to predict the formation of wormholes does not accurately match the acid jetting data due to the formation of these large cavities, so the optimum flux and pore volume to breakthrough cannot be accurately determined.

DEDICATION

This thesis is dedicated to my wife, Julia.

ACKNOWLEDGEMENTS

I would like to thank my committee chair, Dr. Zhu, and my committee members, Dr. Hill, and Dr. Sun, for their guidance and support throughout the course of this research.

Thanks also go to my friends and colleagues and the department faculty and staff for making my time at Texas A&M University a great experience. I also want to extend my gratitude to the Exxon Mobil, which provided the funding and experimental support, and Richard Beckham, who personally took an interest in me and my research and provided extensive guidance.

Thanks to Vanessa Ndonhong for her help with experiments and equipment.

Finally, thanks to my wife, Julia, for her patience and love.

TABLE OF CONTENTS

LIST OF FIGURES

LIST OF TABLES

1. INTRODUCTION*

1.1 Background

The near-wellbore condition is extremely important in well production and has been an area of extensive study. Radial flow to the well results in higher flow velocities, which in turn creates a larger pressure drop per unit distance while approaching the wellbore. When the near-wellbore condition changes, for example, formation damage reduces the permeability in the near wellbore region, and it results in an additional pressure drop. This pressure drop, known as the skin effect can be added to the pressure drop of the reservoir shown by the following steady-state equation, where s is the skin effect:

$$p - p_{wf} = \frac{q\mu}{2\pi kh}\left(\ln\frac{r}{r_w} + s\right) \tag{1.1}$$

The skin effect can be positive or negative. The lower the skin effect the potentially higher the production from the well.

There are two main ways to reduce the damage skin factor of the well: acidizing and hydraulic fracturing. These techniques lower the skin factor by creating multiple channels from the wellbore into the reservoir. These channels reduce the convergence of

reservoir fluid as it travels to the wellbore, thus lowering the pressure drop near the wellbore.

Matrix acidizing (called “matrix” because the injection pressure is below the formation fracture pressure) can be done in either sandstone or carbonate reservoirs, but long, highly conductive, channels known as “wormholes” are only observed in carbonate rocks. Carbonate acidizing designs usually consist of 15 %wt HCl, which causes a high surface reaction rate. Since the reaction rate is high, mass transfer limits the overall reaction rate which causes a nonuniform dissolution pattern that creates wormholes. Sandstone acidizing generally consists of a 3 wt% HF, 12 wt% HCl mixture known as “mud acid”, and has a much slower reaction rate which causes a uniform dissolution. Therefore, sandstone reservoirs should only be acidized to lower the skin factor by eliminating near-well formation damage, while carbonate reservoirs can be acidized to improve the reservoir’s original potential. (Economides et al, 2013)

Matrix acidizing has been extensively studied the in laboratory. Generally, HCl acid is injected axially into carbonate core samples with diameters ranging from 1” to 4” and lengths ranging from 1” to 20”. The acid is pumped at a constant rate until acid dissolves enough material to break through the opposite end of the core. Until the work of Hoefner and Fogler (1989) it was thought that acid should be pumped at the fastest rate possible in order to form wormholes. Hoefner and Fogler found that there is an optimum injection rate by doing several coreflood experiments on limestone and dolomite at different flow rates. The flow rate that enables the core to consume the least amount of acid volume to break through the core is determined to be the optimum flow

rate. Also, it is determined that the optimum flow rate depends on acid concentration, rock mineralogy, and temperature.

A common model used to predict the propagation of wormholes was developed by Buijse and Glasbergen (2005). It takes the results from coreflood experiments, and places them in a semiempirical equation solving for optimum interstitial velocity and optimum pore volumes to breakthrough. They found that the wormhole propagation is inversely related to the pore volumes to breakthrough and dependent on the interstitial velocity of acid through the core. The following figure shows the model (fitted curve) as it relates interstitial velocity to pore volumes to breakthrough.

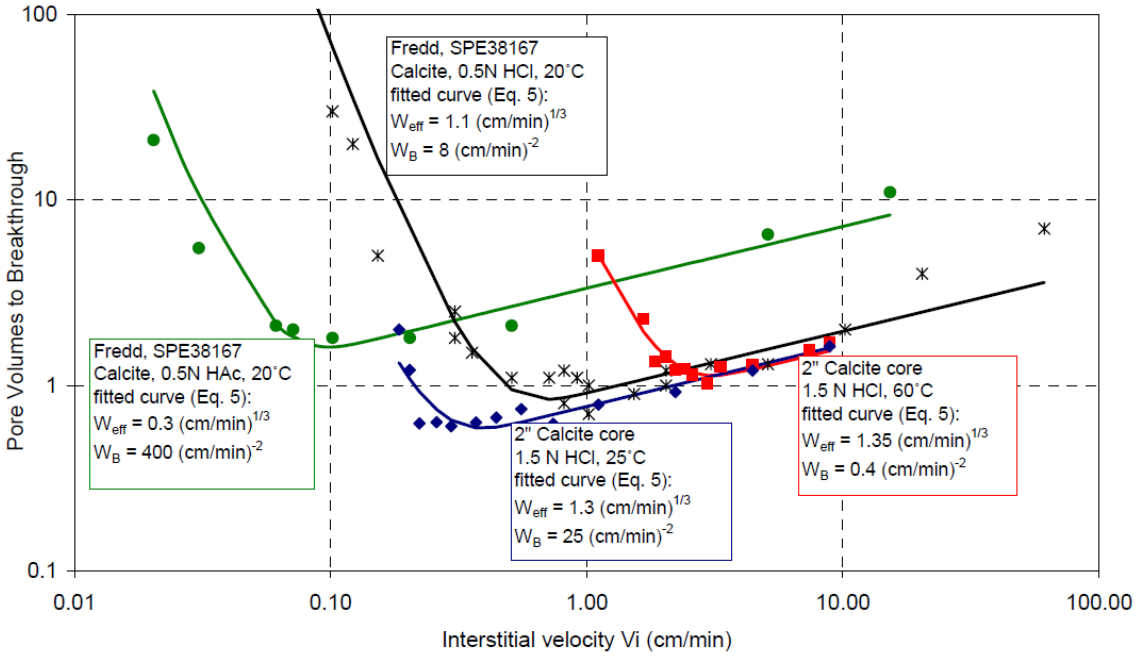

Fig. 1.1 – Interstitial Velocity in relation to Pore Volumes to Breakthrough (Buijse-Glasbergen, 2005)

Acid jetting is a well stimulation technique that is used in carbonate reservoirs that is similar to matrix acidizing. It usually involves injecting acid down hole at high

flow rates through small orifices causing high velocities of acid to strike the borehole wall. The high kinetic energy and chemical reaction of the acid removes drilling mud filter cake from the borehole wall. When injected with overpressure, the acid creates wormholes into the formation as in matrix acidizing. The removal of filter cake and the creation of wormholes reduces the resistance of fluid flow from the reservoir to the well; thus increasing the production of the well.

The most common ways of implementing acid jetting is through coiled tubing, drill pipe, and pre-drilled liners. Coiled tubing with a jetting tool, having jets spiraled around it, is run to TD and can pump up to 6 BPM through nozzles as small as 1/4" in diameter .

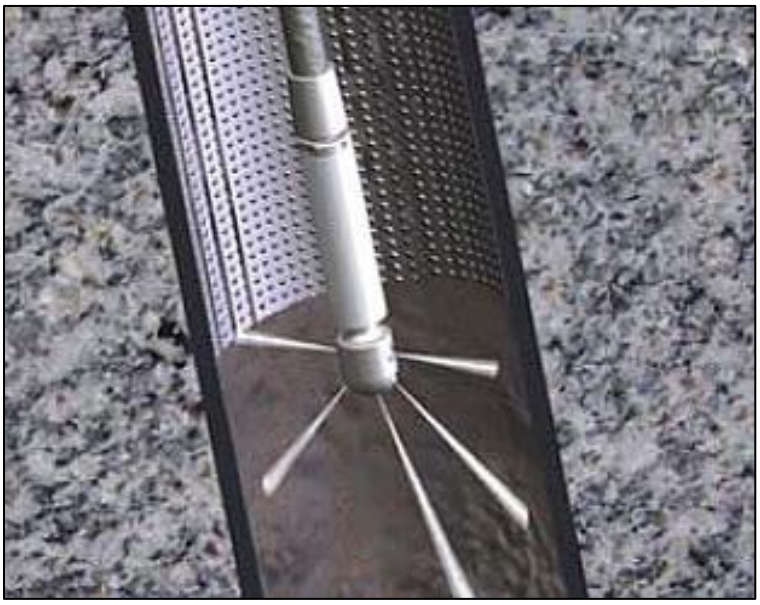

Fig. 1.2 – Coiled Tubing Jetting Attachment (Scope, 2014)

Drill pipe acid jetting is similar to the coiled tubing application, but it can reach farther depths than the coiled tubing. It is also possible to pump at faster rates (up to 25 BPM). (Aslam, 1998)

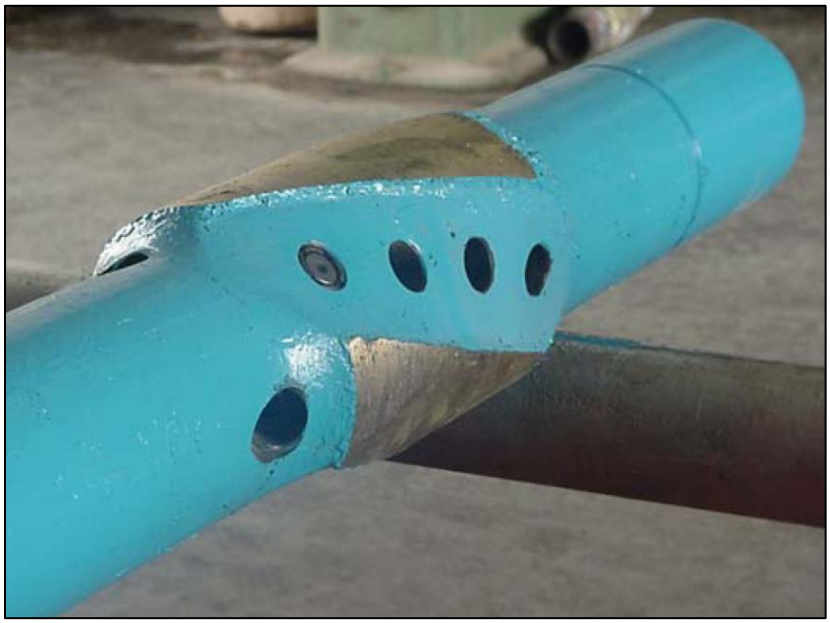

Fig. 1.3 – Drill Pipe Acid Jetting Attachment (Ritchie, 2008)

Pre-drilled, uncemented liners can be used in what is known as a Controlled Acid Jet application. These liners can be up to 9,500 ft long with approximately 200 holes of 1/4" diameter. The pumping vessel is capable of pumping 55 BPM for an average of 0.28 BPM per hole. (Hansen, 2002)

Several factors are involved in the effectiveness of jetting. Impacting force of the jet decreases with an increase of stand-off distance. Laboratory tests have shown that to remove moderate to hard deposits a stand-off of eight times the orifice diameter is needed. Tests have shown that fluid velocity of at least 200 ft/s is needed to remove hard deposits. The jet stream profile is also important. If the profile diverges before it

reaches the jetted surface then the impact force is less than if the profile converges. The pulsation effect from a rotating jet rather than a stationary jet can also be beneficial. (Aslam, 2000)

Investigations have been made in the laboratory to determine how jetting affects the filter cake around the wellbore (Mikhailov, 2008). A filter cake was created by using a fluid loss procedure under conditions that are similar to drilling conditions. The filter cake was applied to the surface of a 4" diameter by 14"- 18" length Indiana limestone cores by using drilling mud that is similar to mud used in drilling operations in the Middle East carbonate reservoirs. In a core holder, the jetting nozzle of 0.05" ID was positioned 0.5" from the surface of the core (10 times nozzle ID). The acid jetting flow rates for these experiments were 100 and 140 ml/min for 10, 45, 60, and 90 seconds. The water jetting flow rates for these experiments were 100 and 140 ml/min for 45, 90 and 180 seconds. Water jetting recovered almost all initial permeability while acid jetting increased the permeability by 2 to 7 times compared with the initial permeability.

A similar study was done but with a constant pressure differential across the core with acid jetting at 100 ml/min and water jetting at 140 ml/min (Zhang, 2009). Also, the jetting nozzle ID is 0.04" and distance between the nozzle and the core surface is 0.32" (8 times nozzle ID). With a nozzle ID of 0.04" the jetting velocities are 6.2 ft/s at 100 ml/min rates and 8.9 ft/s at 140 ml/min. The only major permeability increase was found when injecting acid with a 550 psi pressure differential. All other differential pressures were significantly lower and at best, returned the damage permeability to

original permeability. The 550 psi pressure differential created a flux through the core of 0.3481 cm/min, which generated a wormhole.

1.2 Objectives

Previous experimental work has shown how low velocity water and acid affects the mud filter cake and wormhole creation. The purpose of this study is to:

1. Investigate how high velocity acid affects the surface of rock samples.
2. Investigate the stimulation results between jetting and matrix acidizing by comparing the $PV_{BT\text{-}opt}$ and $V_{i\text{-}opt}$ between acid jetting and matrix experiments.

2. EXPERIMENTAL APPARATUS *

2.1 General Setup

The setup for this research is shown in **Fig. 2.1**. The apparatus involves a pulse pump, hassler type core holder, pressure transducer, hydraulic pump, and two backpressure regulators. A separate device is used to measure the permeability in each core.

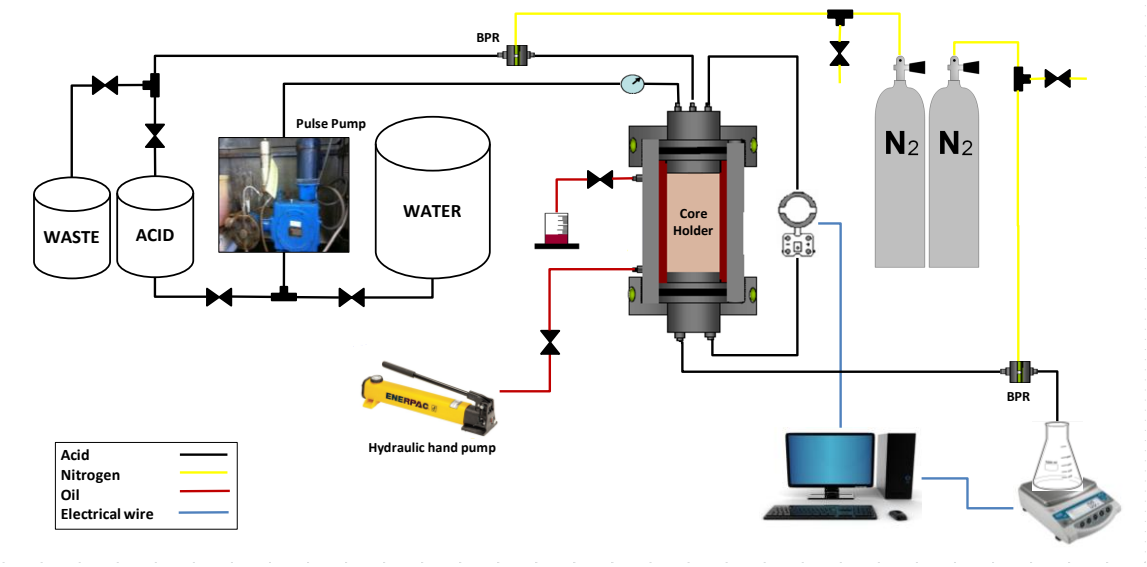

Fig. 2.1 – Schematic

2.2 Pulse Pump

* Figure reprinted with permission from ASCE. "Diffusion of Submerged Jets" by Albertson, M.L., Dai, Y.B., Jensen, R.A. and Rouse, H, 1948.

The Chem/Meter 800 series pulse pump, shown in **Fig. 2.2**, is used to pump water or acid during the experiment. It can deliver a flow rate up to 16.3 GPH or 1,028 ml/min with a maximum operating pressure 2,200 psi.

Fig. 2.2 – Pulse Pump

The flow rate can be adjusted manually by a micrometer type stroke adjustment 0-100% of maximum flow rate. Through internal gear reduction and an eccentric drive, reciprocating motion is created to push a hollow plunger which creates hydraulic displacement. In an opposing direction, a ported control rod is inserted in to the center of the plunger. As the rod is adjusted into or out of the plunger, the volume that the plunger displaces is increased or decreased respectively. The adjustment of that rod by the capacity control knob is how the flow rate is adjusted. Past that point, the diaphragm

is actuated hydraulically. The diaphragm acts as a barrier between the liquid and the rest of the pump, so that the liquid only touches materials suited for the required corrosion resistance.

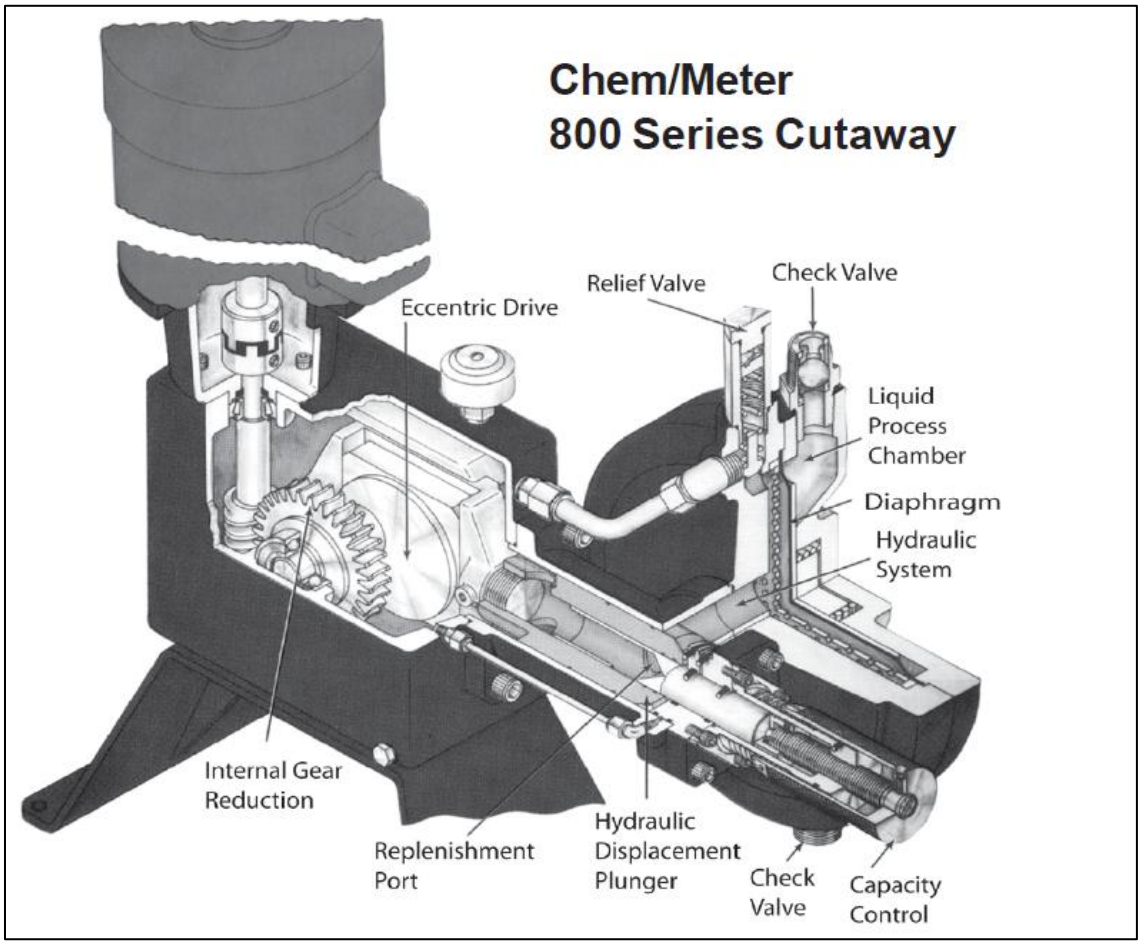

Fig. 2.3 – Pump Diagram (Teikoku, 2014)

With the pump only being rated up to 2,200 psi, the pressure drop across the nozzle is of concern. For the maximum flow rate used during experiments, the pressure drop across the nozzle must be calculated to ensure the pump can handle the pressure. It is calculated by the following equations:

$$\frac{\partial p}{\partial L} = \frac{f\rho v^2}{2g_c \mathrm{D}} \tag{2.2}$$

$f = 0.316 \times Re^{-0.25}$ for turbulent flow (2.3)

$$Re = \frac{\rho v D}{\mu} \tag{2.4}$$

If the maximum flow rate is 940 ml/min and the nozzle diameter is 0.0225 inch:

$$A = \frac{\pi}{4}\left(\frac{0.0225}{12}\right)^2 = 2.761 \times 10^{-6}\, ft^2 \tag{2.5}$$

$$v = \frac{q}{A} = \frac{940\ \frac{ml}{min}}{2.761 \times 10^{-6}\, ft^2} \times \frac{3.5315 \times 10^{-5}\ \frac{ft^3}{ml}}{60\ \frac{s}{min}} = 200.37\ \frac{ft}{s} \tag{2.6}$$

And viscosity is:

$$1.3cp = 8.71 \times 10^{-4}\, \frac{lbm}{ft \cdot s} \tag{2.7}$$

$$Re = \frac{\rho v D}{\mu} = \frac{66.80\, \frac{lbm}{ft^3} \times 200.37\, \frac{ft}{s}}{8.71 \times 10^{-4}\, \frac{lbm}{ft \cdot s}} = 28{,}760 \tag{2.8}$$

$$f = 0.316 \times 28{,}760^{-0.25} = 0.02426 \tag{2.9}$$

$$\frac{\partial p}{\partial L} = \frac{0.02426 \times 66.80\, \frac{lbm}{ft^3} \times \left(200.37\, \frac{ft}{s}\right)^2}{2 \times 32.17\ \frac{ft \cdot lbm}{lbf} \times 0.0225in \times \frac{1ft}{12in} \times \frac{144in^2}{ft^2}} = 3745.6\, \frac{psi}{ft} \tag{2.10}$$

Since,

$$L = 1\ in \times \frac{1ft}{12in} = 0.0833\ ft \tag{2.11}$$

then the friction pressure drop is:

$$3745.6\frac{psi}{ft} \times 0.0833ft = 312.0\,psi \quad (2.12)$$

This pressure must be added to the desired upstream backpressure, **Section 3.8**, to calculate the maximum pressure with pump will experience.

2.3 Core Holder

The core holder, **Fig. 2.4I**, is a metallic cylinder consisting of three components: main body, inlet holder, and outlet holder. The three components are made of Hastelloy C276, which is a Nickel-Molybdendum-Chromium alloy with Tungsten. The reason for the use of Hastelloy is the highly corrosion resistant characteristics. The core holder is capable of reaching pressures up to 3,000 psi and temperatures of 300° F. It can accommodate a 4 inch diameter by 20 inch length core and is manufactured by Phoenix Instruments.

The main body consists of a metal cylinder with male threads on both ends, **Fig. 2.4A**, an inlet cap, **Fig. 2.4C**, and an outlet cap, **Fig. 2.4E**. Inside the main body is a Viton® 70-75 fluoroelastomer sleeve, **Fig. 2.4H**. The sleeve is secured by the inlet and outlet caps, which have female threads and are screwed on to the main body's threads.

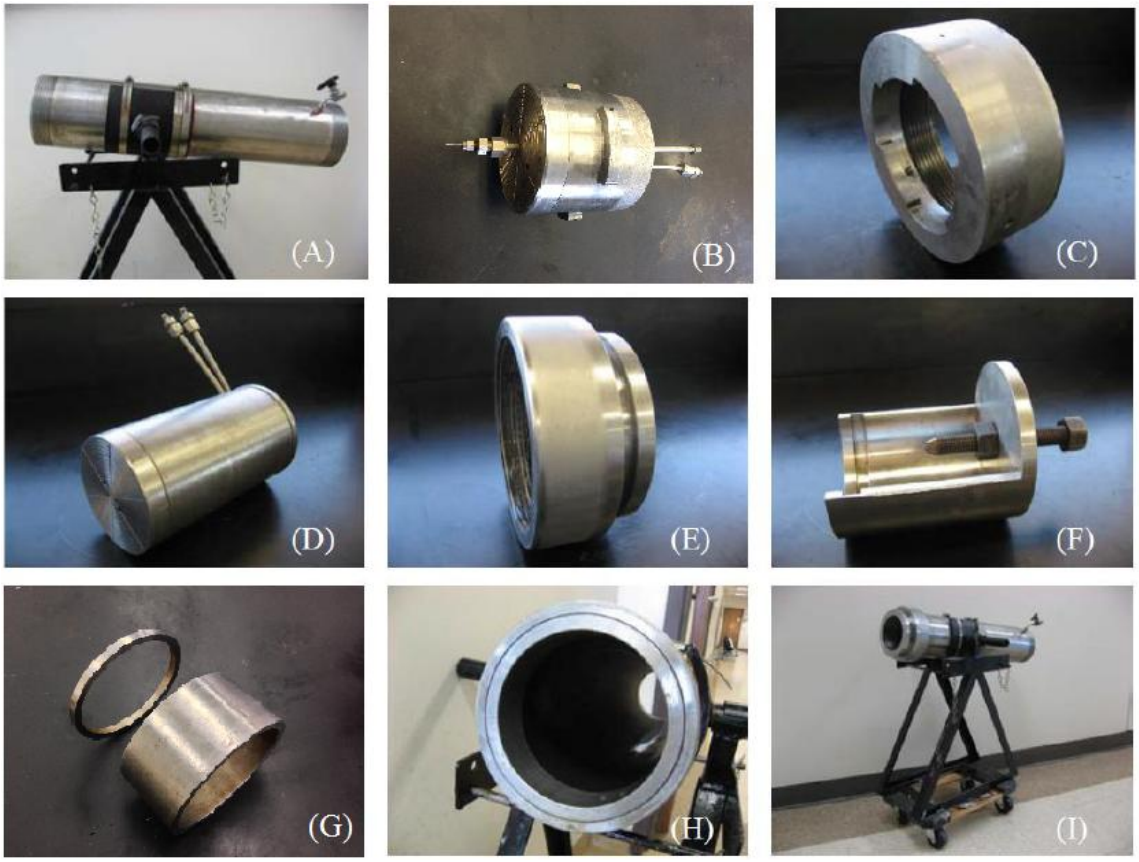

Fig. 2.4 – Core Holder

The inlet holder, **Fig. 2.4B** and **Fig. 2.5**, secures in the inlet side of the core holder. It contains the inlet line, return line, and pressure transducer line, shown in **Fig. 2.5**.

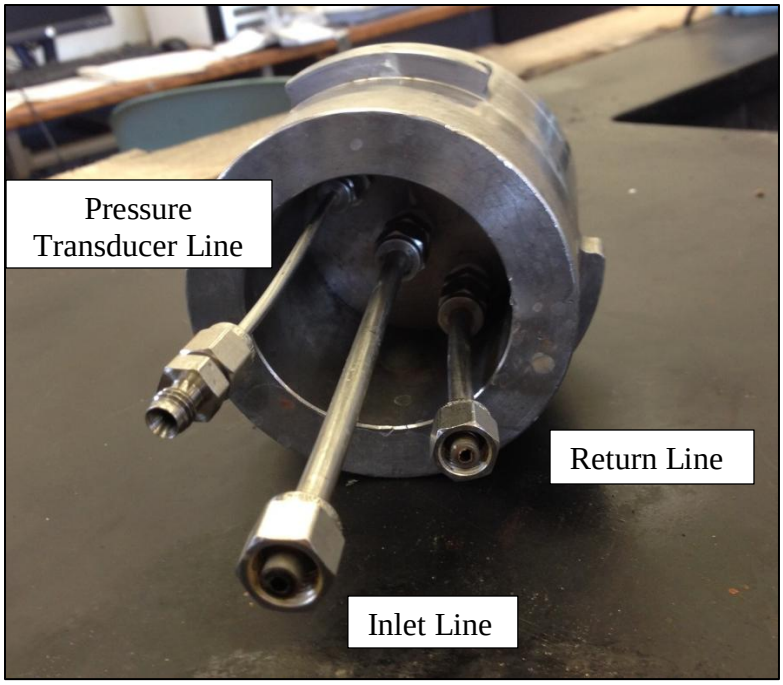

Fig. 2.5 – Inlet holder

The inlet line is 1/4” OD x .049” wall thickness 316 stainless steel tubing. It is connected to the inlet holder via a 1/4” T x 1/4” MNPT (Male National Pipe Thread) bored-through 316 stainless steel fitting. The MNPT threads of the fitting are secured to the FNPT (Female National Pipe Thread) threads on the inlet holder. The fitting is bored-through so that the tubing can pass through the fitting into the core holder so that the jet nozzle can be attached. Once the 1/4” tubing is fully inserted to a predetermined length, the tubing is secured to the 1/4” T side of the 1/4” T x 1/4” MNPT bored-through 316 stainless steel fitting with a nut and ferrule.

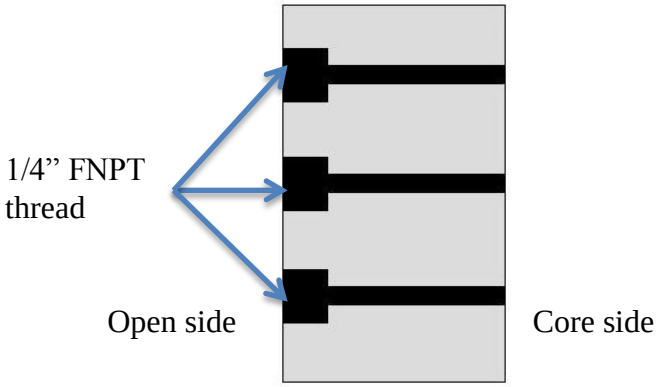

Fig. 2.6 – Inlet Holder Cross Section

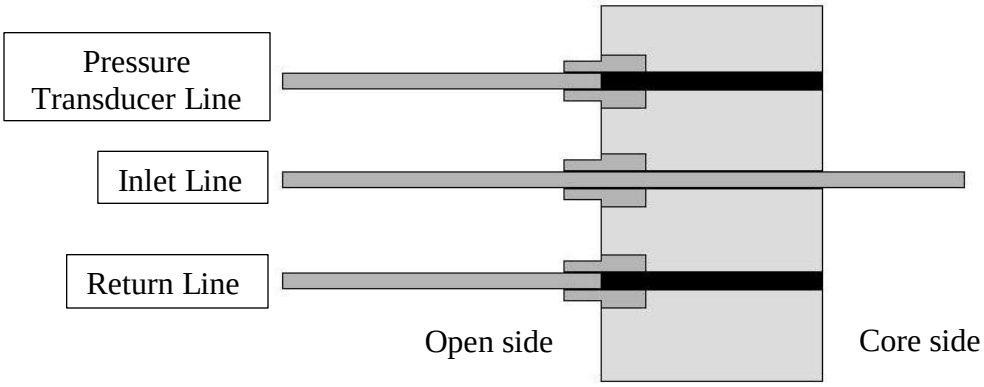

Fig. 2.7 – Inlet Holder Cross Section with MNPT Fitting and Tubing

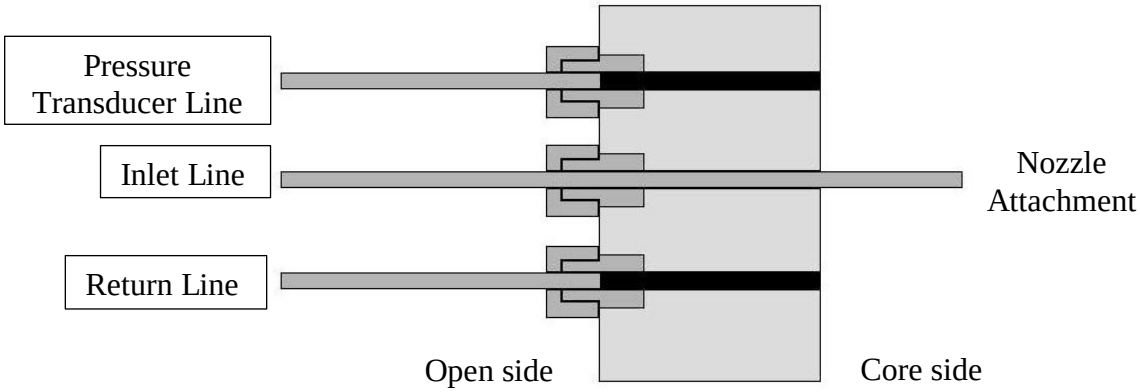

Fig. 2.8 – Inlet Holder Cross Section with MNPT Fitting, Tubing, and Nut

The return line is connected the same way as the inlet line, but the MNPT fitting is not bored-through because the tubing does not need to pass through into the core holder.

The pressure transducer line is 1/8” OD x .028” wall thickness 316 stainless steel tubing. It is connected to the inlet holder via a 1/8” T x 1/4” MNPT 316 stainless steel fitting.

The jet nozzle is attached on the core side of the inlet line. It is constructed by attaching a 1/4” x 1/16” Tube OD Reducing Union to the core side of the inlet line with a nut and ferrule. Then, 1/16” OD x .020 wall thickness tubing is attached with a nut and ferrule.

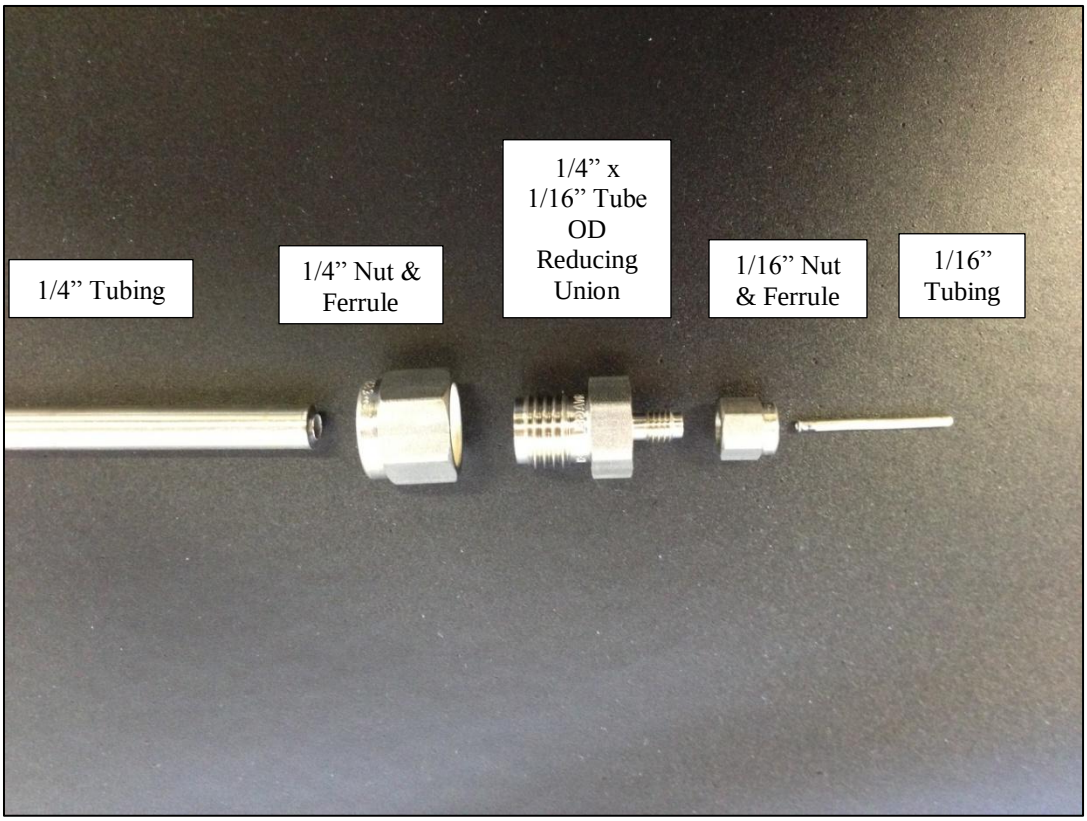

Fig. 2.9 – Nozzle Construction

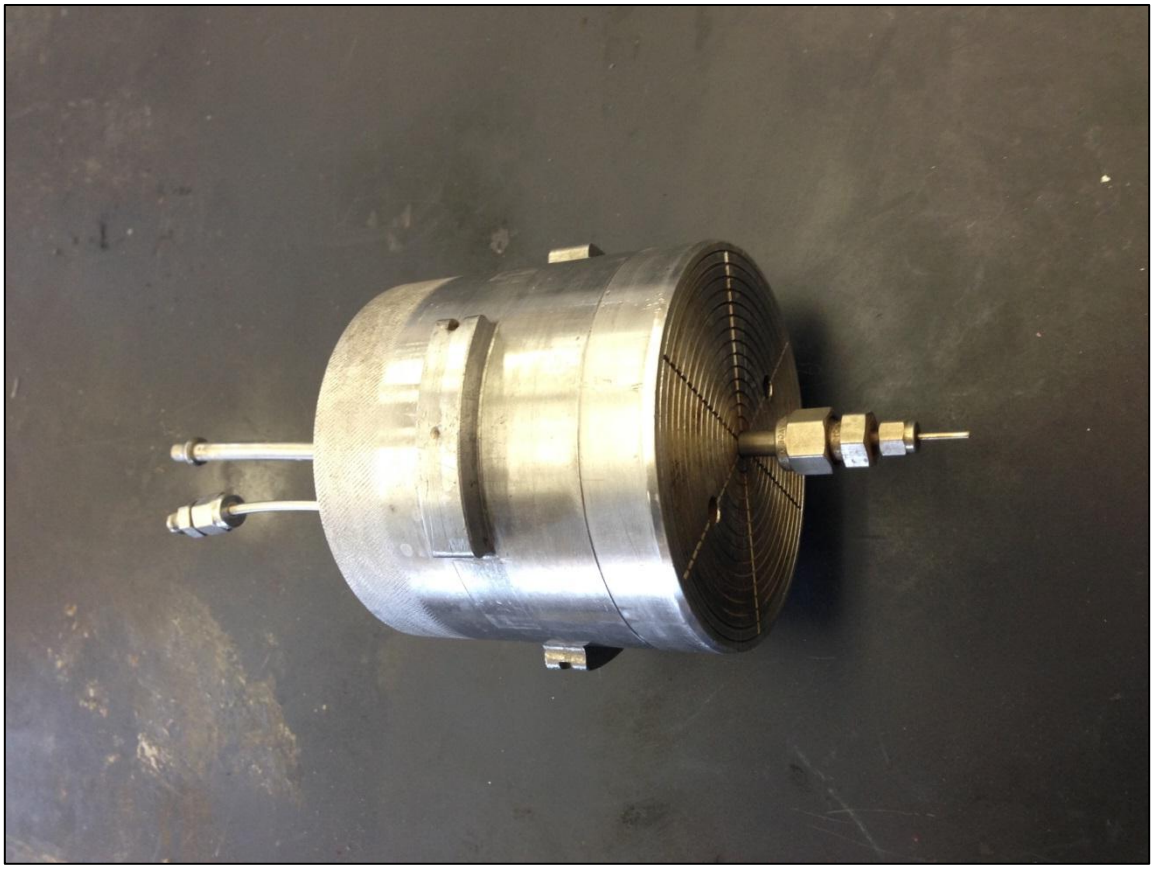

Fig. 2.10 – Jet Nozzle

The length of the nozzle tubing/fitting, L_{tub}, is determined by the amount of standoff required between the nozzle and the core surface, L_{so}, and the available spacer distance, L_{sp} ,**Fig. 2.12 (Zhang, 2009)**. The following equation is used to describe the nozzle length:

$$L_{tub} = L_{sp} - L_{so} \tag{2.13}$$

A standoff of 4 times the ID of 1/16" tubing is used for these experiments. According to **Fig. 2.11 (Pekarek, 1963)**, theoretical results show the effects of water travelling through a nozzle in water medium. The fluid velocity exiting the nozzle

decreases the further it gets from the exit. At distances greater than 4.5 times the nozzle diameter the velocity decreases more with distance.

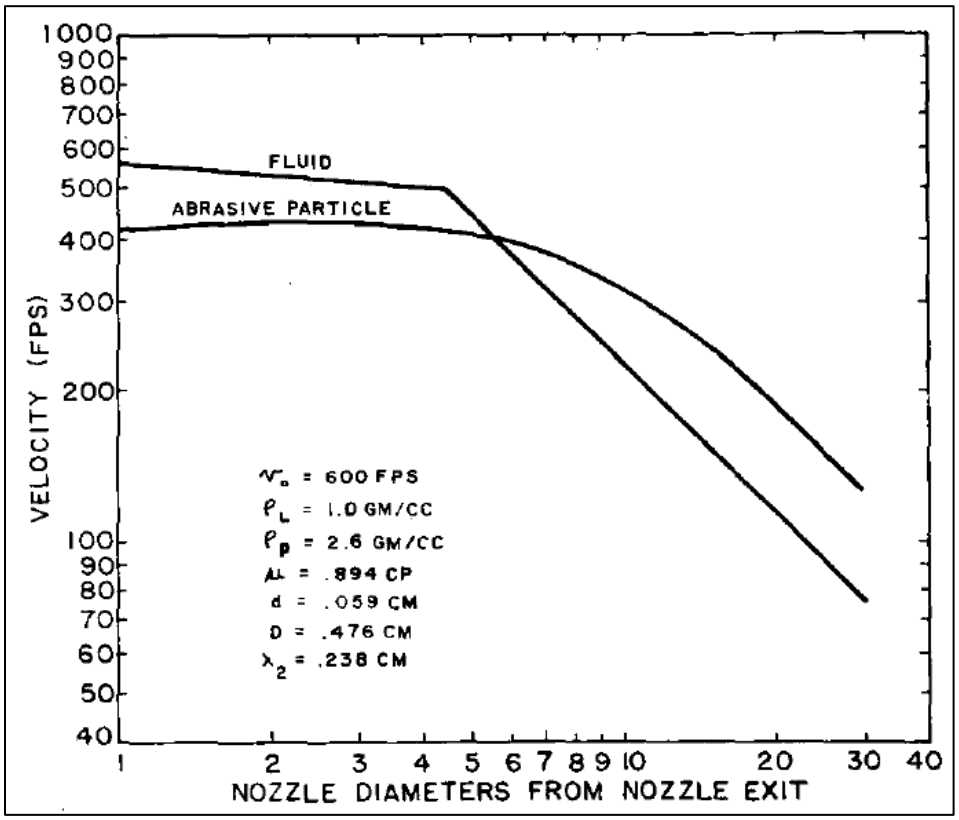

Fig. 2.11 – Fluid Velocity vs. Distance From Nozzle (Pekarek, 1963)

The drop in fluid velocity after 4.5 times the diameter is due to the change in flow regimes. At distances close to the nozzle exit is the initial "zone of flow establishment" shown in **Fig. 2.12 (Albertson, 1948)**. The fluid velocity at the nozzle exit is assumed to be relatively constant, but due to the high shear between the jetted fluid and fluid medium, eddies develop which progress both inward and outward. The lateral mixing causes the fluid within the jet to decelerate while the fluid in the surrounding medium accelerates. This initial zone is limited to where the eddies of the surrounding fluid have not fully penetrated into the centerline of jet stream. When the centerline of the jet has

become fully turbulent, the "zone of established flow"is formed and the jet velocity decreases in greater magnitude at a given distance from the nozzle exit. For this theoretical work it is assumed that there is no transition zone between the flow regimes, and it should be noted that the distance of 4.5 times nozzle diameter is different for fluid mediums other than water.

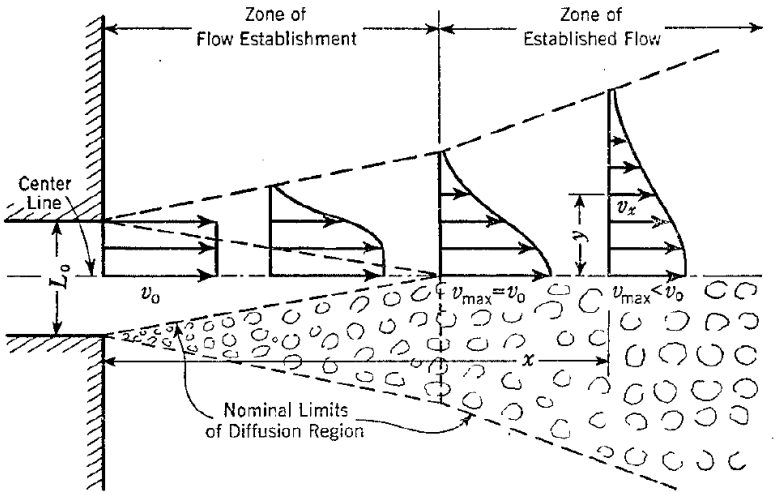

Fig. 2.12 – Jet Stream Diffusion (Albertson, 1948)

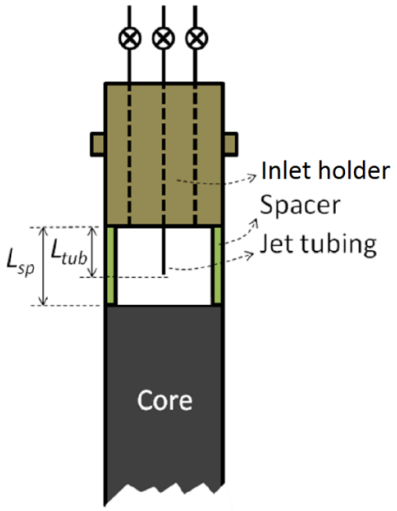

Fig. 2.13 – Nozzle Spacing (Zhang, 2009)

Since the ID of the tubing is 0.0225" (1/16"-2*.020"), L_{so} is 0.09".

Two spacer cylinders, **Fig. 2.4G,** are used to provide distance from the core to the inlet holder. The distance allows clearance for the nozzle located inside the core holder. Both spacers have an OD of 4" and an ID of 3.5". One spacer ring has a 2" length and the other has a 0.25" length for a total L_{sp} of 2.25". Therefore, from Eq. 2.13:

$$L_{tub} = 2.25" - 0.09" = 2.16" \quad (2.14)$$

The outlet holder, **Fig. 2.4D** secures the outlet side of the core holder. The outlet holder is secured in place by bolt which screws the outlet holder in place, **Fig. 2.4F**. One outlet line is connected to the pressure transducer, and the other line is connected to the downstream backpressure regulator.

2.4 Hydraulic pump

The hydraulic hand pump, **Fig. 2.14**, is an Enerpac Co. Model P392. It has a maximum operating pressure of 10,000 psi and a fluid capacity of 900 ml. AW32 hydraulic oil is pumped between the inside diameter of the metallic core holder and the outside diameter of the Viton® sleeve to provide confining pressure to the core inside the core holder.

Fig. 2.14 –Hydraulic Hand Pump

2.5 Backpressure Regulator

Two backpressure regulators are used to control the upstream and downstream pressure of the core holder. The upstream pressure in controlled by a Mity-Mite S-91W, **Fig. 2.15**, which has a pressure range of 100-2,000 psi.

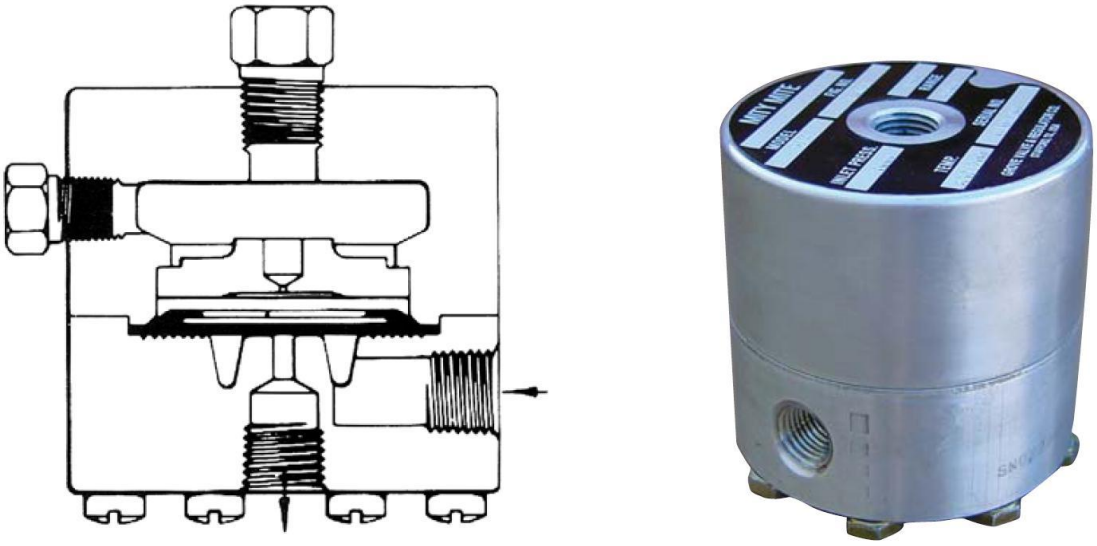

Fig. 2.15 – Mity-Mite S-91W Backpressure Regulator (Dresser Inc., 2014)

Model	Basic Fig #	Dome	Body	Diaphragm	Temperature Range	Back Pressure Range (psig)	Max C_V	Weight (lbs)
90W	10448	Al - Alloy	Al - Alloy	Nitrile	0° to 165°F			1.6
SD90W	11521	Al - Alloy	Al - Alloy	FKM	0° to 200°F	10-2000	0.44	2.5
S90W	11508	316 SST	316 SST	FKM	0° to 200°F			4
91LW	10451	Al - Alloy	Al - Alloy	PTFE				1.6
SD91LW	11522	Al - Alloy	316 SST	PTFE	-65°F to 200°F	25-400	0.44	2.5
S91LW	11504	316 SST	316 SST	PTFE				4
91W	10454	Al - Alloy	Al - Alloy	PTFE				1.6
SD91W	11523	Al - Alloy	316 SST	PTFE	-65°F to 200°F	100-2000	0.38	2.5
S91W	11505	316 SST	316 SST	PTFE				4
91XW	10457	Al - Alloy	Al - Alloy	PTFE				1.6
SD91XW	11524	Al - Alloy	316 SST	PTFE	-65°F to 200°F	100-3000	0.17	2.5
S91XW	11506	316 SST	316 SST	PTFE				4
91	M12519-G	316 SST	316 SST	FKM	0° to 200°F	60-6000	0.12	4

Order Code =

Al = Aluminum
316 SST = 316 Stainless Steel

Fig. 2.16 – Mity-Mite S-91W Specs (Dresser Inc., 2014)

This backpressure regulator is an angle pattern regulator with a diaphragm that senses upstream pressure on the underside which is balance by the dome pressure on the upper side. The dome pressure is regulated by nitrogen from a tank in the lab. Two connections are provided in the dome. The top connection is for a gauge to monitor the pressure inside the dome, while the other is for nitrogen supply line that applies the dome pressure. Two connections are provided for the lower side. One is for the inlet of the fluid, while the other is for the outlet. When the pressure of the inlet fluid matches the pressure of the dome, the diaphragm opens and allows the fluid to flow. If the pressure of the inlet fluid remains lower than the dome pressure, the diaphragm will remain closed.

The downstream backpressure regulator is an Equilibar EB1HP1-SS316, **Fig. 2.17**, which has a pressure range of 0-3,000 psi. It is made from 316 stainless steel, and operates in the same way as the Mity-Mite regulator.

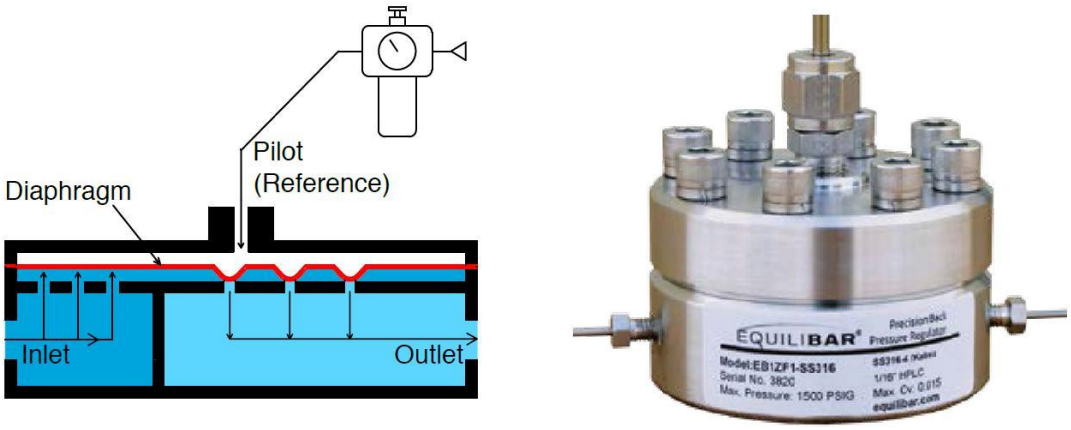

Fig. 2.17 – Equilibar Backpressure Regulator (Equilibar, 2013)

2.6 Data Acquisition

The data acquisition system comprises of a pressure transducer, weight scale, National Instruments signal processing board and PC with National Instruments LabView 2012 software.

The pressure transducer, **Fig. 2.18**, is a Foxboro model IDP10-A26E21F-M1, which measures the pressure differential across the core, has a range of 0-3,000 psi. The transducer has two 1/4" FNPT ports. One, labeled "H", is where the higher, or upstream, pressure is connected. The other port, labeled "L", is where the lower, or downstream, pressure is connected. Both ports are connected to the core holder via a 1/8" T x 1/4" MNPT fitting and 1/8" OD x .028" wall thickness 316 stainless steel tubing. Inside the transducer is a diaphragm that senses the difference in pressure of the two ports. As the diaphragm bends, a corresponding current signal is sent to the NI signal processing board.

Fig. 2.18 – Pressure Transducer

The weight scale, **Fig. 2.19**, used is an A&D Company electronic balance model EP-20KA.

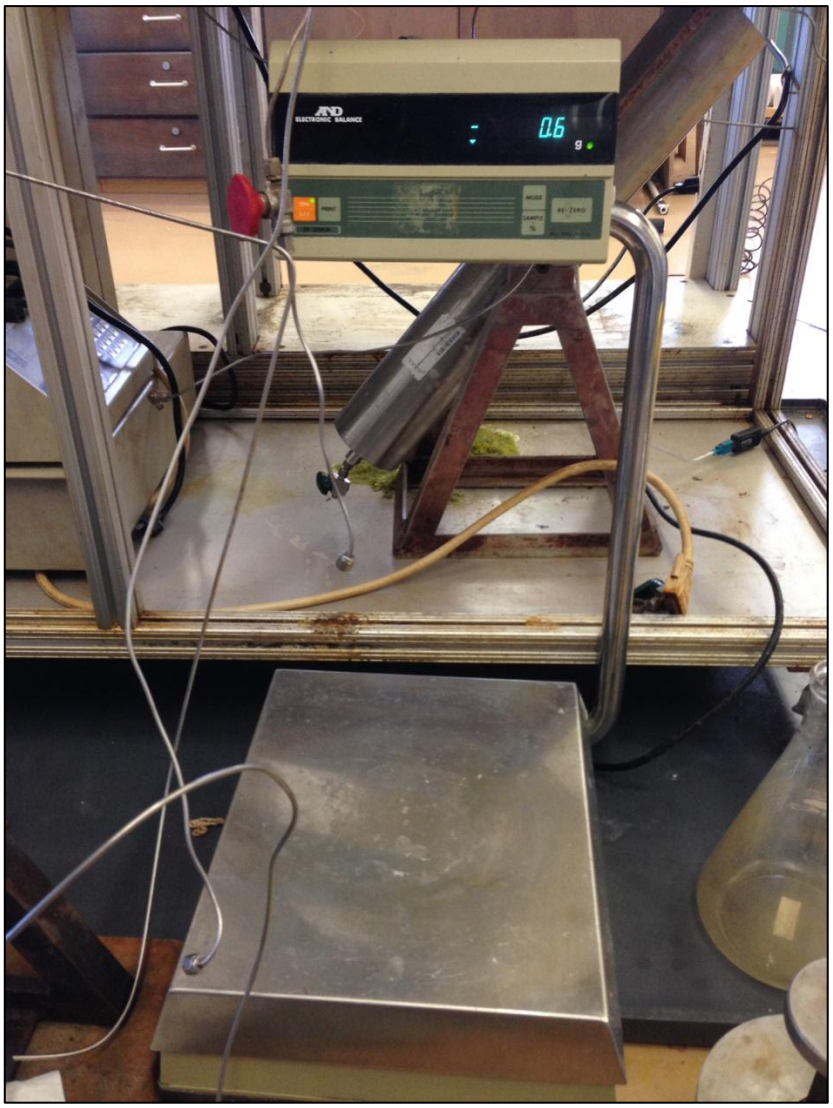

Fig. 2.19 – Weight Scale

The specifications are listed in **Table. 2.1**.

Table 2.1 – Weight Scale Specifications

Max. Capacity Grams	20,000g
Resolution Grams	0.1g
Repeatability Std. Dev.	0.1g
Linearity (Grams)	±0.2g
Sensitivity Drift 10-30°C	±3ppm/°C

Table 2.1 Continued

Resolution Pounds	0.0005lb
Resolution lb/oz	0.1oz
Sample 100% Min. Weight	50g/0.01%
Sample Counting (10 PCS)	10g Min
Counting Capacity (Max)	300,000pcs
Stabilization time	3 seconds
Operating Temp.	32°F -104°F
Pan Dimensions	11.2” W x 13.5” D
External Dimensions	13.8” W x 17.1” D x 25.1” H
Weight	30lb 11oz

The scale has RS232C output connector. A RS232C to USB adapter is used to connect the scale to the computer, **Fig. 2.20**.

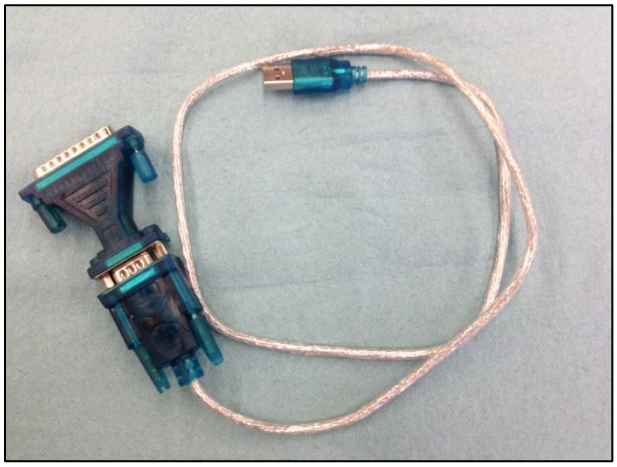

Fig. 2.20 – RS232C – USB Adapter

For the scale to communicate properly with the computer it must be set up in the following way:

1. With the display turned off, press and hold the “RE-ZERO” key

2. Press the “ON/OFF” key, and the display will read “A-XXXXX” (the “X” being an integer)
    - A triangle will appear under the “A”
    - To move the triangle, press the “RE-ZERO” key
    - To change the value above the triangle, press the “PRINT” key
3. With the triangle under the “A”, press the “PRINT” key and the display will read “b-XXXXX”
4. Press the “RE-ZERO” key two times so that the triangle is under the second X
5. Press the “PRINT” until the “X” is a “3”
6. The “b” screen, **Fig. 2.22**, should read “b-03000” and the “A” screen, **Fig. 2.21**, should read “A-00000”

Fig. 2.21 – “A” Screen

Fig. 2.22 – “B” Screen

This set-up puts the scale in “Command Mode”. When the computer sends the scale a “read” command, the scale will send back to the computer what is read on the scale’s weight display.

The NI signal processing board is model CB-68LP. The signal from this board is then sent to a PC via a RS232 cable. Installed on the computer is National Instruments LabView 2012 software. The software is used to write the code for recording the data from the pressure transducer and weight scale. The code is known as a VI file. Before each experiment the VI file is run and it records the data in a text file. The entire code for the VI file is found in Appendix A.

The pressure transducer sends a current signal to the CB-69LP. The DAQ Assistant reads the pressure data from the CB-68LP board. The value is then processed through a filter, which smooths out the signal, and then outputs it to a graph and text file, **Fig. 2.23**.

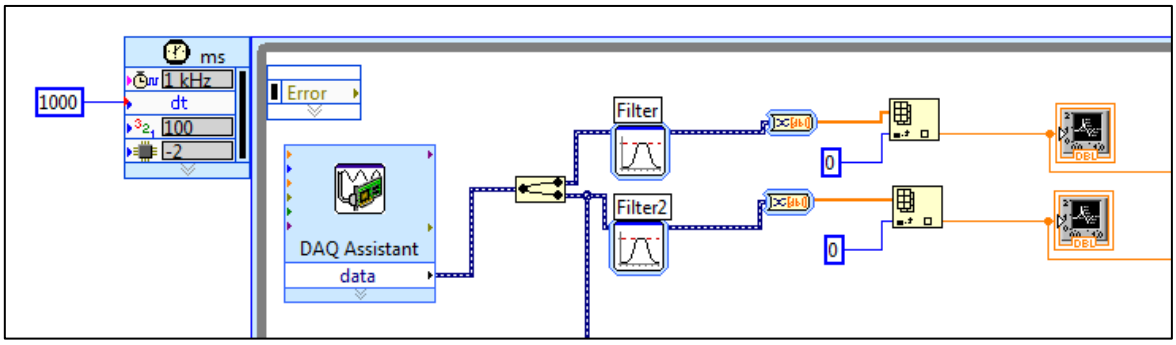

Fig. 2.23 – Pressure Code

LabView VISA function, **Fig. 2.24**, reads the data sent from the weight scale from a USB port on the CPU

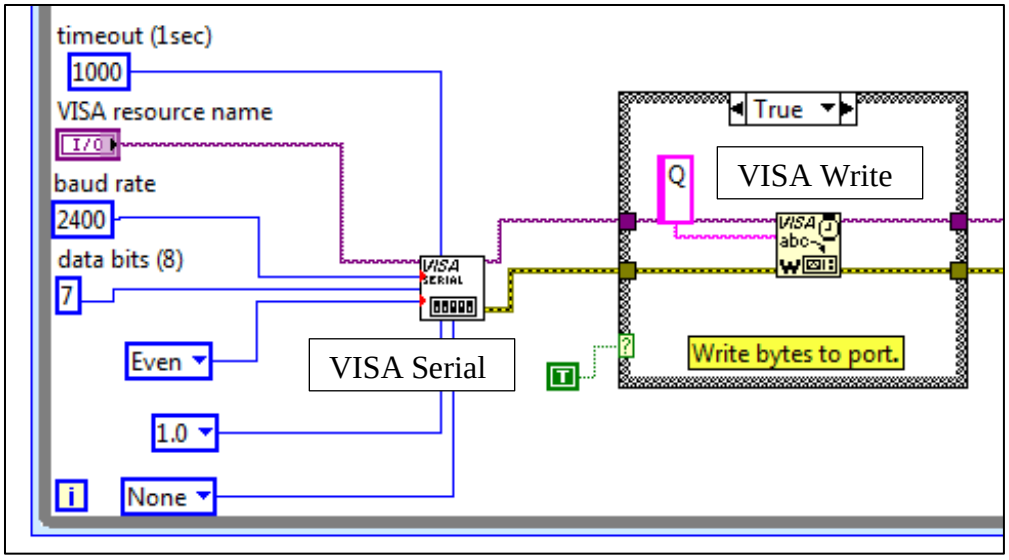

Fig. 2.24 – Weight Scale Input

. The VISA resource name (USB port), **Fig. 2.25**, is chosen on the front panel

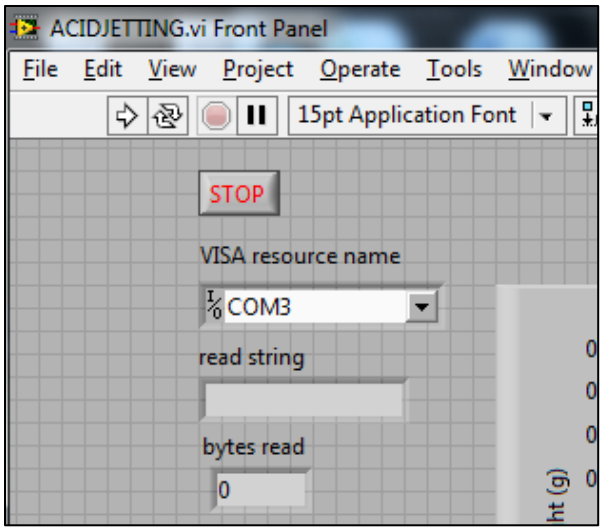

Fig. 2.25 – VISA Resource Name

The resource name depicts which USB port LabView reads from. All the other inputs to the VISA Serial such as baud rate (2400), data bit (7), stop bit (1) and parity bit (EVEN) settings can be found in the instruction manual for the scale. These settings are how the

scale communicates with LabView. The VISA Write function gives the scale an ASCII command "Q", which is a command for the balance to transmit. The scale transmits whatever is on the display. Since the scale was set up to be in command mode (b-03000), the scale knows to transmit based on the "Q" command. The VISA Write function, **Fig. 2.26**, takes the output from the scale in a series of bytes and turns them into a string (pink box).

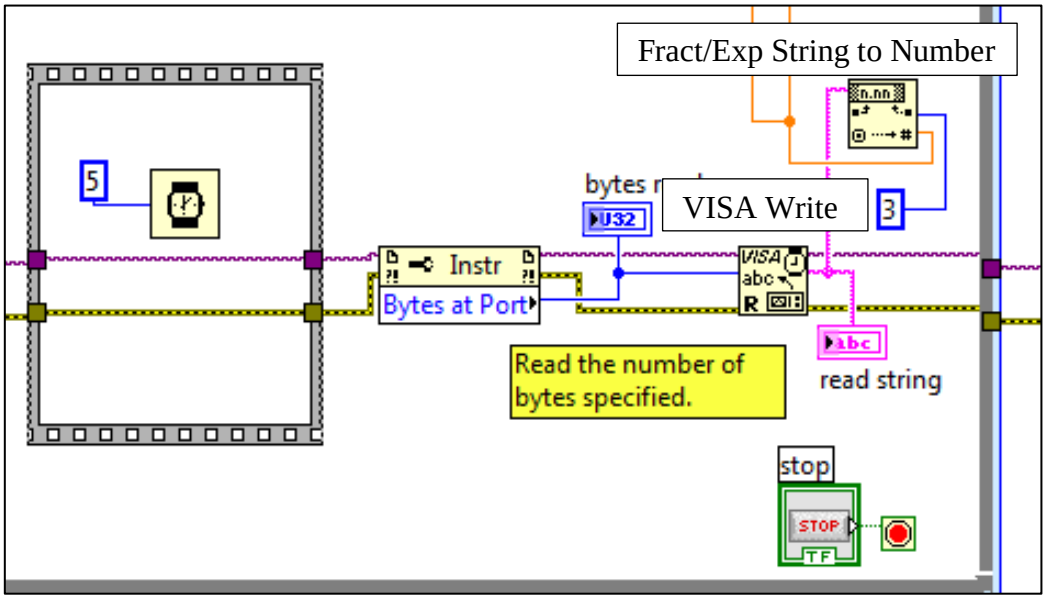

Fig. 2.26 – VISA Write

The string is then formatted from a string to a number with the Fract/Exp String to Number function so it can be displayed on a graph and written in the text output file.

2.7 Permeability Measuring Device

To properly measure permeability, a known, constant flow rate through the core must be used. Therefore, it makes sense to use a syringe pump instead of the pulse pump previously described. A syringe pump is set up with a separate apparatus. A detailed description of the apparatus used can be seen in the Texas A&M University

Master's thesis, "Matrix Acidizing Core Flooding Apparatus: Equipment and Procedure Description" by E. Grabski (2012). The permeability measurement schematic is shown in **Fig. 2.27**, and the apparatus is shown in **Fig. 2.28**.

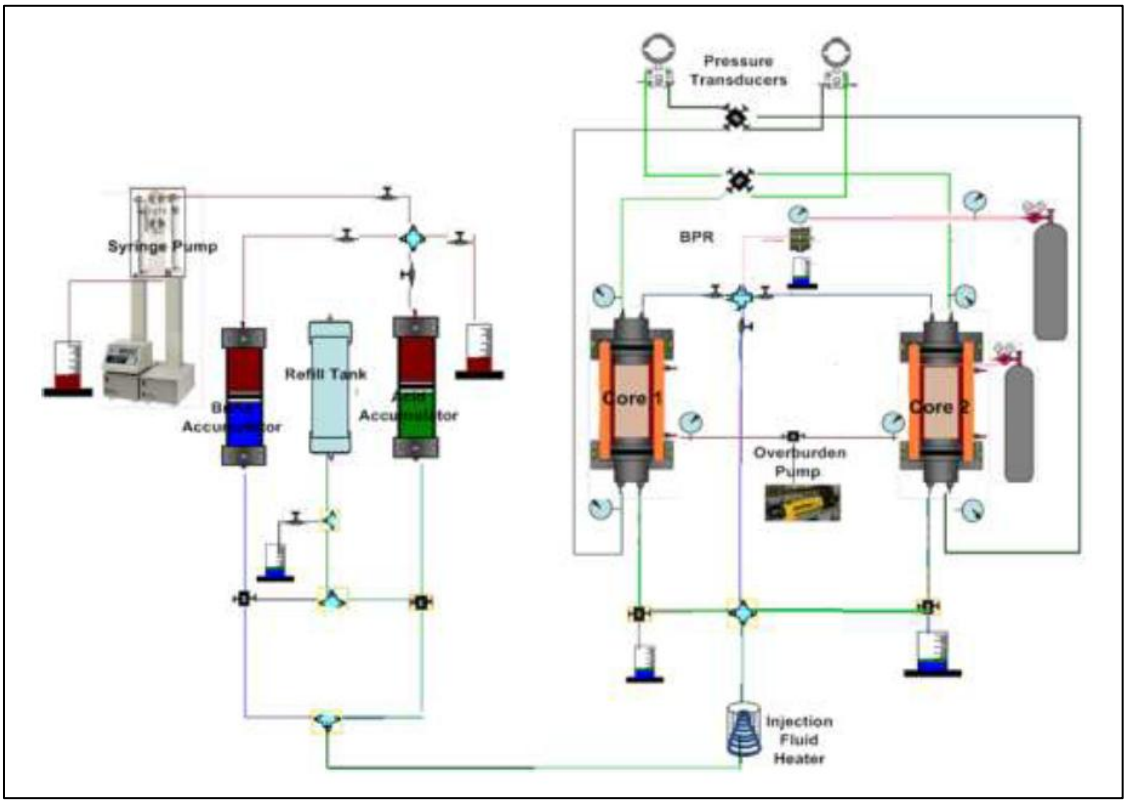

Fig. 2.27 – Permeability Test Apparatus Schematic (Grabski, 2012)

Fig. 2.28 – Permeability Test Apparatus (Grabski, 2012)

2.8 Time Recording

In order to accurately match the pressure and weight data with the moment acid reaches the core, the time must be known. When the LabView program is run, it records the time of the CPU (Central Processing Unit), **Fig. 2.29**.

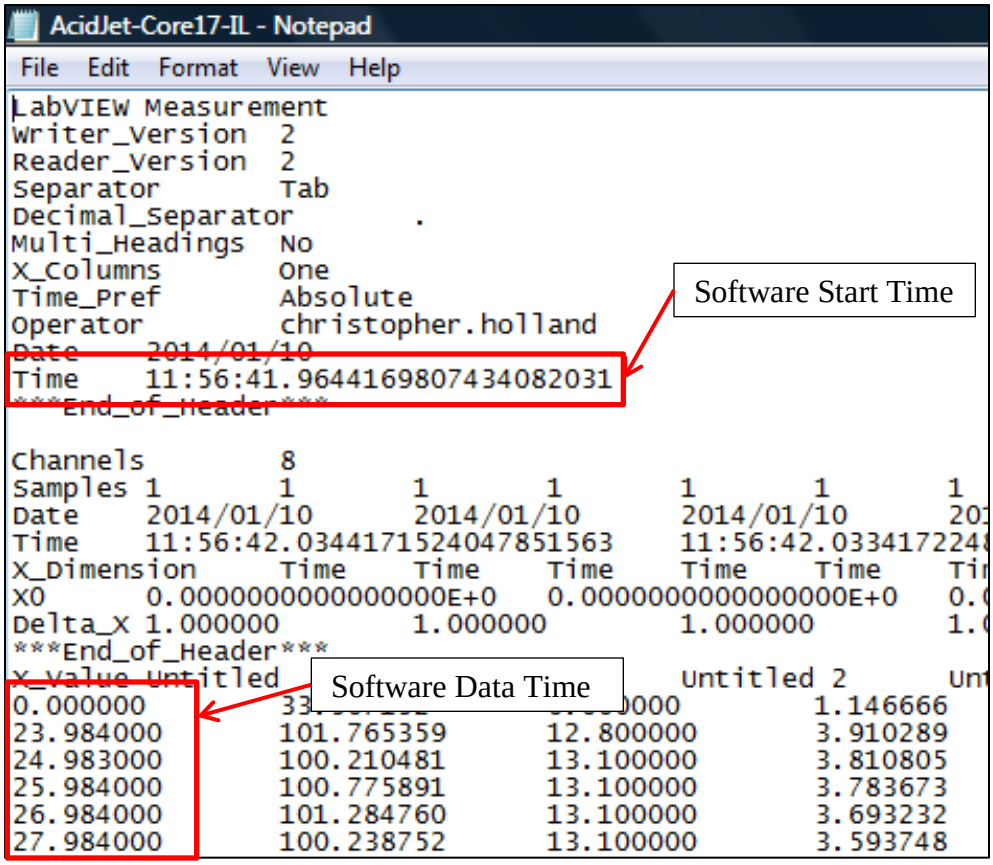

Fig. 2.29 – LabView data

After the file name is created and saved, LabView data is recorded every second. Therefore, the time of LabView data is known. Any type of clock or timer can be used to record events of the experiment. Emerald Timestamp, an iPhone application, **Fig. 2.30**, is used for these experiments. It enables the user to record time with the push of a button, label each time's event, and email these events. It is usually within one second of the CPU clock. The time from the timestamp can be matched with the LabView time to know the exact moment of the experiment that each pressure and weight data is captured.

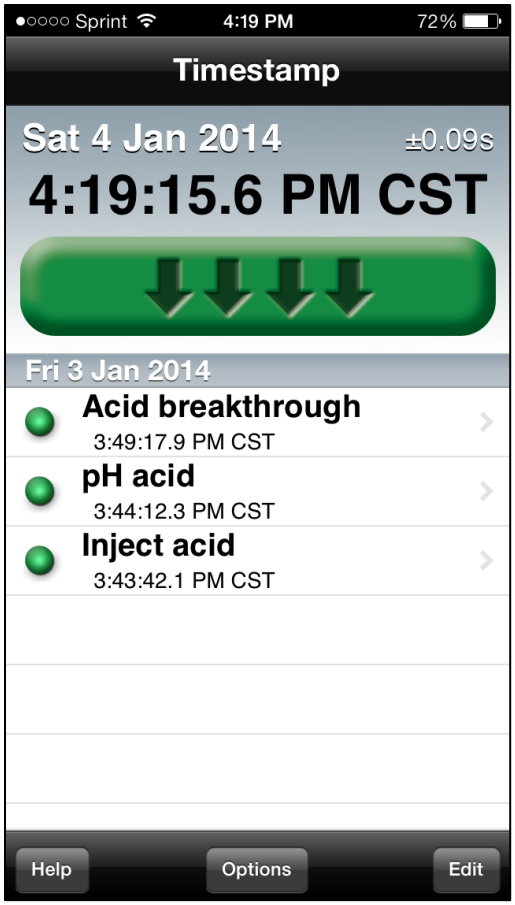

Fig. 2.30 – Emerald Timestamp

3. EXPERIMENTAL PROCEDURE

This section describes in detail the procedures for preparations before acid jetting and the acid jetting experiment itself. The cores need to be weighed after it is saturated with water so that porosity can be determined. The permeability must be determined by injecting water through the core at a known rate. Section 3.1 will describe the general procedure for an acid jetting experiment. More detailed descriptions of major steps will be given in later sections.

3.1 General Experiment

1. Weigh dry core on scale and record dry weight
2. Saturate core in brine with vacuum pump for at least 8 hours
3. Weigh wet core on scale and record wet weight
4. Calculate porosity
5. Set up core in core holder attached to syringe pump to run permeability test
6. Set the syringe pump to desired flow rate and run pump to inject brine into the core
7. Once the pressure across the core has stabilized, stop pump and terminate permeability test
8. Remove core from permeability test apparatus and install core in acid jetting apparatus
9. Prepare 15% wt HCl with corrosion inhibitor and pour in acid container
10. Run pulse pump at desired flow rate to inject brine

11. Apply 1,000 psi downstream backpressure
12. Apply upstream backpressure to give desired flux through the core (pressure must be above downstream backpressure to give a positive pressure differential)
13. Once the pressure differential and flux through core have stabilized, shut off brine and inject acid and record the time
14. Continue to inject acid for 20 minutes or until acid breaks through the core
15. Shut off acid and inject water for 2 minutes
16. Release upstream backpressure
17. When pH of fluid reaches neutral, shut off pump and release downstream backpressure
18. Weigh acidized core
19. Perform post acidizing permeability test if acid did not break through

3.2 Cores

All cores are purchased from Kocurek Industry Co. and are Indiana limestone lithology. They are 4" diameter by 16" length. Permeability ranges from 1 md to 10 md and porosity is around 15%.

3.3 Core Preparation

After cores are cut and arrive at the lab they are numbered and weighed. The dry weight is recorded to be used to calculate porosity.

The core is placed in a large PVC container that is filled with brine. Make sure the core is fully submerged with several inches of water over the top of the core. The

water level will decrease as the pores are filled with water. The PVC is covered with a lid that is attached to a vacuum pump shown in **Fig. 3.2**.

Fig. 3.1 – PVC Container

Fig. 3.2 – Vacuum Pump

When the vacuum pump is turned on, the suction pressure should be maintained around 90 kPa. Apply vacuum grease as needed to seal any leaks. The vacuum pump should run for at least 8 hours to make sure the core is fully saturated.

3.4 Porosity Measurement

After the cores are fully saturated, they are immediately weighed to get the saturated weight. The dry weight and saturated weight are used to calculate porosity. Porosity is calculated by the following:

$$\emptyset = \frac{V_{pore}}{V_{bulk}} \times 100\% \qquad (3.1)$$

$$V_{bulk} = A \cdot L = \frac{1}{4}\pi d^2 \cdot L \tag{3.2}$$

$$V_{pore} = \frac{M_{saturated} - M_{dry}}{\rho_{brine}} \tag{3.3}$$

3.5 Permeability Test

After each core is saturated and weighed, it must undergo a permeability test. Permeability, k, is the property that describes the ability of fluids to flow in a porous medium, and is described by the following equation:

$$k = 96.13\frac{q \times L \times \mu}{\Delta p \times A} \tag{3.4}$$

If q is in cm/min, L in inches, μ in cp, Δp in psi, and A in square inches, 96.13 converts these units into millidarcy by:

$$\frac{1\ \frac{ml}{min} \cdot 1 \times 10^{-6}\frac{m}{ml} \cdot \frac{1\ min}{60\ s} \cdot 0.0254\frac{m}{in} \cdot 0.001\ \frac{Pa \cdot s}{cp}}{6896.6\frac{Pa}{psi} \cdot 6.4516 \times 10^{-4}\frac{m^2}{in^2} \cdot 9.9 \times 10^{-16}\frac{m^2}{cp}} = 96.13 \tag{3.5}$$

The test is as follows:

For the initial fill of brine, see steps below and **Fig. 3.3**:

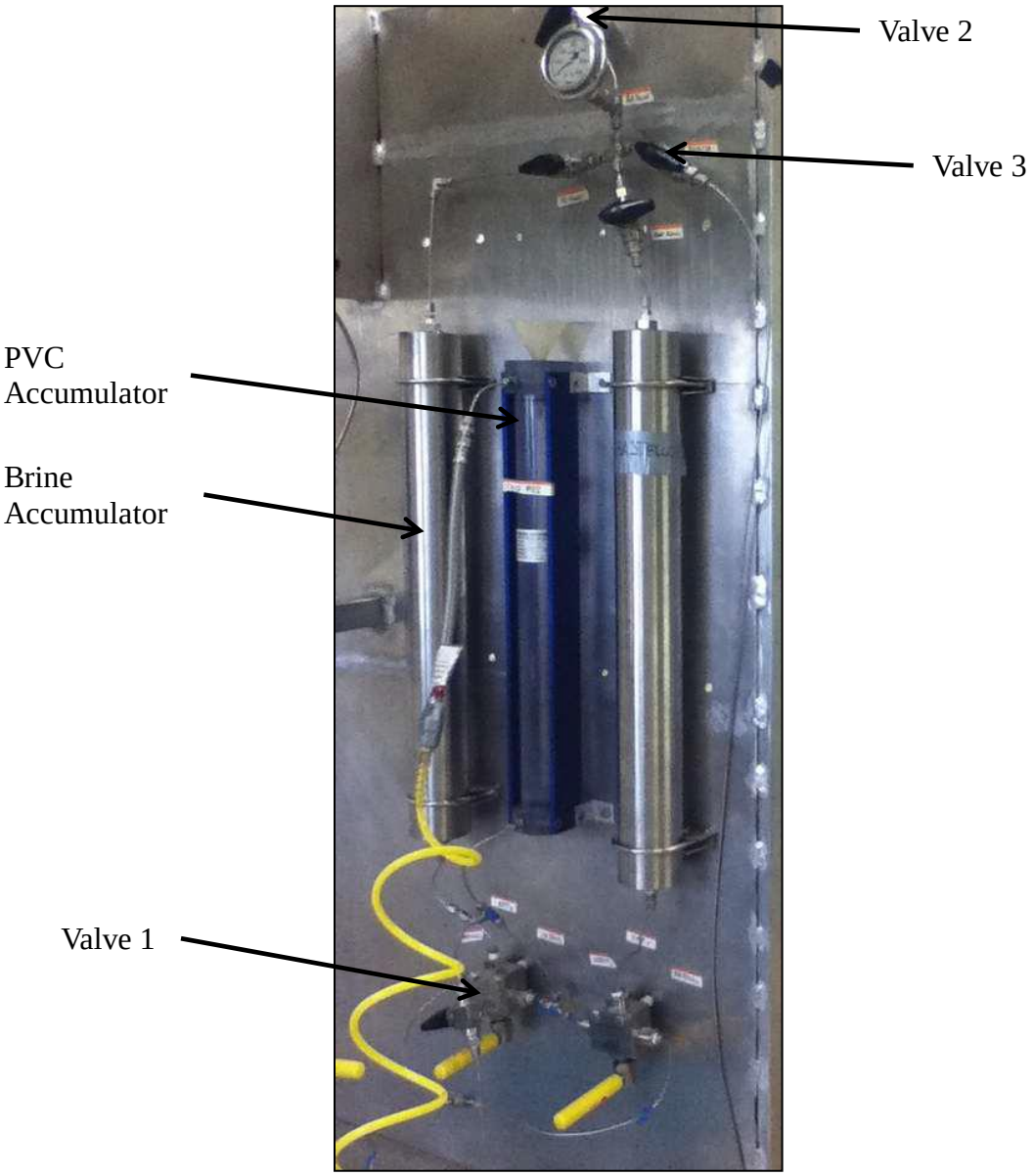

Fig. 3.3 – Permeability Test Apparatus (Grabski, 2012)

1. Pour brine in clear PVC accumulator and secure with nut
2. Set Valve 1 to “Refill” (left)

3. Close Valve 2
4. Open Valve 3
5. Open air pressure (on wall)
6. Once refill is complete set Valve 1 to “Off” (centered)
7. Shut off air pressure (on wall)
8. Open Valve 2

For the permeability test, see steps below, **Fig. 3.3 and Fig. 3.4**:

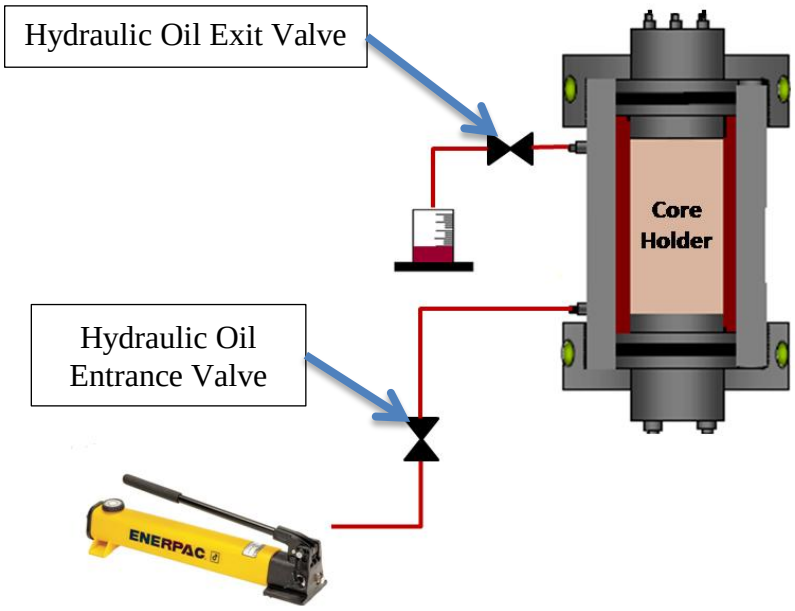

Fig. 3.4 – Hydraulic Oil Valves Schematic

1. Load core in core holder.
2. Insert lower holder
3. Rotate core upright
4. Insert spacer ring on top of core
5. Attach hydraulic oil fitting and open all Hydraulic Oil Valves

6. Pump hydraulic oil until a steady stream is flowing out of the Hydraulic Oil Exit Valve
7. Close Hydraulic Oil Exit Valve
8. Apply 8 pumps of Enerpac hand pump
9. Pour water on top of core to fill spacer ring void
10. Attach upper holder
11. Attach all tube fittings
12. Apply 500 psi confining pressure (hydraulic oil)
13. Open bypass valve
14. Make sure Valve 2 and Valve 3 are open and Valve 1 is "Off" (centered)
15. Start syringe pump (20 ml/min)
16. After constant flow is established, close Valve 3
17. Set Valve 1 to "Inject" (right)
18. Start LabView program (C drive, final labview, Matrix Acidizing 1001)
19. Close bypass valve
20. Monitor pressure and adjust confining pressure (300-500 psi over pressure display)
21. Adjust pump rate to 50 ml/min to speed up pressure buildup
22. When pressure reaches 100 psi, slow down pump rate to 20 ml/min
23. MAKE SURE PRESSURE DISPLAY DOES NOT EXCEED 1,500 PSI, ADJUST PUMP RATE ACCORDINGLY

During test Refill:

24. When brine accumulator becomes empty, stop pump, set Valve 1 to “Off”

25. If confining pressure is above 1,000 psi, adjust confining pressure to 1,000 psi by releasing the Release Valve (A) on the Enerpac pump

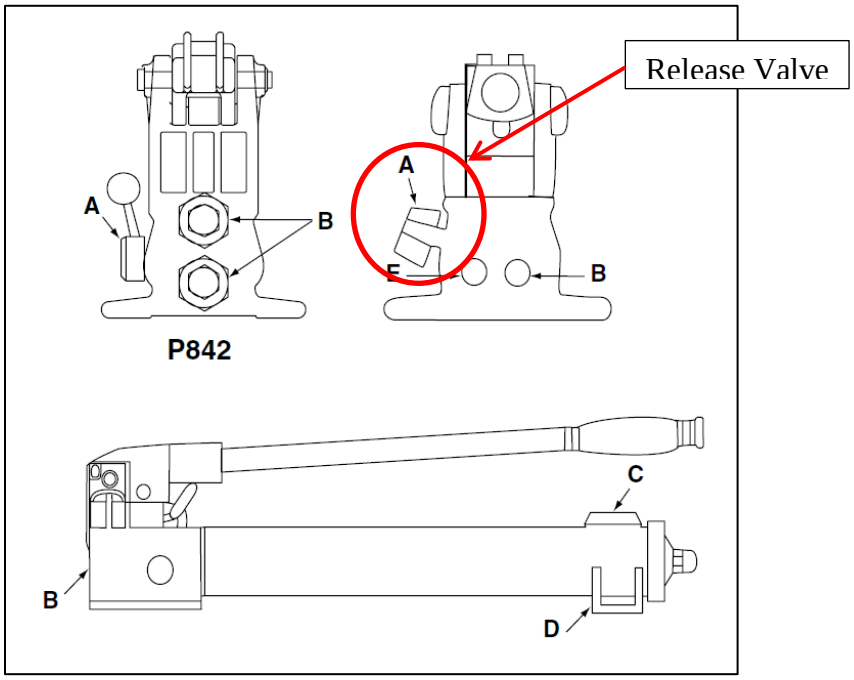

Fig. 3.5 – Hydraulic Oil Pump (Enerpac, 2014)

If confining pressure is below 1,000 psi, do not adjust

26. Open Valve 3

27. Close Valve 2

28. Set Valve 1 to “Refill”

29. Open air pressure (on wall)

30. Once refill is complete set Valve 1 to “Off”

31. Shut off air pressure (on wall)

32. Open Valve 2

33. When refill is complete, do steps 15-18

To shut down the Permeability Test:

34. When pressure has reached steady-state, **Fig. 3.6**, stop pump

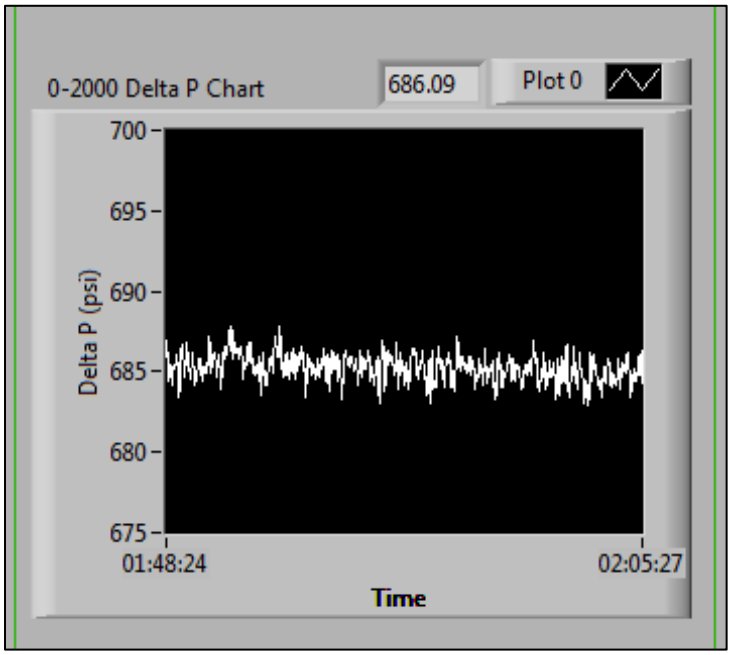

Fig. 3.6 – Steady State Pressure

35. Set Valve 1 to “Off”

36. Make sure system pressure is below 500 psi

37. Lower confining pressure to 500 psi

38. Open bypass valve

39. Stop LabView program

40. When system pressure has reached close to 0 psi, release all confining pressure

41. Disassemble

A typical permeability test pressure curve should look like **Fig. 3.7**.

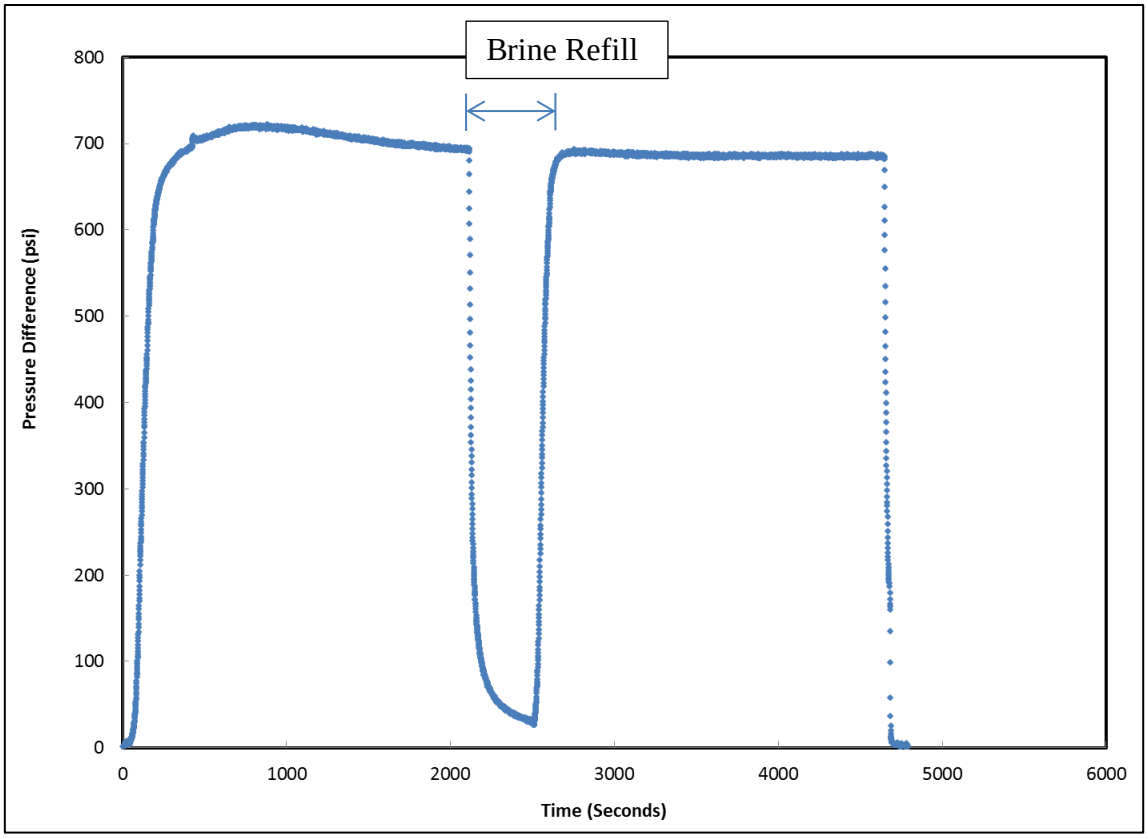

Fig. 3.7 – Permeability Test Pressure Curve

Permeability is calculated with Δp found in this test and Eq. 3.4.

3.6 Acid Preparation

The HCl acid that is used in the lab is from Macron Chemical Co., and comes standard with a concentration of 36.46% by weight. In order to achieve the needed concentration for the experiment of 15% by weight, the acid must be diluted. **Table 3.1** shows how the acid should be diluted for a total volume of 5L.

Table 3.1 – Acid Volume

	Concentration	Density (g/cm^3)
HCl from stock	36.46%	1.18
HCl for experiment	15%	1.07

Table 3.1 Continued

Density 15%	1.07	
Total Vol (mL)	Vol Acid (mL)	Vol Water (mL)
5,000	1865.290032	3134.709968

The volume of acid and water needed to get the experiment concentration:

$$V_{experiment\ acid} = \frac{C_{experiment\ acid} \cdot \rho_{experiment\ acid}}{C_{stock\ acid} \cdot \rho_{stock\ acid}} \cdot V_{total} \tag{3.6}$$

$$V_{water} = V_{total} - V_{experiment\ acid} \tag{3.7}$$

Once, the acid is prepared, it is poured into the acid accumulator, shown in **Fig. 3.8**, with Schlumberger A262 corrosion inhibitor. The corrosion inhibitor concentration used is 0.5% by volume, so each experiment that uses 5L of acid uses 25mL of A262.

Fig. 3.8 – Acid Accumulator

3.7 Pressure Differential Calculation

Prior to starting an acid jetting experiment the pressure differential across the core must be determined in order to achieve the desired initial flow rate through the core. Since L, μ, k, and A are known, Δp can found by defining q and rearranging Equation 3.4:

$$\Delta p = \frac{q \times L \times \mu}{96.13 \times k \times A} \tag{3.8}$$

3.8 Acid Jetting Procedure

1. Attach inlet holder to main body of core holder.
2. Turn core holder to vertical position with inlet on bottom

3. Insert spacer rings in core holder so that they fall inside the core holder and are flush with inlet holder
4. Insert saturated core into core holder so that it becomes flush with spacer rings
5. Attach outlet holder
6. Rotate core holder 180 degrees so that the inlet holder is now on top.
7. Attach all tube fittings
8. With both Hydraulic Oil Valves open, **Fig. 3.9**, pump the hydraulic hand pump until a steady stream of hydraulic oil is flowing out of the exit

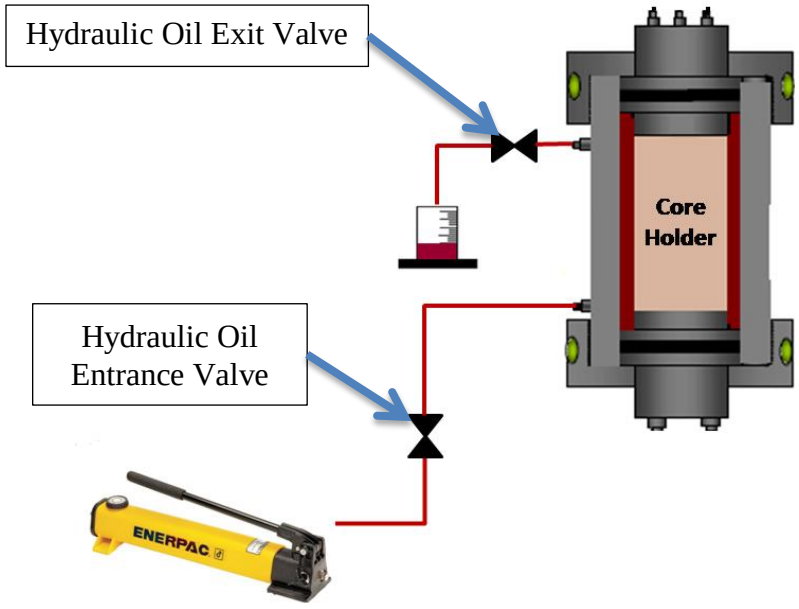

Fig. 3.9 - Hydraulic Oil Valves Schematic

9. Close the Hydraulic Oil Exit Valve
10. Add 750 psi of confining pressure with the hydraulic hand pump
11. Open Water Accumulator Valve, **Fig. 3.10**

Fig. 3.10 – Water Accumulator Valve

12. Open Waste Valve and close Acid Recycle Valve, **Fig. 3.11**

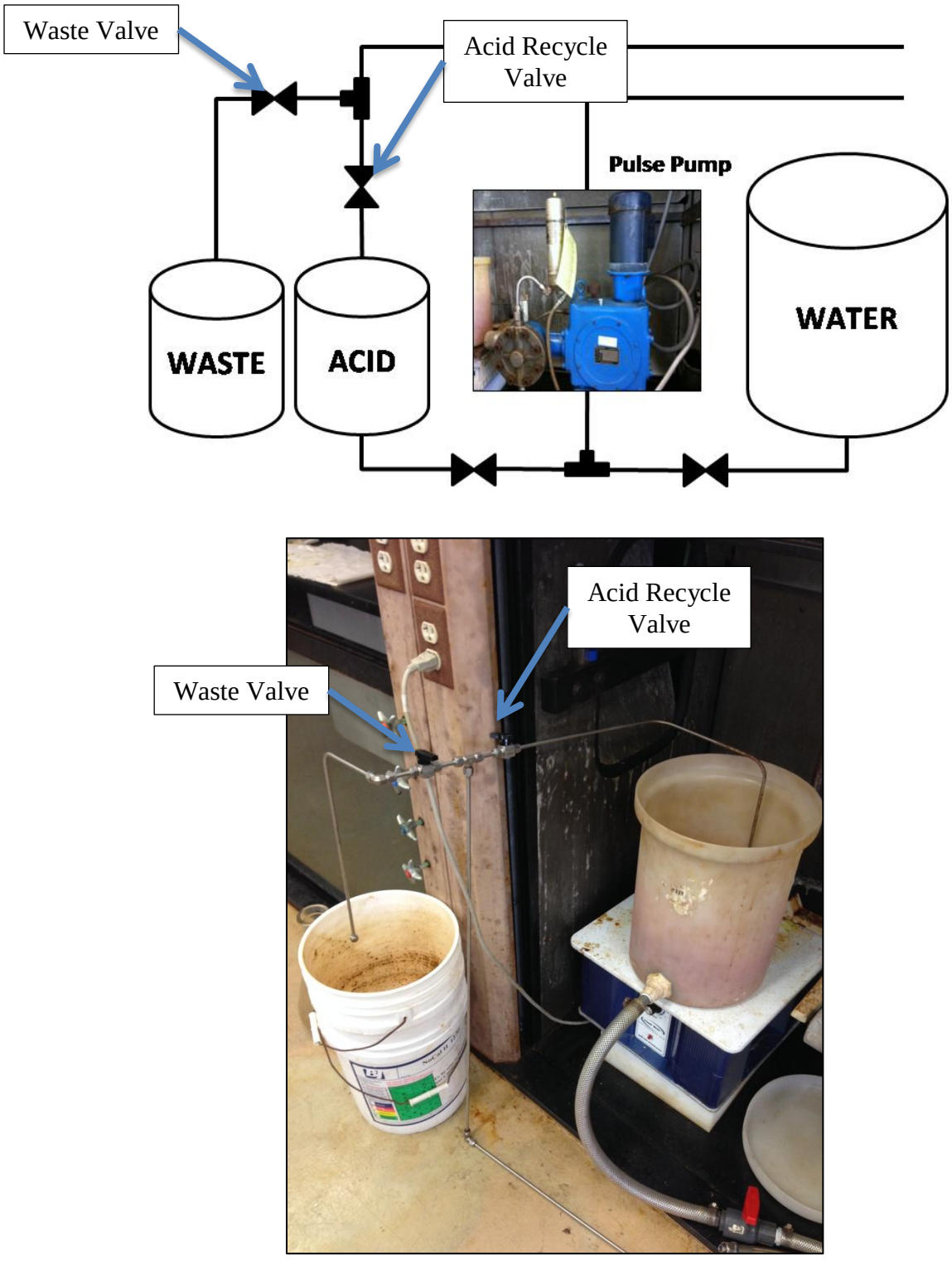

Fig. 3.11 – Waste and Recycle Valves

13. Start pump
14. Allow water to fill lines and exit with a constant flow into the waste accumulator
15. Set downstream backpressure regulator, $P_{downstream}$, to 1,000 psi, **Fig 3.12**

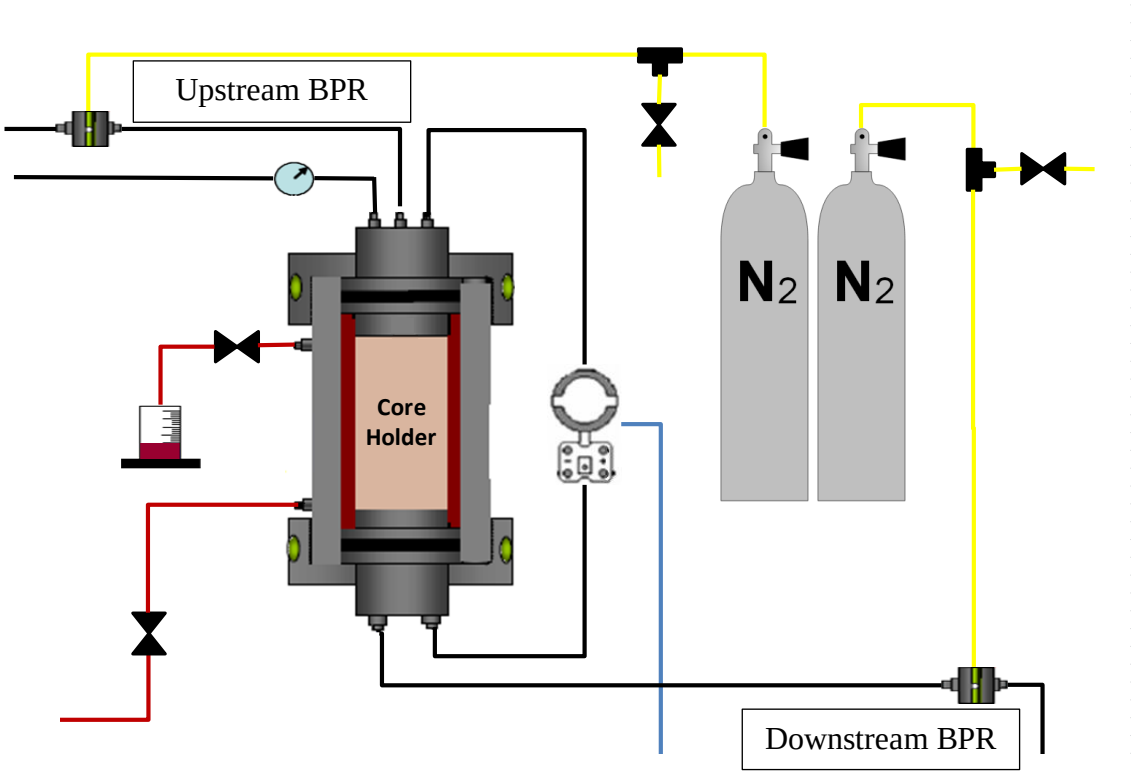

Fig. 3.12 – Backpressure Regulators

16. Set upstream backpressure regulator to 250 psi, **Fig. 3.12**
17. Increase confining pressure to 1,000 psi
18. Set upstream backpressure regulator to 500 psi
19. Allow pressure to equalize across core
20. Increase confining pressure to 1,500 psi
21. Set upstream backpressure regulator to 1,000 psi

22. Allow pressure to equalize across core
23. Set upstream backpressure regulator, $P_{upstream}$, to pressure above downstream backpressure regulator that will net the desired pressure differential across the core, i.e. if the desired pressure differential across the core, ΔP_{core}, is 100 psi, set upstream backpressure regulator to 1,100 psi

$$P_{upstream} = P_{downstream} + \Delta P_{core} \quad (3.9)$$

24. Increase confining pressure to maintain 500 psi above $P_{upstream}$
25. Start LabView program
26. Allow pressure differential across core to stabilize and observe a constant flow exiting the core
27. Simultaneously close Water Accumulator Valve and open Acid Accumulator Valve, and record time.

Fig. 3.13 – Acid Valve

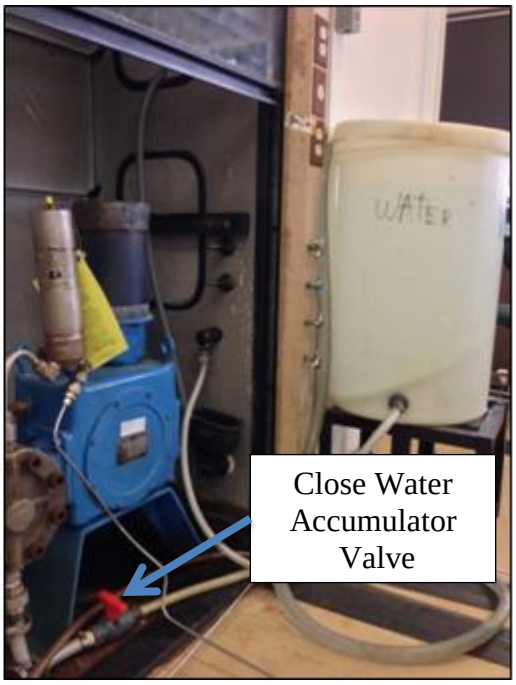

Fig. 3.14 – Water Valve

28. Hold pH tester strip under water stream at the waste exit
29. When pH tester strip indicates acid, open Acid Recycle Valve and close Waste Valve
30. Allow acid to inject for 20 minutes or until acid breaks through the core, whichever happens first
31. Close Acid Accumulator Valve, open Water Accumulator Valve and record time
32. Close upstream backpressure regulator nitrogen tank and lower upstream backpressure to 750 psi
33. Lower confining pressure to 1,250 psi
34. Lower upstream backpressure to 500 psi
35. Lower confining pressure to 1,000 psi
36. Lower upstream backpressure to 250 psi
37. Lower confining pressure to 750 psi
38. Lower upstream backpressure to 0 psi
39. Slowly release downstream backpressure to 0 psi
40. Let water flush through the system until pH of exit fluid becomes neutral
41. Stop pump
42. Slowly lower confining pressure to 0 psi
43. Disassemble core holder and remove core
44. Weigh core

3.9 Post Acid Jetting Permeability Test

For experiments where acid did not break through the core, a post experiment permeability test must be completed if a CT scanner is not available. A CT scanner will show the inside of the core revealing the exact length of the wormhole. With this test, the wormhole length can be approximated assuming 100% homogeneity of the core and 100% conductivity of the wormhole. The procedure for this test is exactly the same as the initial permeability test in **Section 3.5**. For experiments that broke through the core, a post permeability test is not needed because the length of the wormhole is known (the full length of the core). The calculation for the wormhole length, L_{WH}, is as follows:

$$L_{WH} = L - L_{eff} \tag{3.10}$$

$$L_{eff} = \frac{k_{orig} \times A \times \Delta P_{new}}{96.13 \times \mu \times q_{new}} \tag{3.11}$$

Where L is the full length of the core, k_{orig} is the original permeability found in **Section 3.5**, A is the cross sectional area of the core, Δp_{new} is the Δp found in the post permeability test in **Section 3.8**, μ is the viscosity, and q_{new} is the flow rate used in the post permeability test in **Section 3.8**.

The calculated wormhole lengths compared the CT scanner measured lengths are found in **Table 3.2**.

Table 3.2 – Calculated L_{WH} and Measured L_{WH}

Core #	Calculated L_{WH} (in)	Measured L_{WH} (in)
Core 2	7.00	9.43
Core 6	8.87	9.32
Core 10	9.01	8.58
Core 13	3.85	4.58
Core 14	7.57	7.53

4. RESULTS

4.1 Jetting Velocity

As mentioned in **Section 1.2**, jetting velocities of 100 ft/s, 150 ft/s, and 200 ft/s are used to inject acid. Since the flow rate of the fluid coming out of the pump is known, and the nozzle inner diameter is known, the fluid velocity can be calculated. The maximum pump rate is 16.3 GPH, which converts to the desired ft/s by the following: The pump is adjusted to 48.75 % capacity, which yields a flow rate of:

$$q = 16.3\frac{gal}{hr} \times .4875 = 7.946\frac{gal}{hr} \tag{4.1}$$

$$7.946\frac{gal}{hr} \times 0.133681\frac{ft^3}{gal} \times \frac{1\ hr}{3{,}660\ s} = 2.9506 \times 10^{-4}\ \frac{ft^3}{s} \tag{4.2}$$

For a nozzle ID of 0.0225 in:

$$A = \frac{\pi}{4}D^2 = \frac{\pi}{4}\left(0.0225in \cdot \frac{1ft}{12in}\right)^2 = 2.7612 \times 10^{-6} ft^2 \tag{4.3}$$

$$v = \frac{q}{A} = \frac{2.9506 \times 10^{-4}\ \frac{ft^3}{s}}{2.7612 \times 10^{-6} ft^2} = 106.86\ ft/s \tag{4.4}$$

Using equations 4.1-4.4 and a pump rate adjusted to 68.50% and 91.50%, the jetting velocity is 150.01 ft/s and 200.38 ft/s respectively.

4.2 Flux

The flux, also known as interstitial velocity, v_i, is the rate flow per unit area and is described by the following equation:

$$v_i = \frac{q}{A\phi} \tag{4.5}$$

where q is the flow rate, A is cross-sectional area and ϕ is porosity

$$A = \frac{\pi}{4}D^2 = \frac{\pi}{4}\left(4in \cdot 2.54\frac{cm}{in}\right)^2 = 81.07cm^2 \quad (4.6)$$

Since acid is injected at a constant pressure, the flux varies as acid dissolves the core. Therefore the average flux used.

4.3 Pore Volume to Breakthrough

Pore Volume to Breakthrough, or PV_{bt}, is a dimensionless number that is a ratio of the volume of acid injected to the pore volume of the core. It can be written as:

$$PV_{bt} = \frac{V_{acid}}{V_{pore}} = \frac{V_{acid}}{V_{core} \cdot \varphi} \quad (4.7)$$

The pore volume to breakthrough is a parameter to measure the efficiency of acidizing.

4.4 Acid Jetting

A typical acid jetting experiment results in the following graph, **Fig. 4.1**.

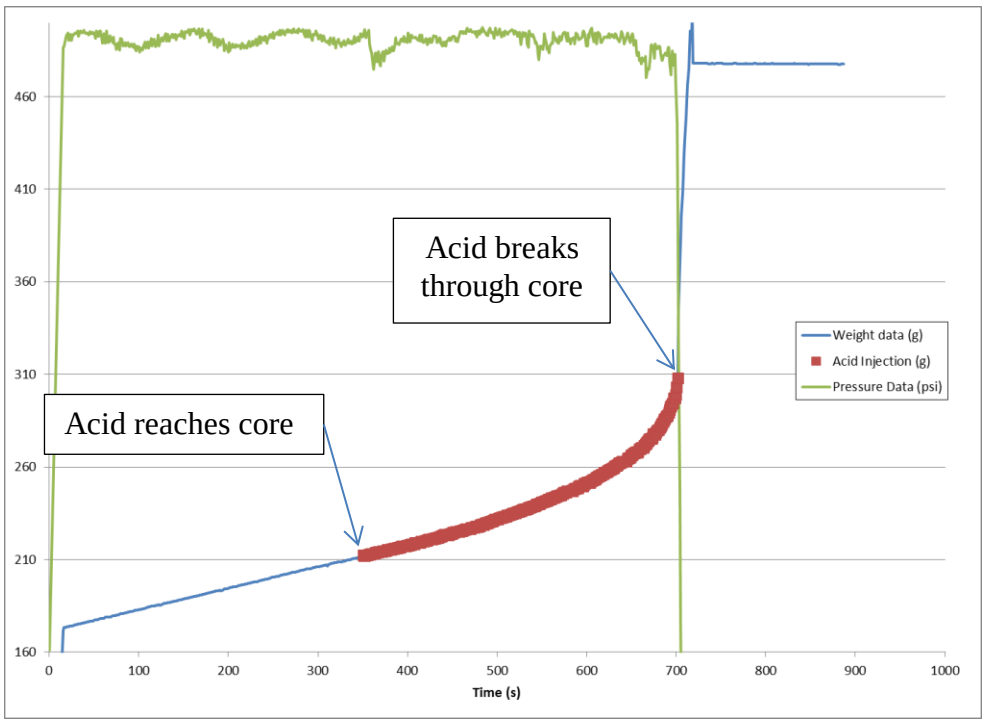

Fig. 4.1 – Acid Jetting Data Graph

The green line represents the pressure differential across the core. The blue line represents the mass read on the scale. Since the mass (grams) is known and the density of the fluid is assumed to be 1 gram/cc, the volume can be calculated.

$$V = \frac{m}{\rho} \tag{4.8}$$

So each gram can be calculated to be a milliliter. The red line represents the duration of the acid injected into the core. The time the acid takes to reach the core from the acid accumulator can be calculated. The flow rate of the pump in known and the volume of pipe can be calculated since the length and inner diameter is known. The volume of pipe is calculated to be 16.7 in^3.

Pipe 1 Length = 153 in; ID = 0.152 in

$$V_1 = \frac{\pi}{4} D^2 \times L = \frac{\pi}{4} 0.152in^2 \times 153in = 2.8in^3 \tag{4.9}$$

Pipe 2 Length = 29 in, ID = 0.75 in

$$V_2 = \frac{\pi}{4} D^2 \times L = \frac{\pi}{4} 0.75^2 \times 29 = 12.8in^3 \tag{4.10}$$

Pipe 3 Length = 9 in, ID = 0.402 in

$$V_3 = \frac{\pi}{4} D^2 \times L = \frac{\pi}{4} 0.402^2 \times 9 = 1.1in^3 \tag{4.11}$$

$$V_T = V_1 + V_2 + V_3 = 16.7in^3 = 9.66 \times 10^{-3} ft^3 \tag{4.12}$$

With the pump set at 48.75%, the flow rate from the pump is 2.9506×10^{-4} ft^3/s; therefore the time for the acid to reach the core is:

$$T = \frac{V}{q} = \frac{9.66 \times 10^{-3} ft^3}{2.9506 \times 10^{-4} \frac{ft^3}{s}} = 32.7s \tag{4.13}$$

Since the time is recorded when the acid is turned on, the exact time the acid touches the core surface is known; therefore the exact volume through the core is known. The

known volume over the known time allows for the calculation of the average rate through the core, thus the average flux can be calculated with Eq. 4.5.

As acid is jetted onto the core's surface, the surface begins to dissolve. After several minutes, a cavity inside the core begins to form as shown in **Fig. 4.2**. The force of the jet causes the acid to circulate in the cavity, which creates a bulb type shape.

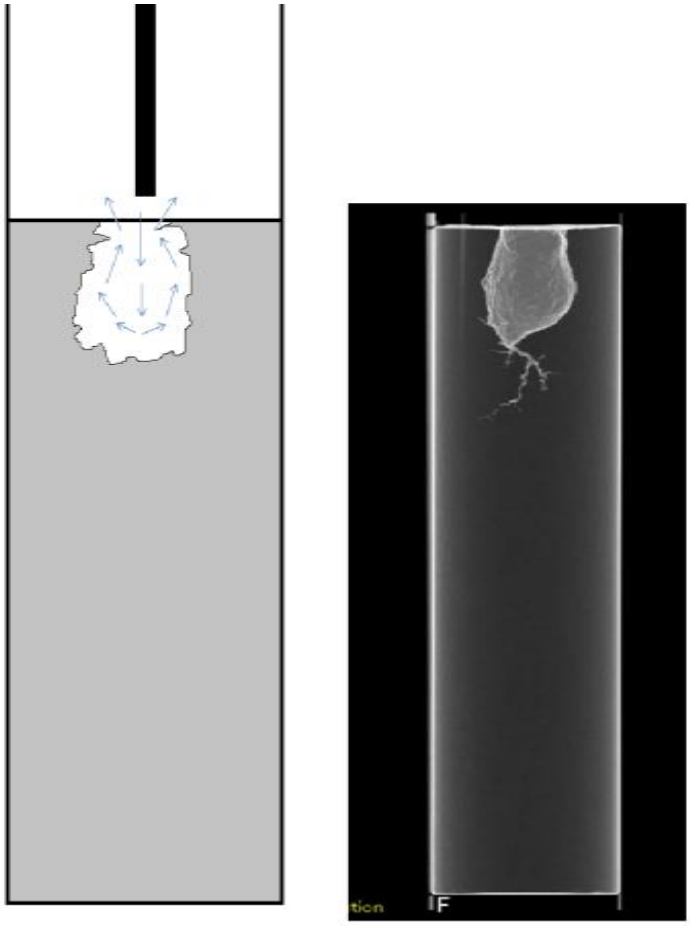

Fig. 4.2 – Acid Jet Cavity

Fig. 4.3 shows the typical results of an acid jet experiment. The bulb forms as a result of the jet, and the wormhole forms as a result of the acid flux through the core.

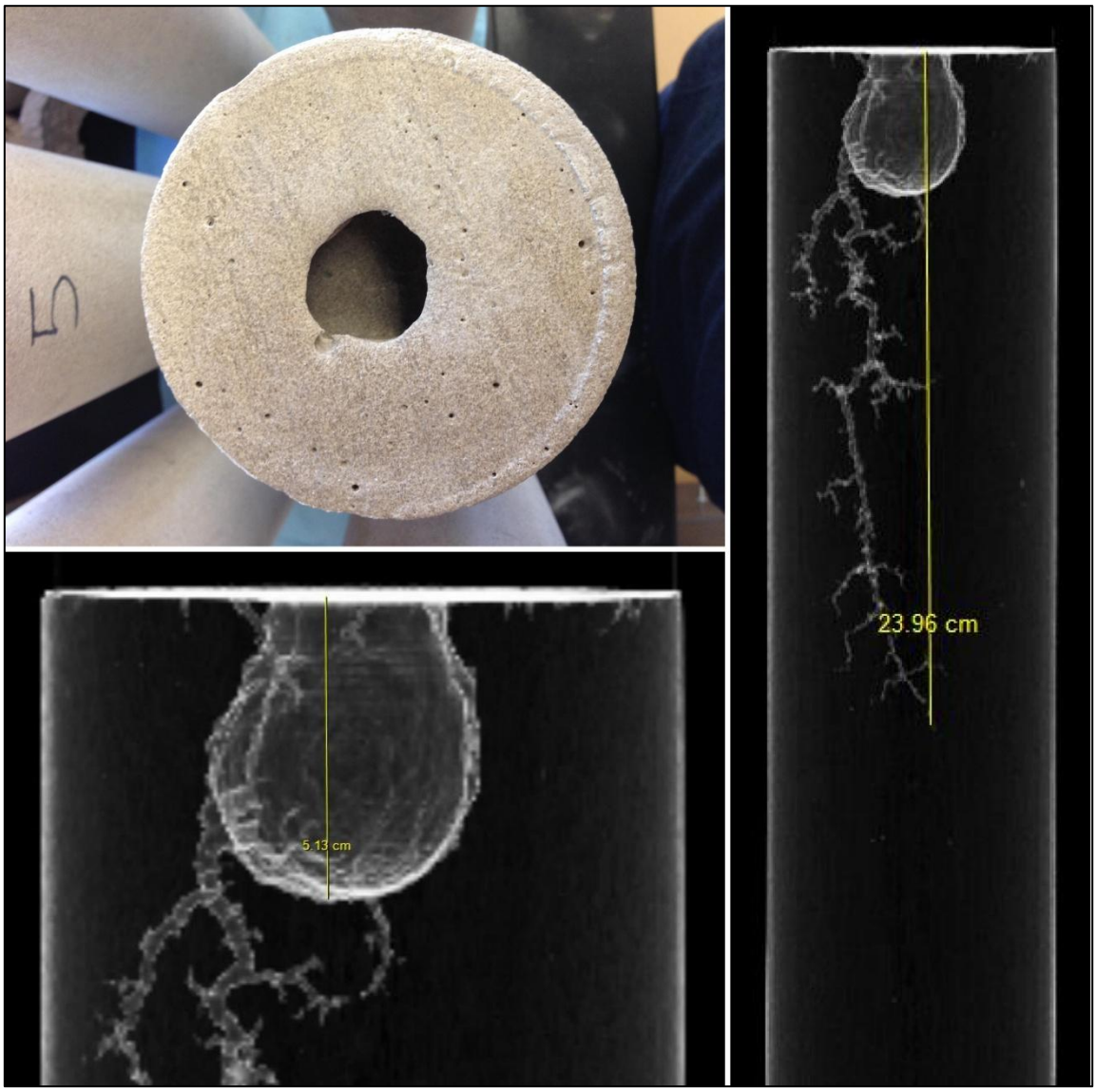

Fig. 4.3 – Bulb and Wormhole Formation during Acid Jetting

The cavity depth is compared among the three velocities in **Table. 4.1**.

Table 4.1 – Jetting Velocity vs Cavity Depth

Jetting Velocity vs Cavity Depth			
	Velocity (ft/s)	Time (s)	Cavity Depth (cm)
Core 1	106.86	451	4.79
Core 2	106.86	1239	5.13
Core 4	106.86	613	4.09
Core 10	106.86	1203	5.96
Core 17	106.86	978	4.64
Core 5	150.01	457	4.83
Core 6	150.01	1200	6.66
Core 11	150.01	351	4.18
Core 12	150.01	500	4.77
Core 13	150.01	1200	6.57
Core 7	200.38	768	6.66
Core 14	200.38	1137	6.78
Core 15	200.38	322	4.21

Fig. 4.4 shows that with increasing velocity, the cavity depth increase. Cores 3, 8, and 9 are omitted because they were tested at high temperatures or high acid concentration or both. Core 16 is omitted because the experiment failed due to equipment malfunction. As jetting time increases, the cavity depths of the 150 ft/s velocity diverge from the cavity depths of the 106 ft/s, and the cavity depths of the 200 ft/s velocity diverge from the 150 ft/s, as shown by the fitted linear regression.

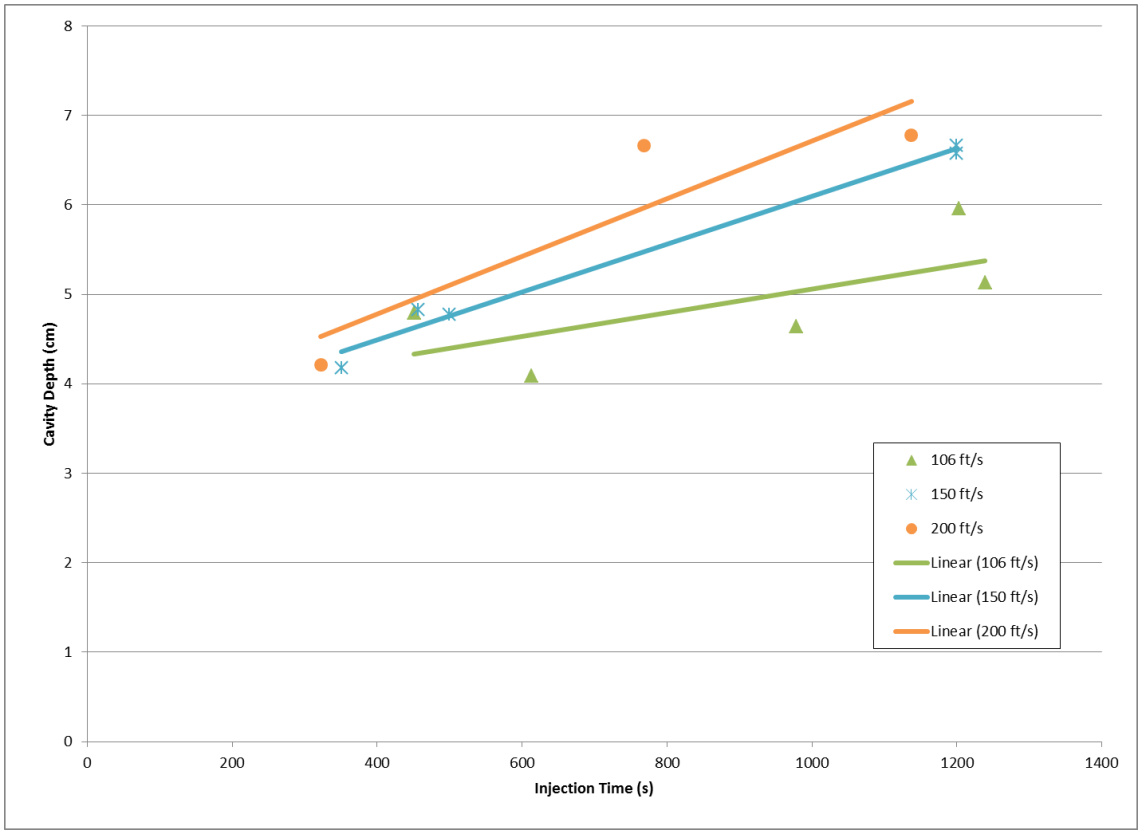

Fig. 4.4 – Cavity Depth vs Time

Prior to the acid jetting of cores 1, 5, and 7, water was jetted for up to 20 minutes. After these water injections, the surface of the cores was visually inspected to find that there was no change to the core due to water jetting.

4.5 Matrix Acidizing

In order to compare acid jetting and matrix acidizing, matrix acidizing data is obtained from experiments conducted by Jin (2013). In his study, 4" diameter by 8" length Indiana Limestone cores were injected with 15 %wt HCl acid at constant rates without a jetting nozzle. The results from the matrix acidizing experiments are shown in **Table 4.2.**

Table 4.2 – Matrix Acidizing Data

Core#	Perm(mD)	Porosity	Acid injection rate(ml/min)	Interstitial Velocity(cm/min)	PVbt
1	2.5	14.53	6.3	0.53	0.34
2	0.55	14.46	10.5	0.90	0.22
3	0.86	14.74	35.1	2.94	0.28
4	0.86	14.3	3.5	0.30	1.47

The interstitial velocity and PV_{bt}, plotted on a log-log scale in **Fig. 4.5**, are shown by the black dots.

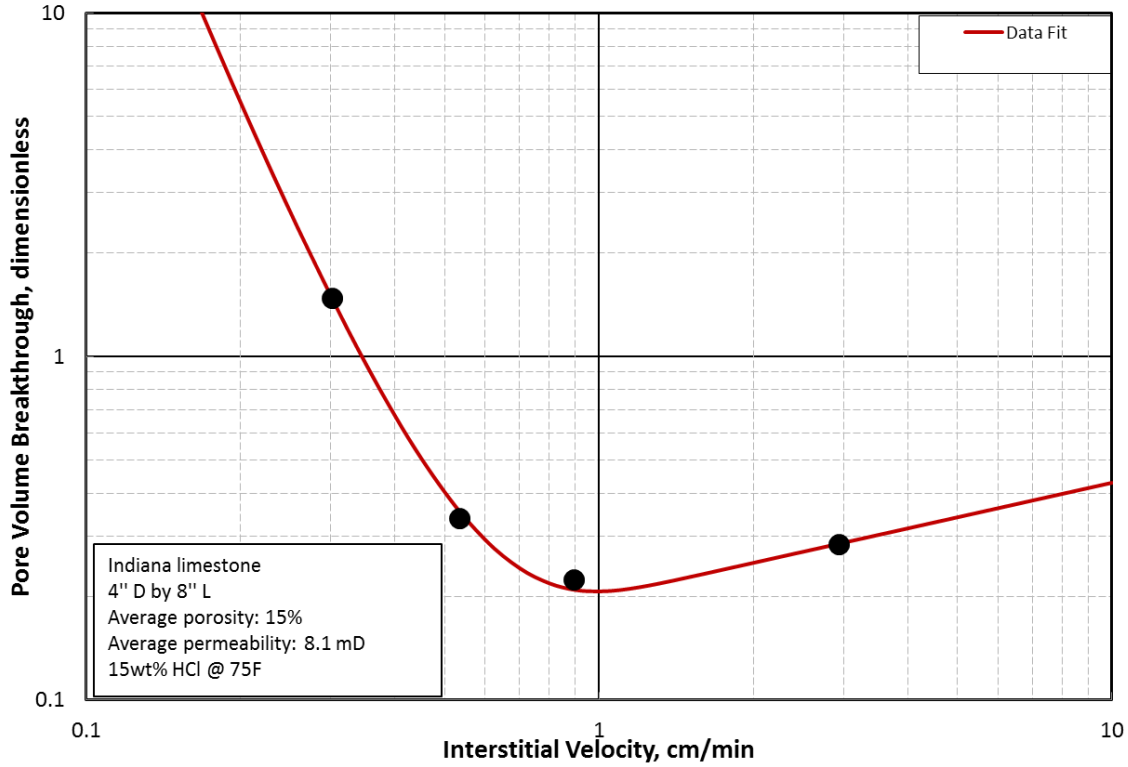

Fig. 4.5 – Matrix Wormhole Efficiency Graph

The red line on the graph represents a data fit line, which uses Buijse and Glasbergen's semiempirical model and can be described by the following equations:

$$PV_{bt} = \frac{V_i^{1/3}}{W_{eff} \cdot B(V_i)} \tag{4.14}$$

$$W_{eff} = \frac{V_{i-opt}^{1/3}}{PV_{bt-opt}} \tag{4.15}$$

$$B(V_i) = [1 - \exp(-W_B \cdot V_i^2)]^2 \tag{4.16}$$

$$W_B = \frac{4}{V_{i-opt}^2} \tag{4.17}$$

The equations above are related to PV_{bt} the following equation:

$$PV_{bt-fit} = PV_{bt-opt}\left(\frac{V_i}{V_{i-opt}}\right)^{1/3}\left\{1 - exp\left[-4\left(\frac{V_i}{V_{i-opt}}\right)^2\right]\right\}^{-2} \tag{4.18}$$

Using the PV_{bt} and V_i obtained from the experiments, the $PV_{bt\text{-}opt}$ and $V_{i\text{-}opt}$ can be solved for by using a least squares method. In this method, the sum is taken of the square difference between each experimental PV_{bt} and the corresponding $PV_{bt\text{-}fit}$, shown by Equation 4.19:

$$J = \sum_i^n \left[PV_{bt}^i - PV_{bt-fit}^i\right]^2 \tag{4.19}$$

Shown in Microsoft Excel, $V_{i\text{-}opt}$ and $PV_{bt\text{-}opt}$ are solved for with the use of the solver function by minimizing J, as shown by **Fig. 4.6** and **Fig. 4.7**.

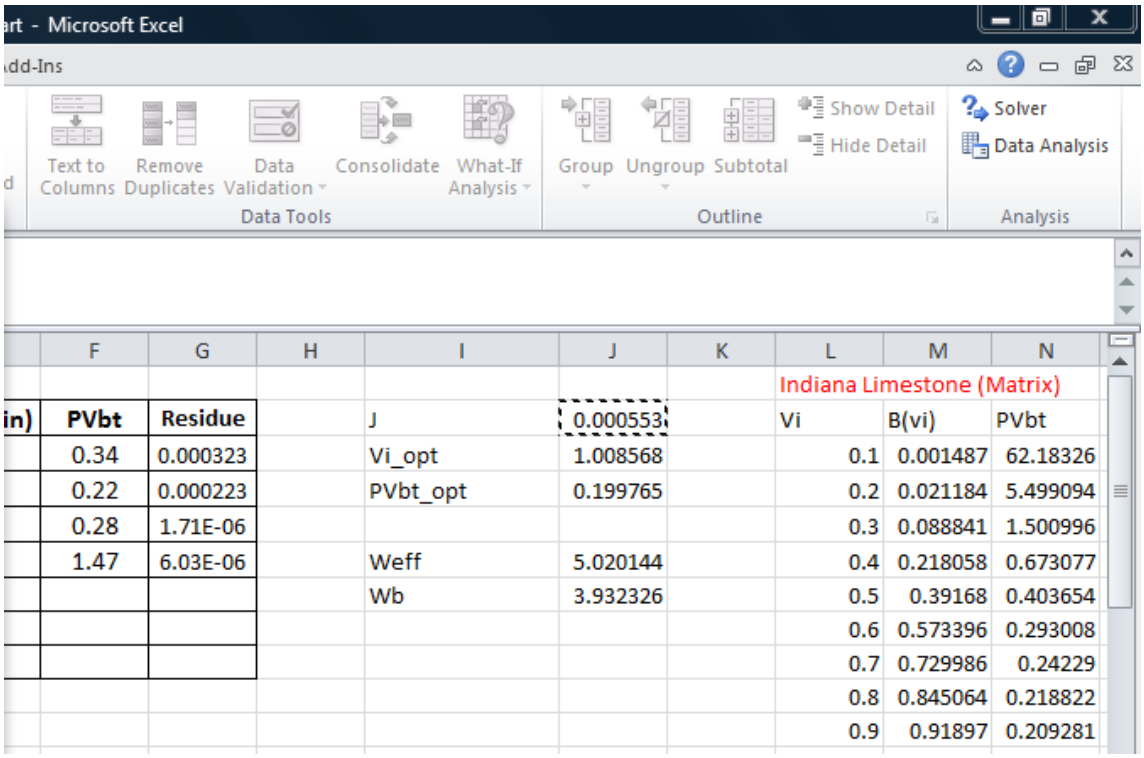

in)	PVbt	Residue		J	0.000553		Indiana Limestone (Matrix) Vi	B(vi)	PVbt
	0.34	0.000323		Vi_opt	1.008568		0.1	0.001487	62.18326
	0.22	0.000223		PVbt_opt	0.199765		0.2	0.021184	5.499094
	0.28	1.71E-06					0.3	0.088841	1.500996
	1.47	6.03E-06		Weff	5.020144		0.4	0.218058	0.673077
				Wb	3.932326		0.5	0.39168	0.403654
							0.6	0.573396	0.293008
							0.7	0.729986	0.24229
							0.8	0.845064	0.218822
							0.9	0.91897	0.209281

Fig. 4.6 – Excel Spreadsheet

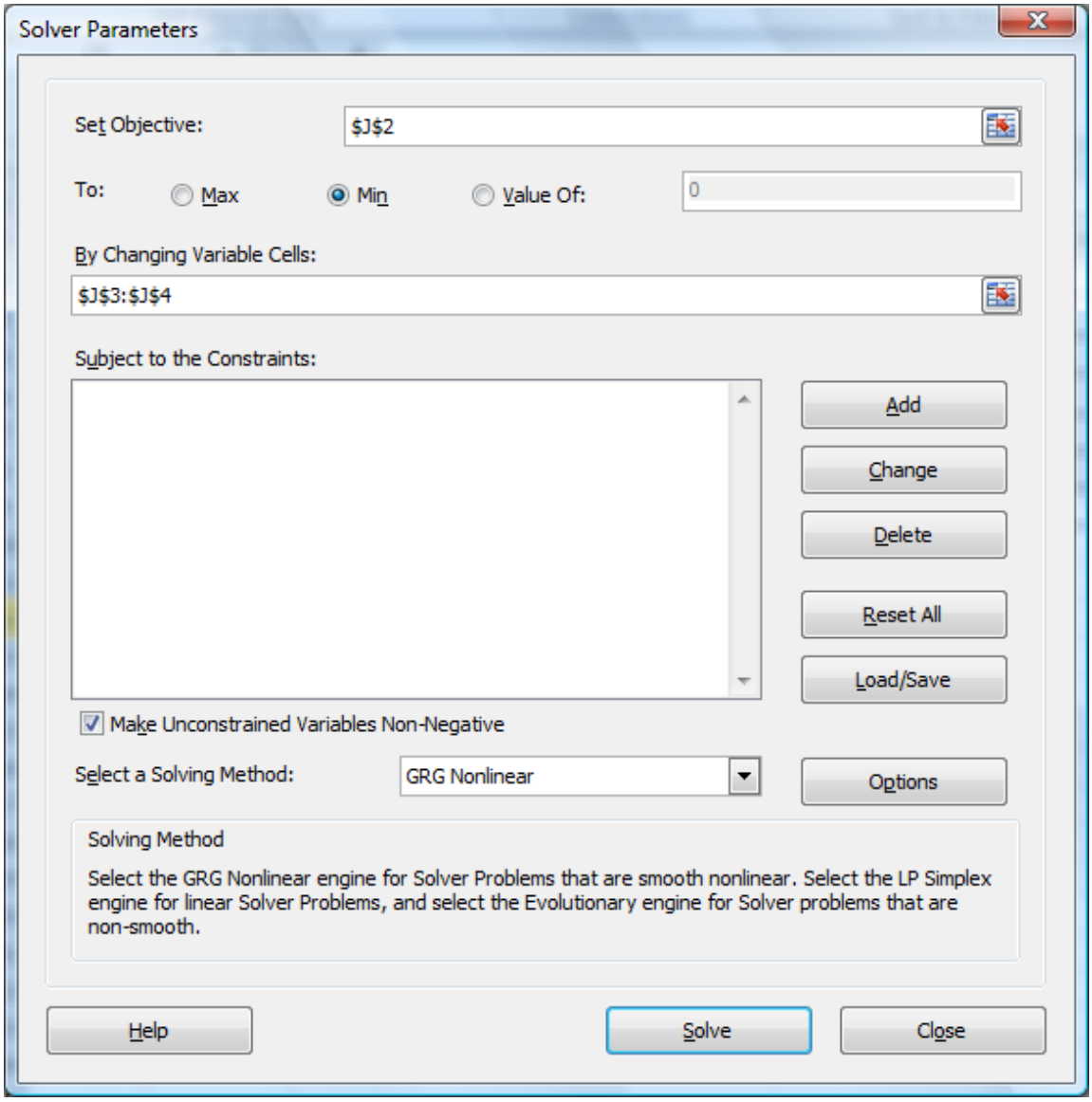

Fig. 4.7 – Excel Solver Function solving for $V_{i\text{-}opt}$ and $PV_{bt\text{-}opt}$

After the Buijse and Glasbergen model is fit to the experimental data, the $V_{i\text{-}opt}$ and $PV_{bt\text{-}opt}$ are determined to be 1.00 cm/min and 0.20 respectively.

4.6 Jet – Matrix Comparison

To properly compare acid jetting and matrix acidizing, the acid jetting experiments must be plotted like the matrix experiments on a log-log plot of PV_{bt} versus V_i. This can be an interesting achievement because the jetting experiments are completed under a constant pressure with the acid flowing through a closed loop system, where acid is circulating in the system, while the matrix experiments are completed with a constant flow rate through an open system where the volume of the acid injected is known. The reason for the jetting setup is to allow for high flow rates that create high acid velocity through the jetting nozzle but keeping a reasonable pressure drop across the core to allow for low flow rates through the core. If the high flow rates were held constant, then the pressure would exceed the pump's capabilities. Since the acid is allowed to escape the upstream backpressure regulator to circulate in the system, the volume of acid used to dissolve the rock cannot be determined through volumetric calculations.

A way to determine the amount of acid consumed in a jetting experiment is through stoichiometry. Indiana limestone is 99% calcite ($CaCO_3$) with the other 1% being quartz (Churcher 1991). The chemical reaction between $CaCO_3$ and HCl is:

$$2HCl + CaCO_3 \rightarrow CaCl_2 + CO_2 + H_2O \quad (4.20)$$

Another way to express the reaction stoichiometry is with "dissolving power." The volumetric dissolving power, χ, is the volume of mineral dissolved by a given volume of acid solution and is represented by the following equations:

$$\chi = \beta \frac{\rho_{acid\ solution}}{\rho_{mineral}} \tag{4.21}$$

$$\beta = \frac{v_{mineral} \cdot MW_{mineral}}{v_{acid} \cdot MW_{acid}} \tag{4.22}$$

According to Eq. 4.20, v_{HCl} is 2 and v_{CaCO_3} is 1. Since, MW_{HCl} is 36.5 and MW_{CaCO3} is 100.1, the reaction between 100% HCl and $CaCO_3$ is:

$$\beta_{100} = \frac{(1) \cdot (100.1)}{(2) \cdot (36.6)} = 1.37 \frac{gCaCO_3}{gHCl} \tag{4.23}$$

$$\beta_{15} = 0.15\beta_{100} = 0.21 \frac{gCaCO_3}{gHCl} \tag{4.24}$$

Since ρHCl is 1.07 g/cm^3 and ρ$CaCO_3$ is 2.71 g/cm^3, from Eq. 4.21:

$$\chi_{15} = \beta_{15} \cdot \frac{\rho_{acid\ solution}}{\rho_{mineral}} = 0.21 \frac{gCaCO_3}{gHCl} \left(\frac{1.07 \frac{g}{cm^3}}{2.71 \frac{g}{cm^3}} \right) = 0.0829 \frac{cm^3 CaCO_3}{cm^3 15\% HCl} \tag{4.25}$$

In order to use Eq. 4.25, it is assumed that 100% of the acid spent consumes 100% of the $CaCO_3$. From Eq. 4.25, the volume of acid consumed can be calculated if the volume of the Indiana limestone (assumed to be 100% $CaCO_3$) dissolved is known. For each experiment, the saturated weight of the core is measured. After each experiment the core is weighed again. The difference of the weights will give the weight of the core dissolved. If the density of the saturated core is known, then the volume of limestone dissolution can be calculated.

$$m_{core-dissolved} = m_{core-initial} - m_{core-final} \tag{4.26}$$

$$\rho_{core} = \frac{m_{core-initial}}{V_{core}} \tag{4.27}$$

$$V_{CaCO_3} = \frac{m_{core-dissolved}}{\rho_{core}} \cdot (1 - \varphi) \tag{4.28}$$

For example, Core 1 has a $m_{core\text{-}initial}$ of 8030.9g and a $m_{core\text{-}final}$ of 7876.2g with a porosity of 14.20%.

$$m_{core-dissolved} = 8030.9g - 7876.2g = 154.7g \tag{4.29}$$

$$\rho_{core} = \frac{8030.9g}{\frac{\pi}{4}\left(4in \cdot 2.54\frac{cm}{in}\right)^2 \left(16in \cdot 2.54\frac{cm}{in}\right)} = 2.437\frac{g}{ml} \tag{4.30}$$

$$V_{CaCO_3} = \frac{154.7g}{2.437\frac{g}{ml}} \cdot (1 - 0.1420) = 54.47cm^3 \tag{4.31}$$

From Eq. 4.25:

$$V_{HCl} = \frac{V_{CaCO_3}}{\chi_{15}} = \frac{54.47cm^3}{0.0829} = 657.1ml \tag{4.32}$$

From Eq. 4.7:

$$PV_{bt} = \frac{V_{acid}}{V_{pore}} = \frac{657.1ml}{\frac{\pi}{4}\left(4in \cdot 2.54\frac{cm}{in}\right)^2 \left(16in \cdot 2.54\frac{cm}{in}\right) \cdot 0.142} = 1.40 \tag{4.33}$$

The PV_{bt} and V_i for all experiments are summarized in **Table 4.3**. Cores 3, 8, and 9 are omitted because they were tested at high temperatures or high acid concentration or both. Core 16 is omitted because the experiment failed due to equipment malfunction.

Table 4.3 – Acid Jetting Experimental Results

Core #	Perm (mD)	Porosity	Acid injection rate (ml/min)	V_i (cm/min)	PV_{bt}
106.86 ft/s					
1	4.96	14.20	15.9	1.38	1.40
2	6.58	14.31	2.7	0.23	2.64
4	3.03	14.27	9.4	0.81	1.11
10	2.41	14.10	1.7	0.15	2.59
17	2.12	14.42	3.6	0.31	1.22
150.01 ft/s					
5	3.21	14.60	7.2	0.61	1.26
6	7.87	15.55	3.5	0.28	4.28
11	1.77	10.02	16.4	2.02	1.28
12	4.10	14.90	12.2	1.01	1.24
13	4.48	14.78	1.1	0.10	6.91
200.38 ft/s					
7	5.04	15.28	7.7	0.62	2.41
14	2.08	14.18	2.2	0.19	5.41
15	1.96	14.33	21.4	1.84	1.11

Acid broke through the entire core for most experiments, but cores with very low V_i did not break through because all experiments were limited to 20 minutes. During initial testing of the acid jetting apparatus, acid was injected for 28 minutes which caused the jetting cavity to grow so large that the core wall collapsed; therefore the 20 minutes time limit was applied. For the cores that did not break through, CT scans, in **Appendix B**, are used to measure the length of the wormhole. The wormhole length is used to calculate the pore volume as if the core is only as long as the wormhole. For example, Core 10 has a wormhole length of 21.80 cm (8.58 in, **Fig. B.10**), porosity is 14.10%, and acid volume of 645.2 ml. In order to calculate proper pore volume to break

$$PV_{bt} = \frac{V_{acid}}{V_{pore}} = \frac{645.2ml}{\frac{\pi}{4}\left(4in \cdot 2.54\frac{cm}{in}\right)^2 \left(8.58n \cdot 2.54\frac{cm}{in}\right) \cdot 0.141} = 2.59 \quad (4.34)$$

through, the core is simulated to be 8.58 in. instead of 16 in. Therefore the PV_{bt} for Core 10 is:

Fig. 4.8 shows each acid jet experiment's V_i and PV_{bt} plotted on a log-log graph along with the matrix acidizing data. The green triangles represent data of the 106 ft/s jet. The blue asterisk is data for the150 ft/s jet and the orange dot is data for the 200 ft/s jet. The respective colored lines are the data fitted by the Buijse-Glasbergen model.

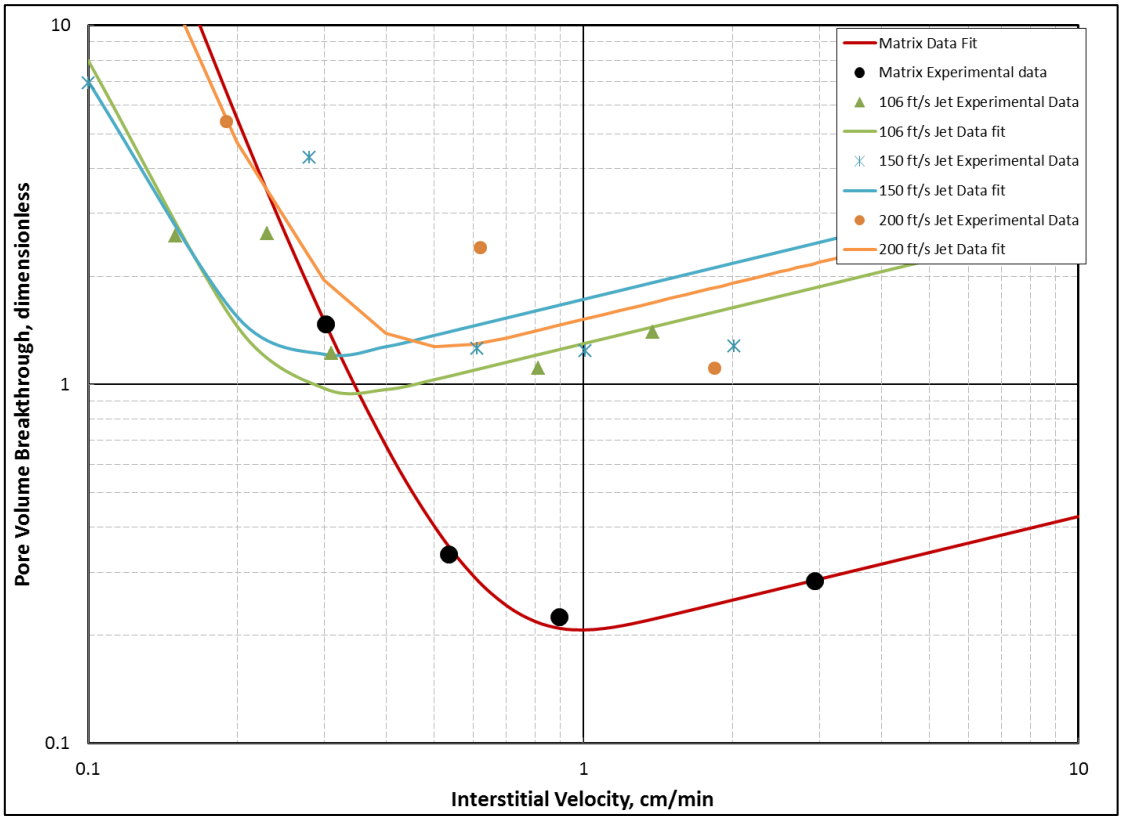

Fig. 4.8 – Acid Jet-Matrix Comparison Graph

Table 4.4 shows the calculated optimum V_i and PV_{bt} for each jetting velocity.

Table 4.4 – Acid Jet $V_{i\text{-}opt}$ and $PV_{bt\text{-}opt}$

Velocity	$V_{i\text{-}opt}$	$PV_{bt\text{-}opt}$
106 ft/s	0.35	0.91
150 ft/s	0.31	1.17
200 ft/s	0.53	1.22

Looking at the acid jetting data in Fig. 4.8 with respect to the Buijse-Glasbergen fit, the data is very scattered and does not fit well. The reason for high scatter is that the model is only meant to account for wormholing. The large cavity that is formed during the jetting process is not described by the model. Also, the Buijse-Glasbergen model uses a constant injection rate to predict wormhole propagation, whereas the injection rate for the jetting experiments is not constant. Therefore, the Buijse-Glasbergen model cannot be used to totally describe the optimum V_i and PV_{bt}, but may be valuable in

Fig. 4.9 shows a single data fit line to all acid jet experiemnts regardless of jetting velocity. This shows how the optimum V_i and PV_{bt} of jetting compares to that of matrix acidizing.

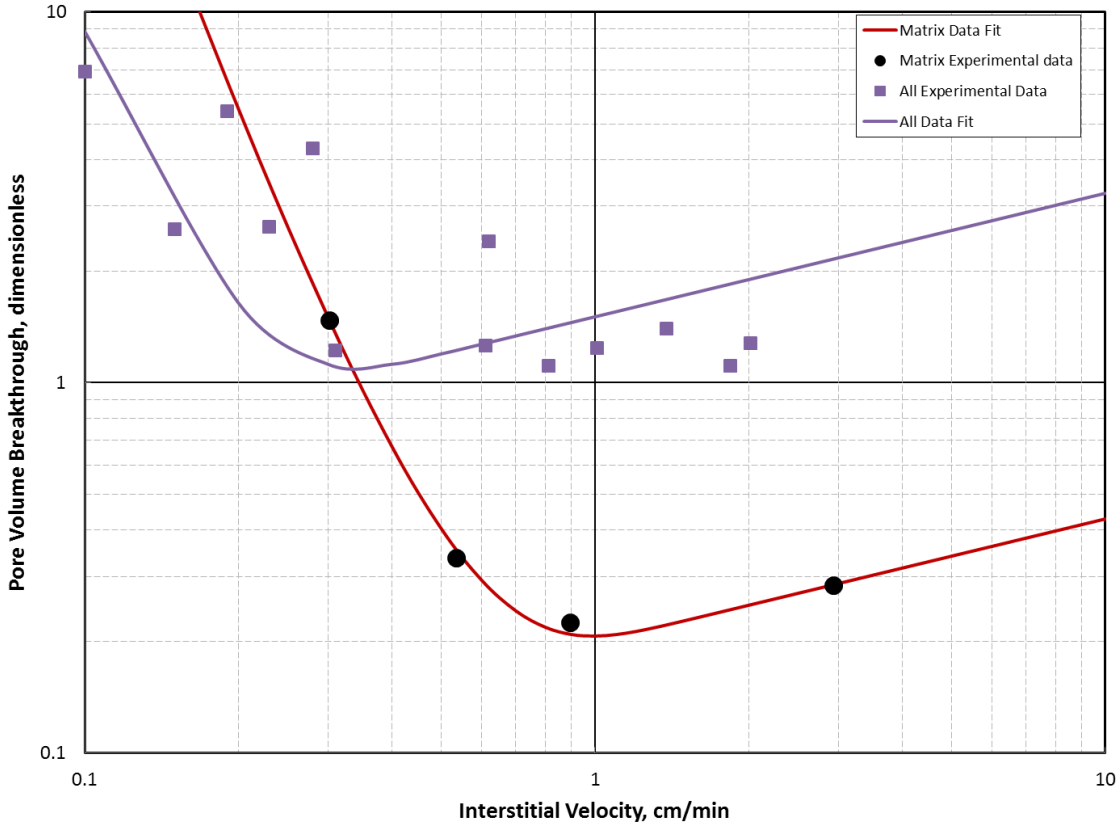

Fig. 4.9 - Acid Jet-Matrix Comparison Graph, All Data

As shown in **Table 4.5**, the optimum PV_{bt} for is jetting is five times higher than for matrix; thus jetting is inefficient in acid usage compared to matrix.

Table 4.5 – Matrix vs Jetting $V_{i\text{-}opt}$ and $PV_{bt\text{-}opt}$

Technique	$V_{i\text{-}opt}$	$PV_{bt\text{-}opt}$
Matrix	1.00	0.20
Jetting	0.35	1.06

The high PV_{bt} can be attributed to the large cavity that is formed by the jetting action. A lot of acid is used to remove this large portion of rock, but it does not penetrate very far

into the core; whereas the wormhole from the matrix experiments continues to penetrate into the core with less acid usage.

5. CONCLUSION AND RECOMMENDATIONS

- Jetting Velocity
    - High velocity acid jetting experiments are successful in creating large cavities, which may be similar to what is happening in the field.
    - According to **Fig. 4.3**, the higher the jetting velocity, the further the penetration from the wellbore. Even with no acid flux into the formation, there is potential for a negative skin factor because the jetted acid will penetrate into the formation by creating cavities. The higher penetration\ will result in a lower skin factor should be penetrations bypass the damaged zone.
- Jetting versus Matrix Acidizing
    - Dominant wormholes always form from the jetted cavity, whereas in matrix acidizing, dominant wormholes form through the path of least resistance. Therefore, acid jetting can be considered an effective mechanism for mechanically placing the acid where wormholes are needed.
    - Under the conditions for these experiments, jetting cannot be directly compared with matrix acidizing. The model used to determine optimum conditions for matrix acidizing does not provide an accurate fit to the jetting data due to the formation of the large cavities and variable flux through the core.
- Future work

- Test different acid concentrations and higher temperatures to see how these variables affect the jetting wormhole creation.
- Test other types of carbonate rock such as dolomite and Winterset limestone
- Use different lengths of cores down to 6 inches to analyze the effect of core length on the kinetic acid transport.
- Determine how to create a constant flux during acid jetting and negate the formation of the jetting cavity to more accurately compare jetting to matrix acidizing.

REFERENCES

Albertson, M.L., Dai, Y.B., Jensen, R.A. and Rouse, H. Diffusion of Submerged Jets. ASCE Paper 2409. December, 1948.

Aslam, J. and Al Salat, T. 1998. Stimulation of Horizontal Wells in Carbonate Reservoirs. Paper SPE 49493 presented at Abu Dhabi International Petroleum Exhibition and Conference, Abu Dhabi, U.A.E., 10/11/1998

Aslam, J. and Al Salat, T. 2000. High-Pressure Water Jetting: An Effective Method to Remove Drilling Damage. Paper SPE 58780 presented at SPE International Symposium on Formation Damage Control. Lafayette, Louisiana. 02/23/2000

Buijse, M.A. and Glasbergen, G. 2005. A Semiempirical Model to Calculate Wormhole Growth in Carbonate Acidizing. Paper SPE 96892 presented at the SPE Annual Technical Conference and Exhibition, Dallas, Texas, 10/09/2005

Churcher, P.L., French, P.R., Shaw, J.C. and Schramm, L.L. 1991. Rock Properties of Berea Sandstone, Baker Dolomite, and Indiana Limestone. Paper SPE 21044 presented at SPE International Symposium on Oilfield Chemistry. Anaheim, California. 02/20/91

Dresser, Inc. 2014. Mity Mite back pressure regulator. http://www.dresser.com/documents/RedQ/regulator_broc_redq_spec_reg_brochure_f.pdf. Downloaded 08 January 2014

Economides, M.J., Hill, A.D., Ehlig-Economides, C, and Zhu, D. 2013. Petroleum Production Systems, Upper Saddle River, New Jersey: Prentice Hall

Enerpac. 2014. Instruction Sheet – Hydraulic Hand Pumps. http://www.enerpac.com/sites/default/files/l1763_i_3.pdf. Downloaded 12 January 2014

Equilibar Precision Control. 2014. Equilibar back pressure regulator. http://www.equilibar.com/PDF/research-back-pressure-regulators.pdf. Downloaded 08 January 2014

Grabski, E.R. 2012. Matrix Acidizing Core Flooding Apparatus: Equipment and Procedure Description. Master of Science. Texas A&M University. College Station, Texas

Hansen, J.H. and Nederveen, N. 2002. Controlled Acid Jet (CAJ) Technique for Effective Single Operation Stimulation of 14,000+ ft Long Reservoir Sections.

Paper SPE 78318 presented at the 13th European Petroleum Conference, Aberdeen, Scotland, U.K. 10/29/2002

Hoefner, M.L., and Fogler, H.S. Fluid-Velocity and Reaction-Rate Effects during Carbonate Acidizing: Application of Network Model, SPEPE, 56-62. February 1989.

Jin, Xiao. 2013, Experimental Investigation for the Effects of the Core Geometry on the Optimum Acid Flux in Carbonate Acidizing. Master of Science. Texas A&M University. College Station, Texas

Mikhailov, M., Zhu, D. and Hill, A. D. 2008. An Experimental Investigation of Drilling-Fluid Filter-Cake Removal by Acid Jetting. Paper SPE 112373 presented ath SPE International Symposium and Exhibition on Formation Damage Control. Lafayette, Louisiana. 02/13/2008

Pekarek, J. L., Lowe, D. K. and Huitt, J. L. 1963. Hydraulic Jetting – Some Theoretical and Experimental Results. Paper SPE 421.

Ritchie, B., Abbasy, I., Pitts, M., White, B. and Rushdun Jaafar, M. 2008. Challenges in Completing Long Horizontal Wells Selectively. Paper SPE 116541 presented at SPE Asia Pacific Oil and Gas Conference and Exhibition, Perth, Australia. 10/20/2008

Scope Production Developments. 2014. Spincat http://www.scopeproduction.com/spincat.php. Downloaded 08 January 2014

Teikoku USA Inc Chempump. 2014. Chem/Meter 800 Series http://www.chempump.com/images/technical_literature/chem_meter/brochures/800series-02.pdf. Downloaded 08 January 2014

Wang, Y., Hill, A.D., and Schechter, R.S. 1993. The Optimum Injection Rate for Matrix Acidizing of Carbonate Formations. Paper SPE 26578 presented at the SPE Annual technical Conference and Exhibition, Houston, Texas, 10/03/1993

Zhang, Y. 2009. Experimental Study of Filter Cake Cleanup by Acid/Water Jetting. Master of Science. Texas A&M University. College Station, Texas

APPENDIX A

A.1 LabView

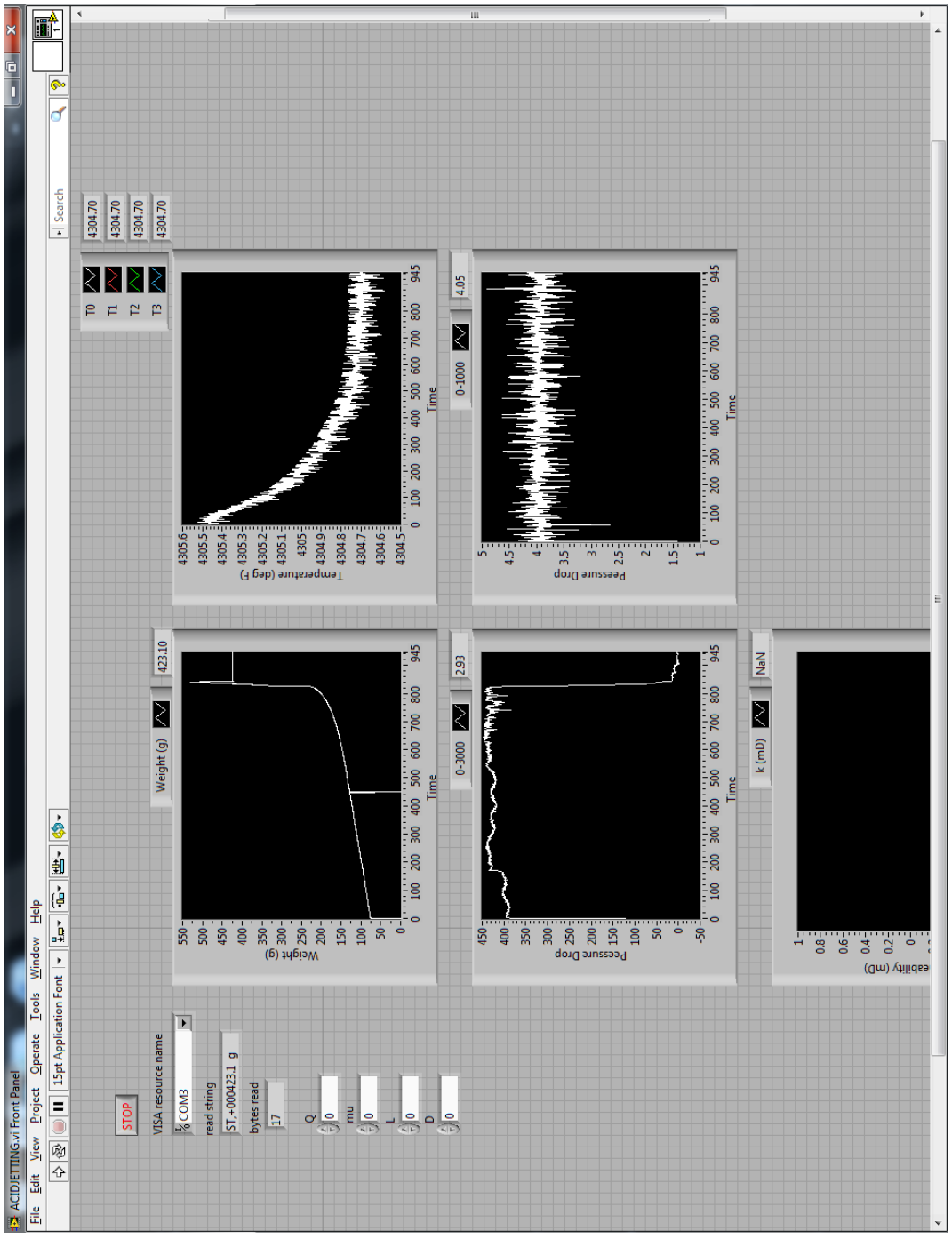

Fig. A.1 – LabView Front Panel

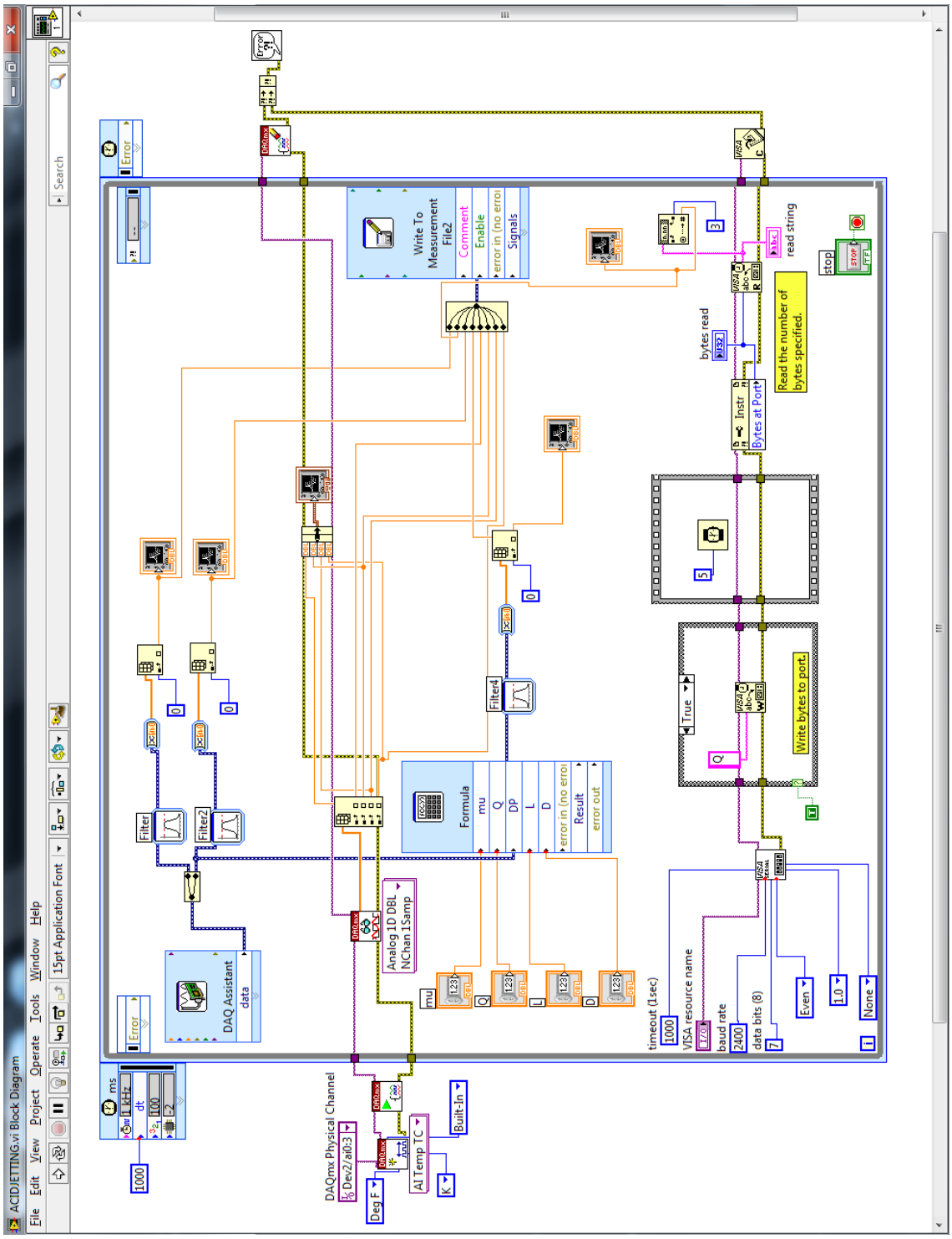

Fig. A.2 – LabView Block Diagram

APPENDIX B

B.1 Core Pictures/CT Scans

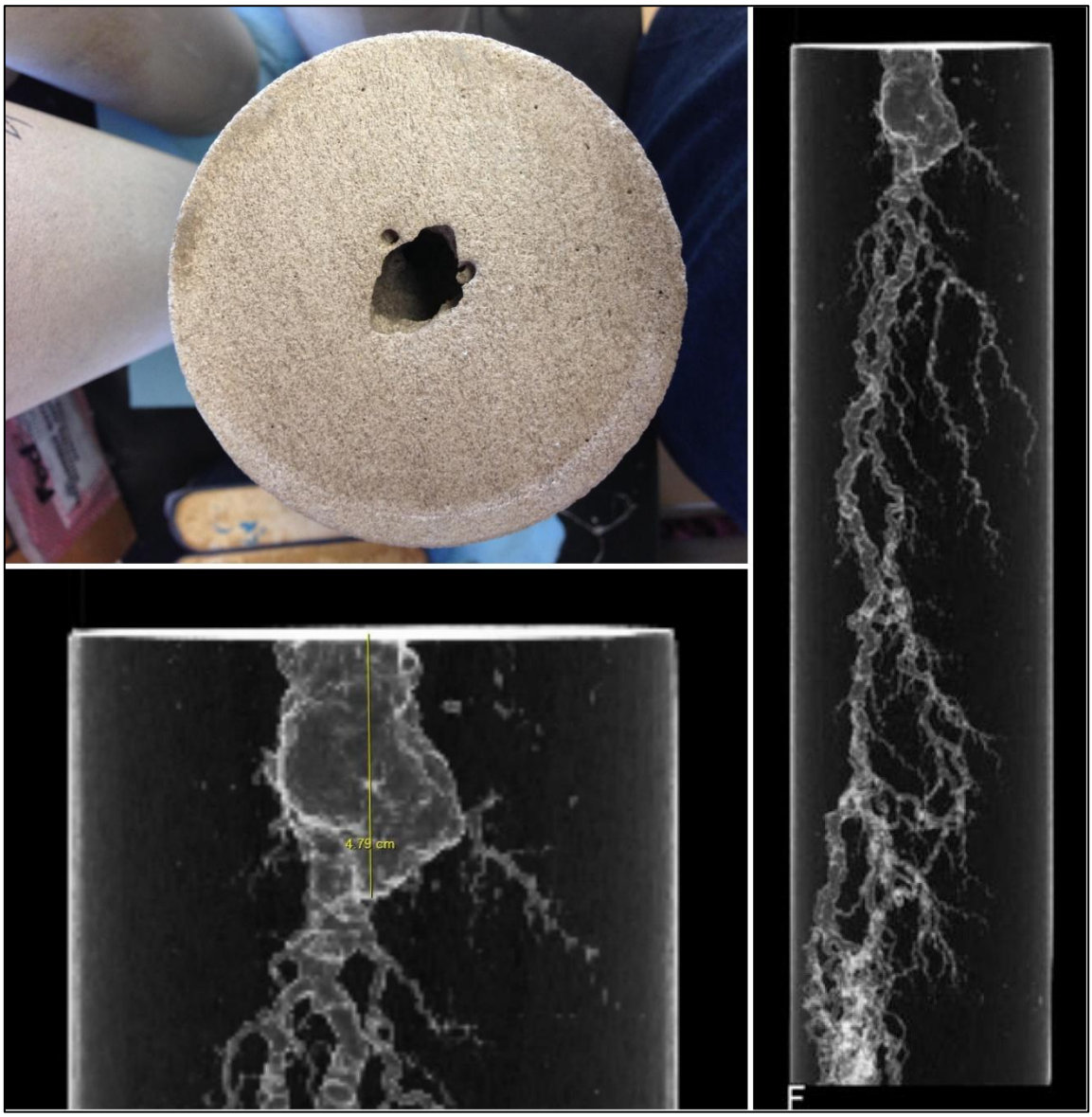

Fig. B.1 – Core 1

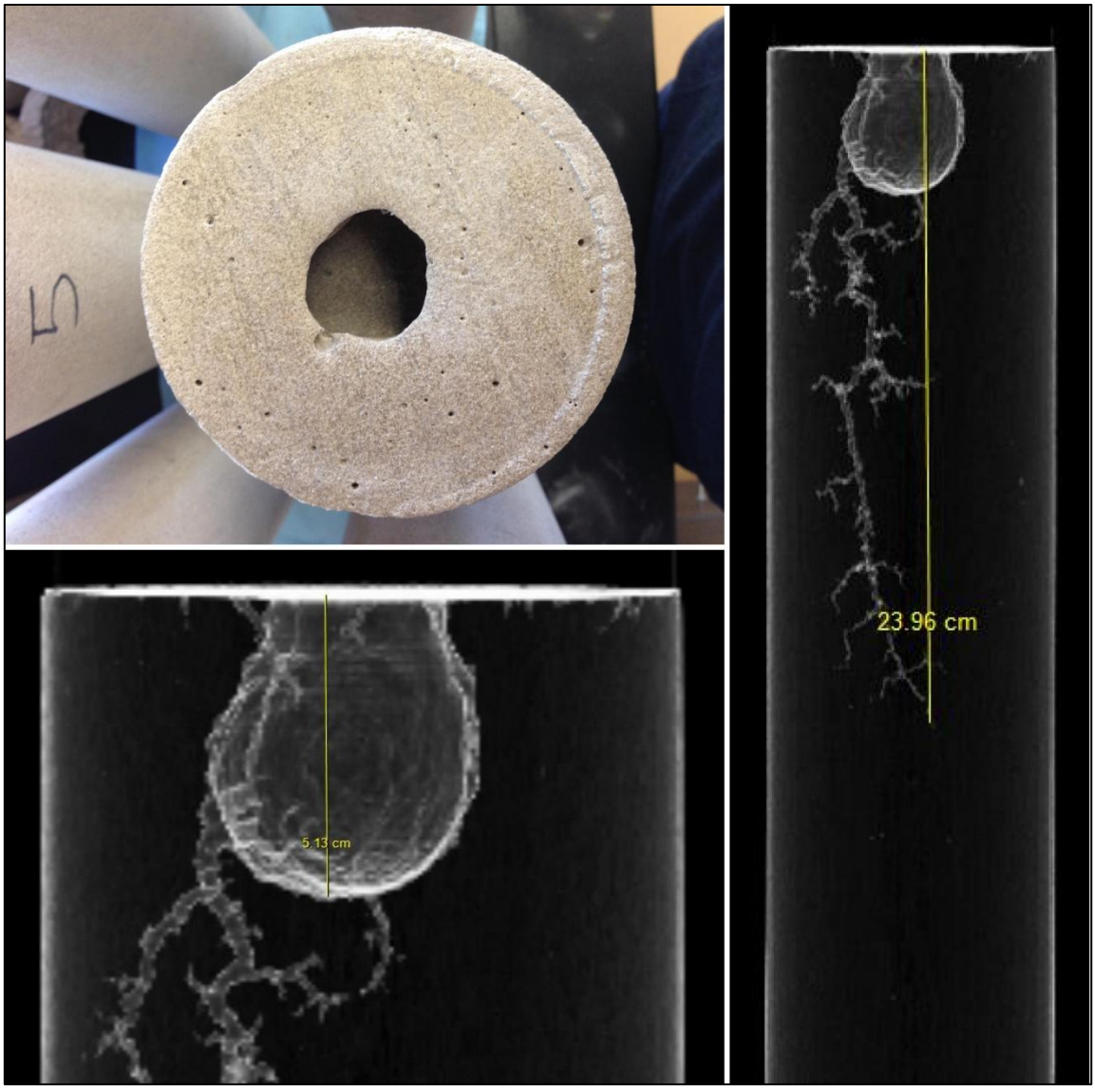

Fig. B.2 – Core 2

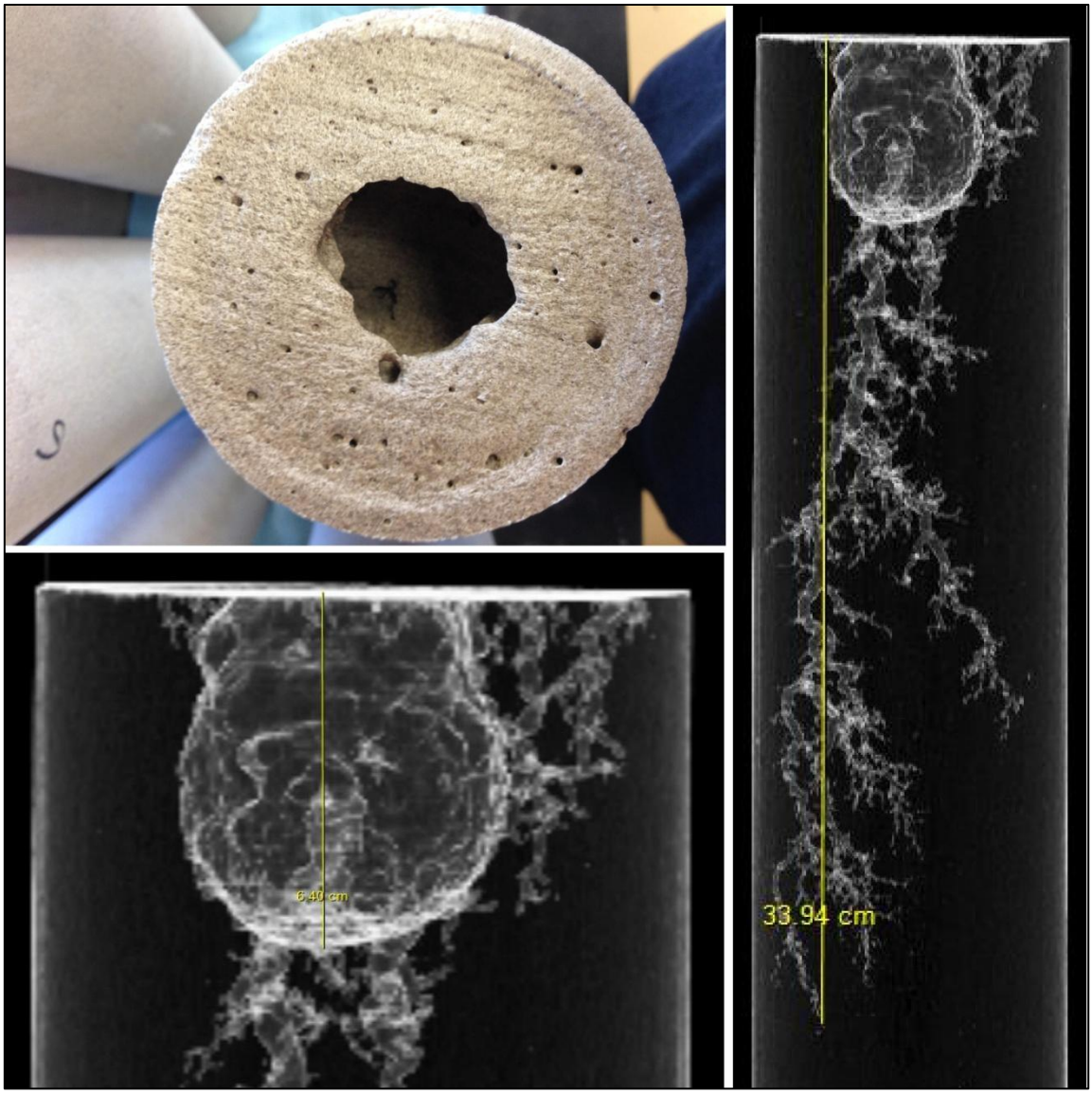

Fig. B.3 – Core 3 (180 °F)

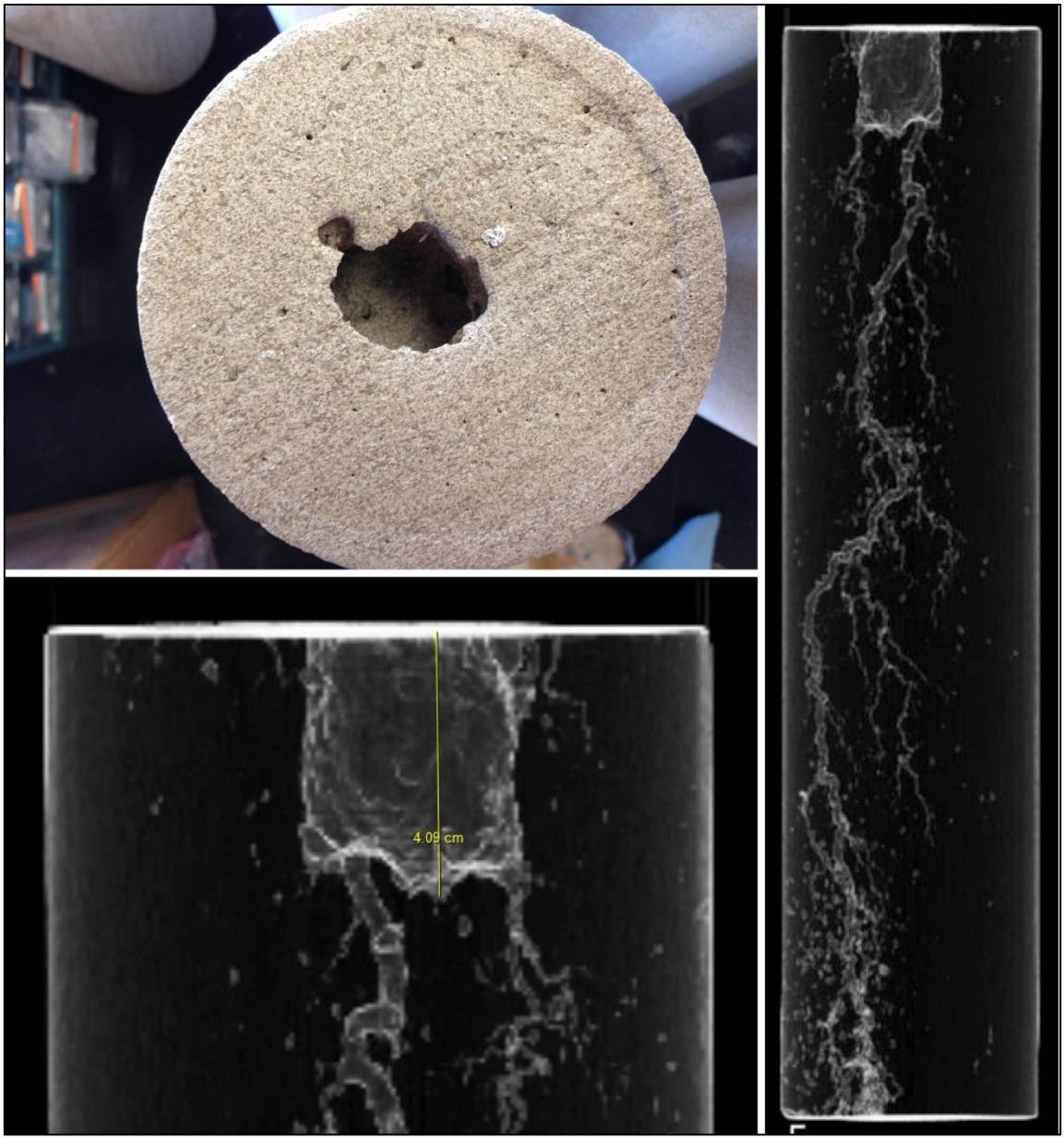

Fig. B.4 – Core 4

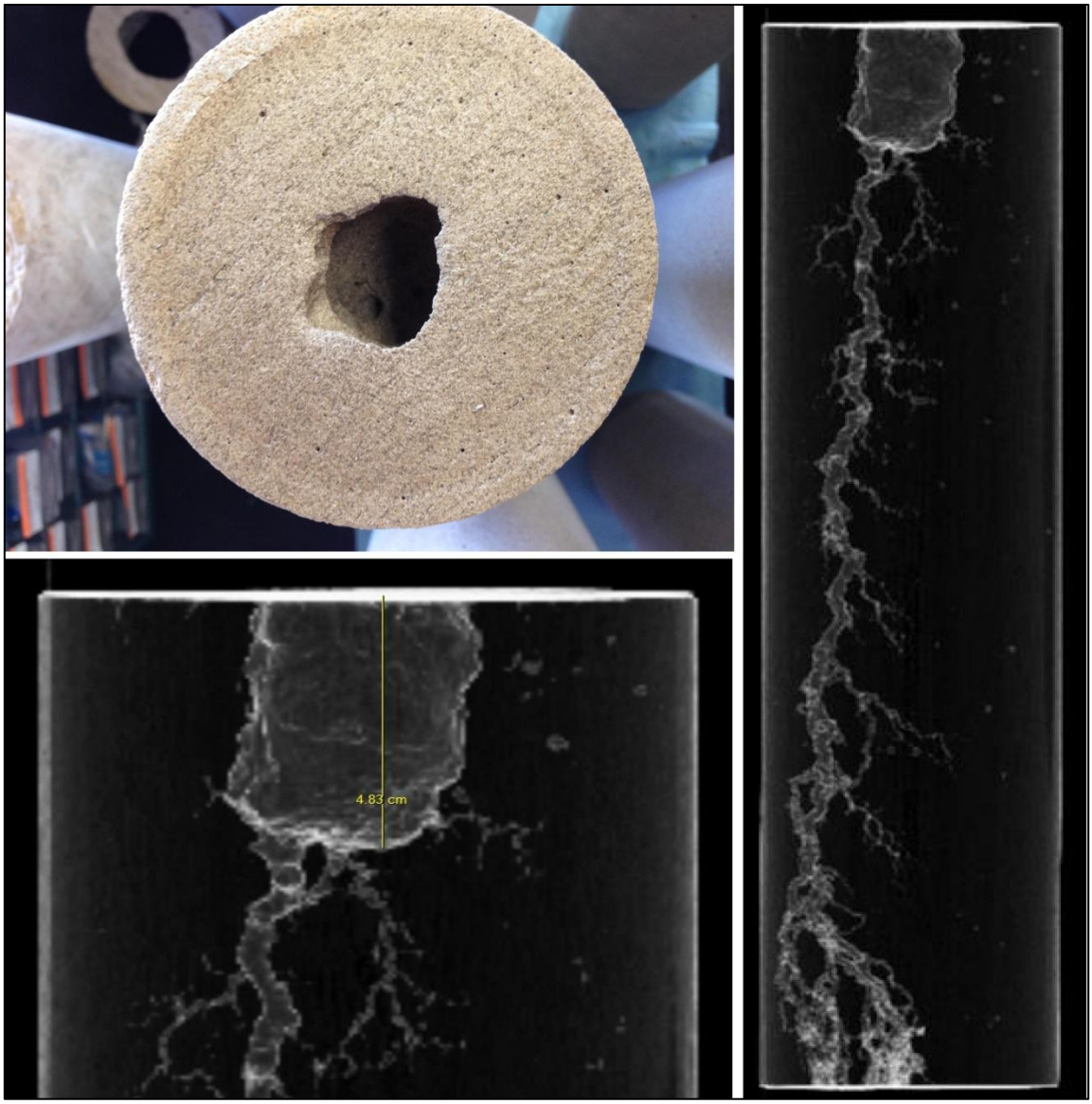

Fig. B.5 – Core 5

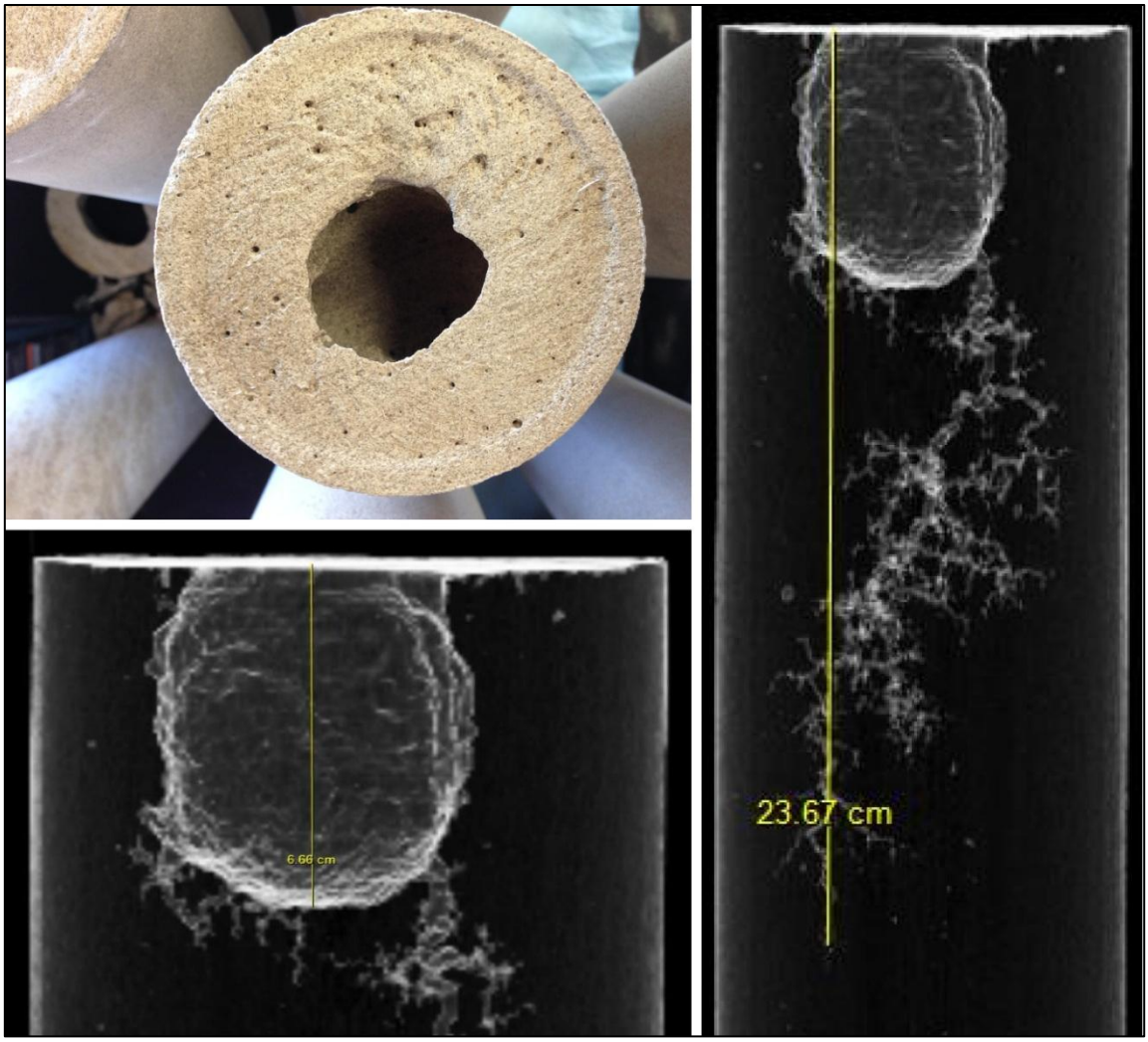

Fig. B.6 – Core 6

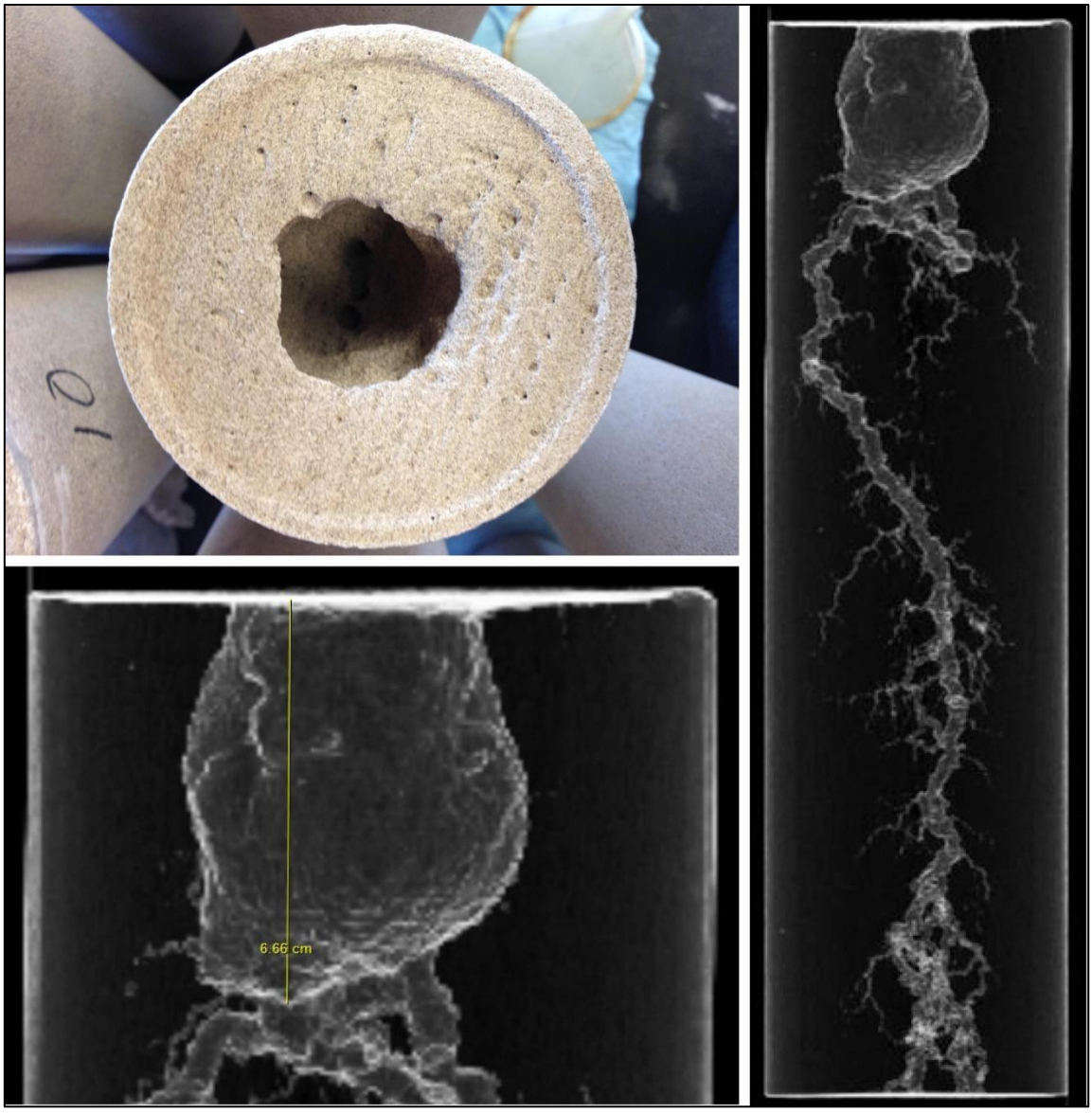

Fig. B.7 – Core 7

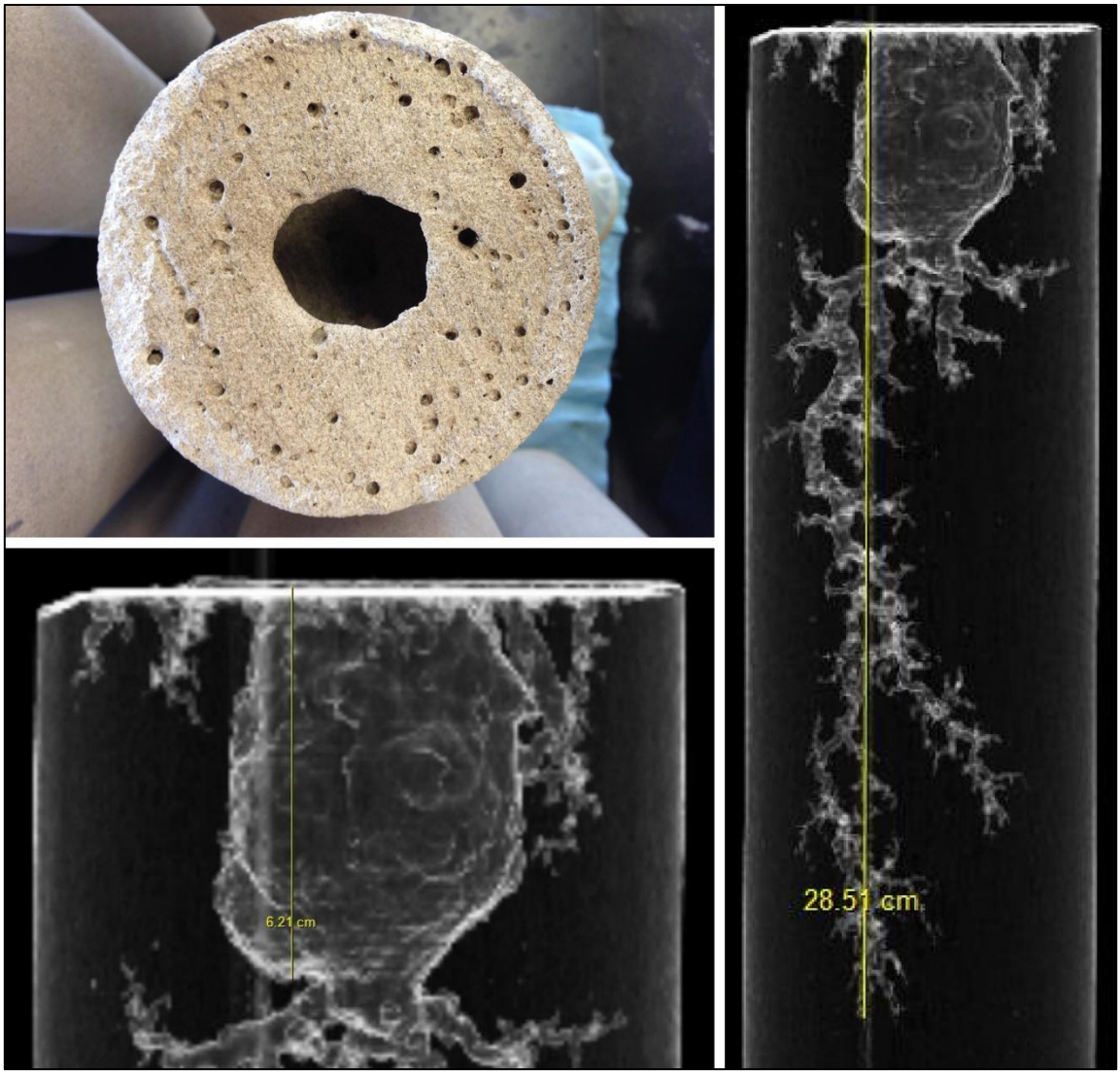

Fig. B.8 – Core 8 (180 °F)

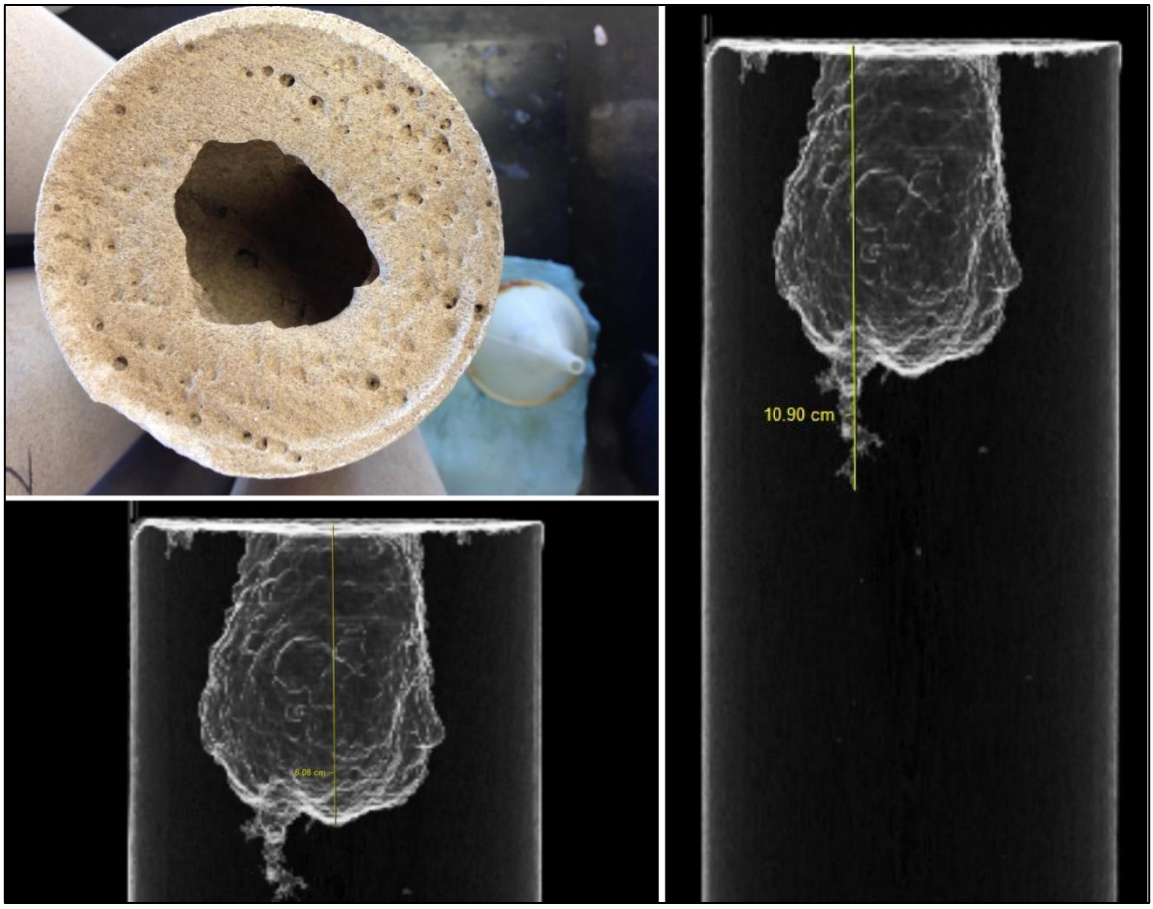

Fig. B.9 – Core 9 (180 °F & 28%wt HCL)

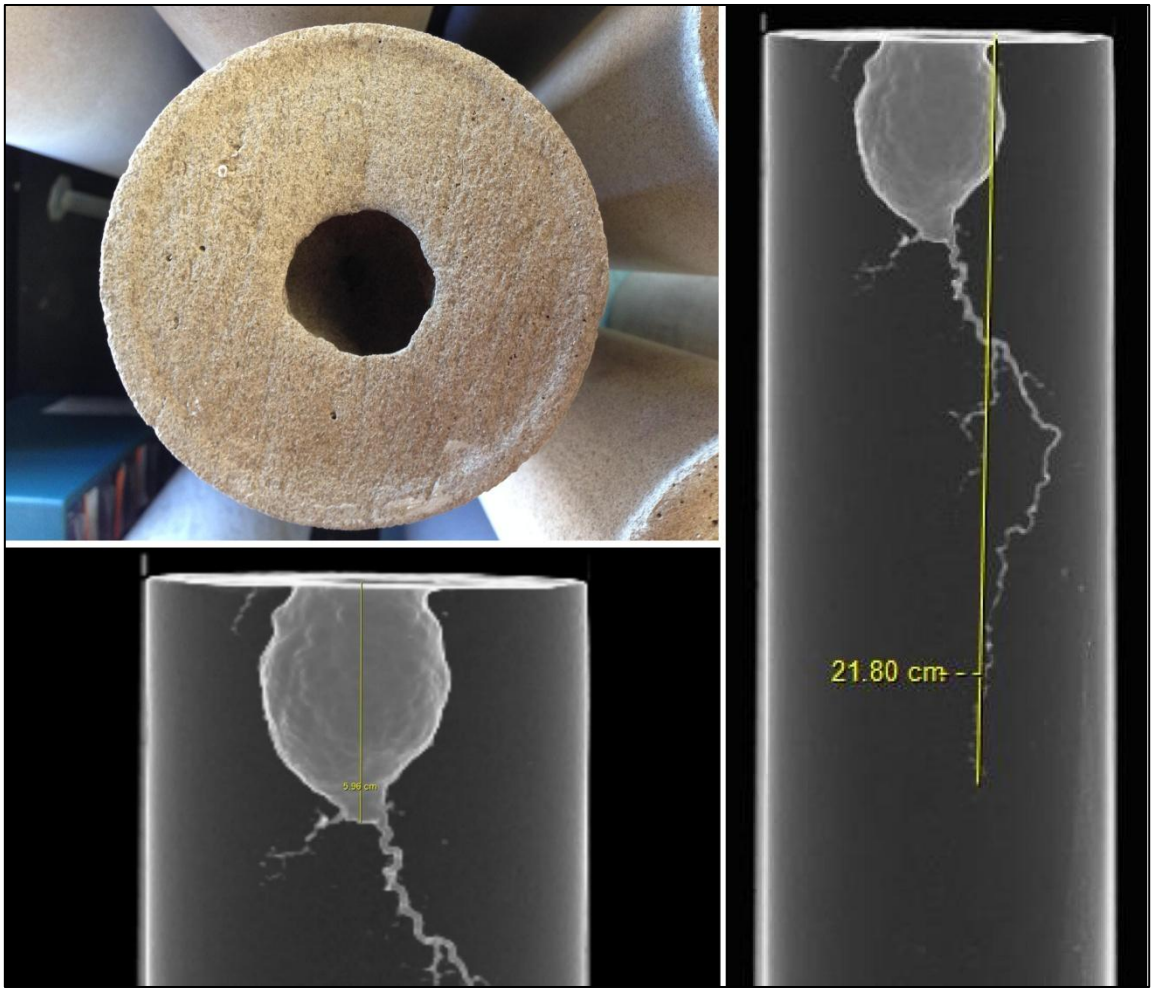

Fig. B.10 – Core 10

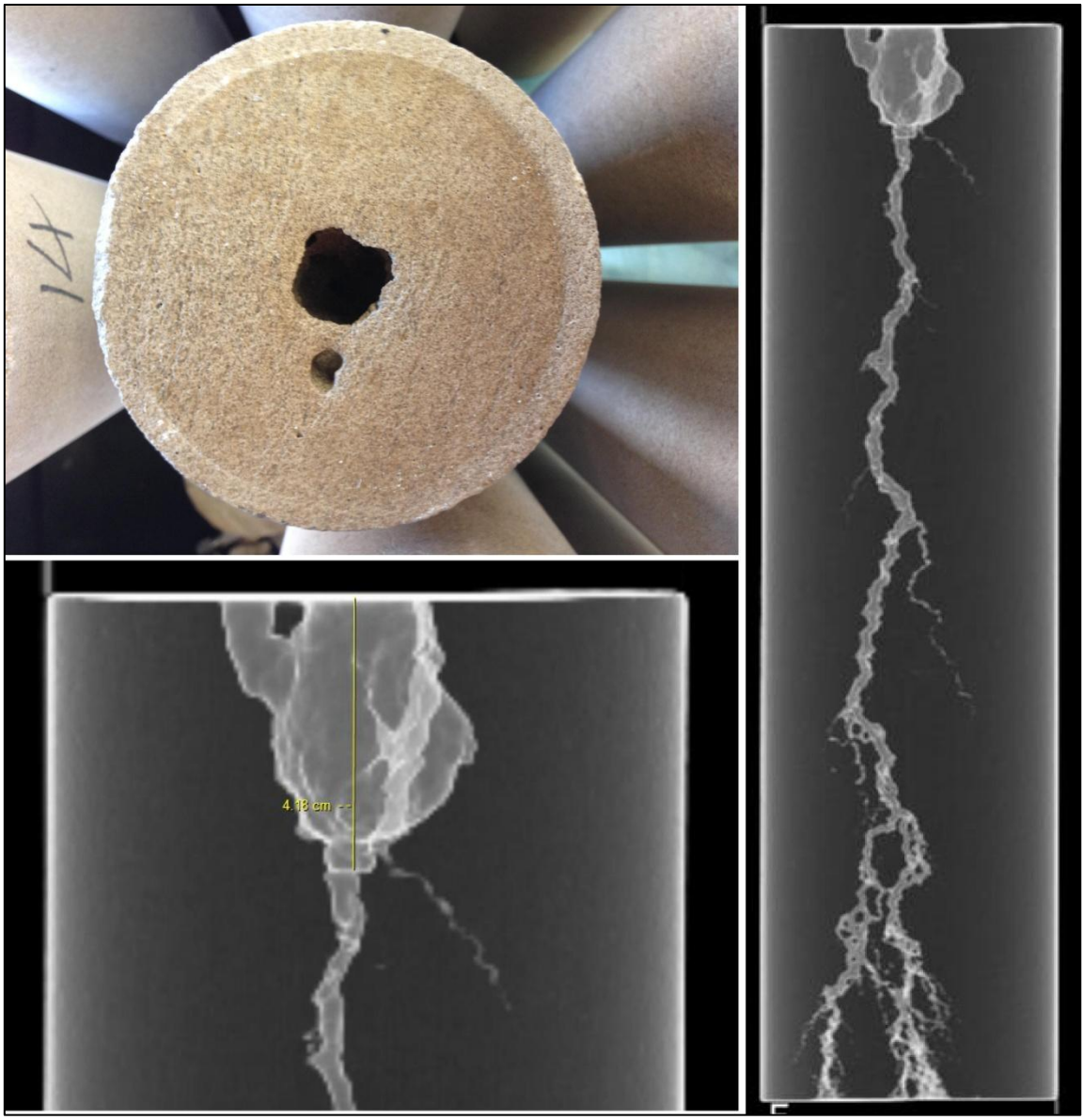

Fig. B.11 – Core 11

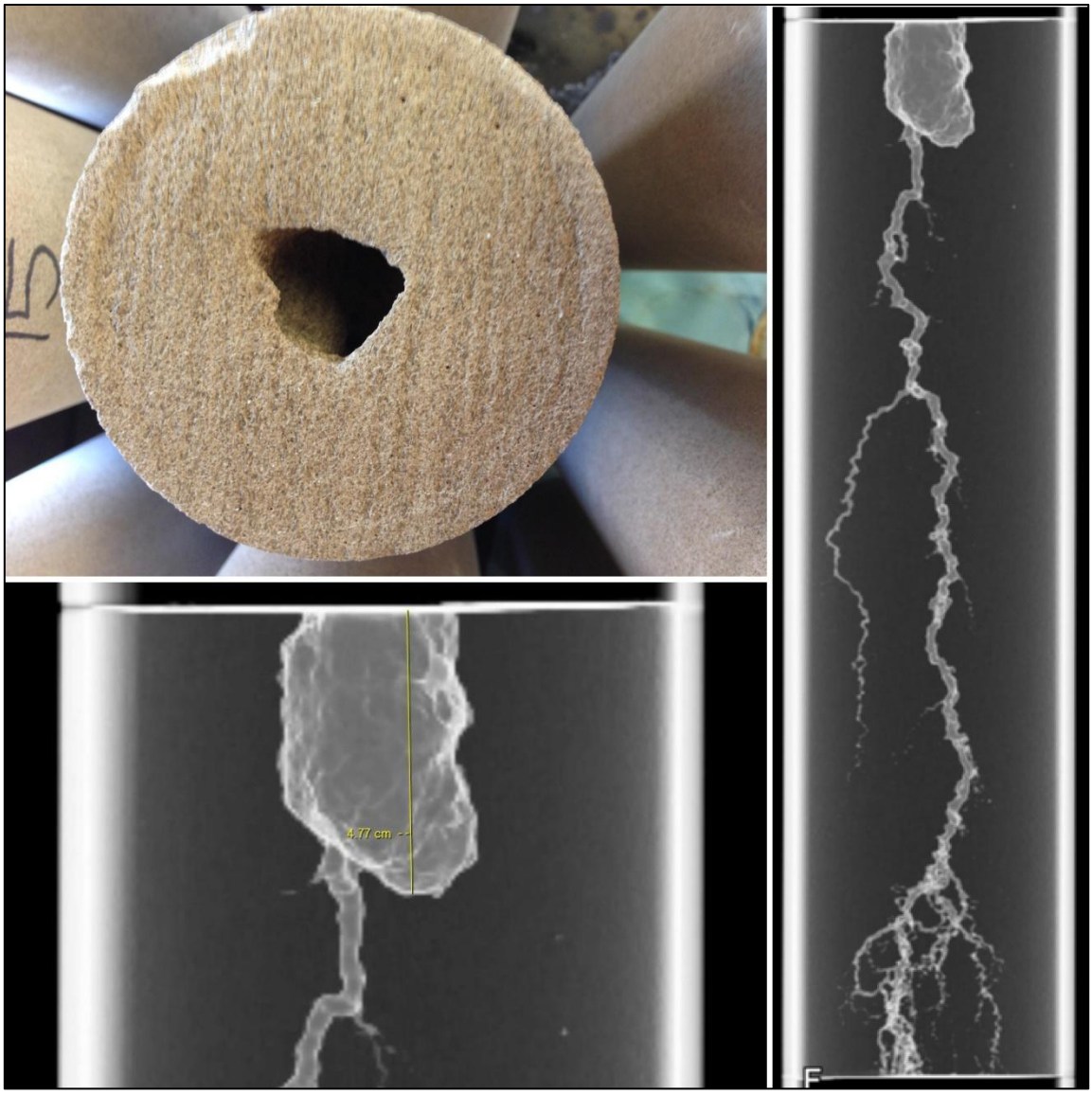

Fig. B.12 – Core 12

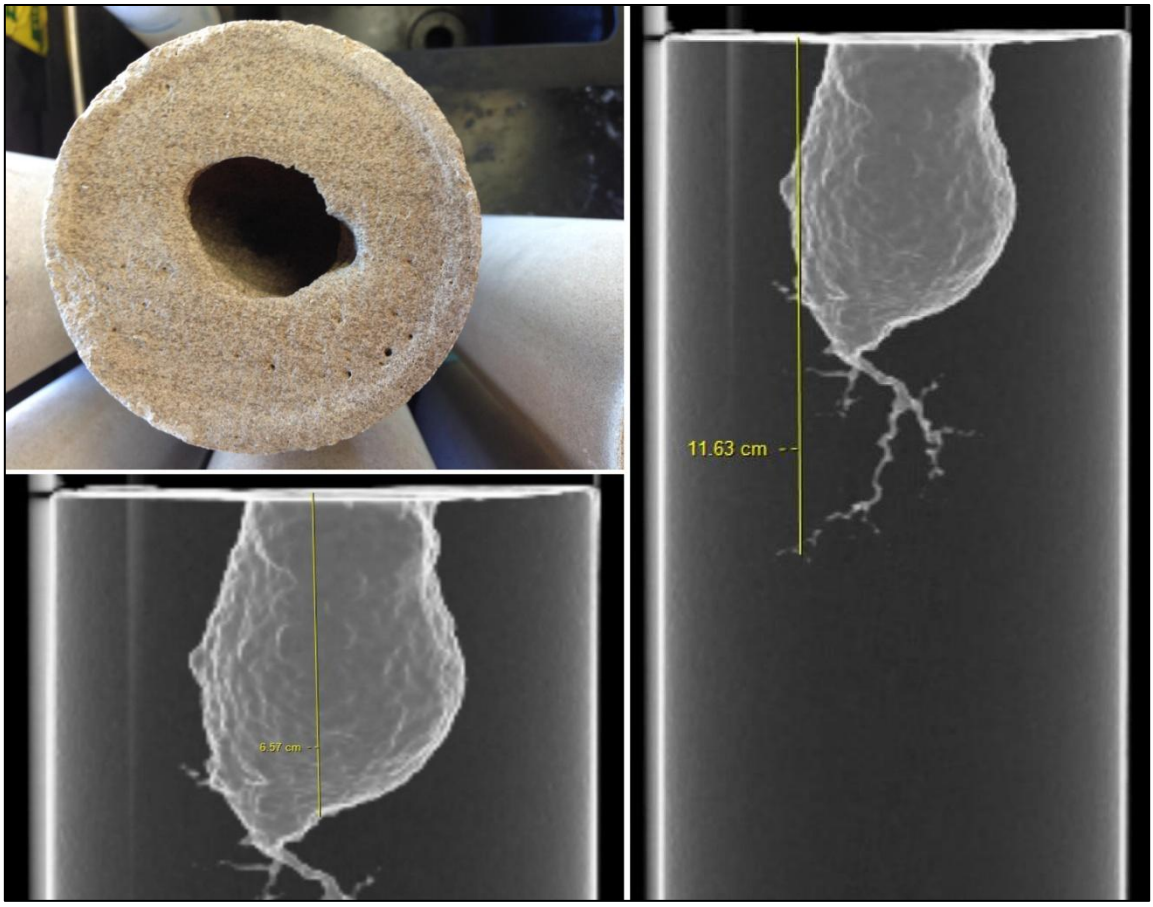

Fig. B.13 – Core 13

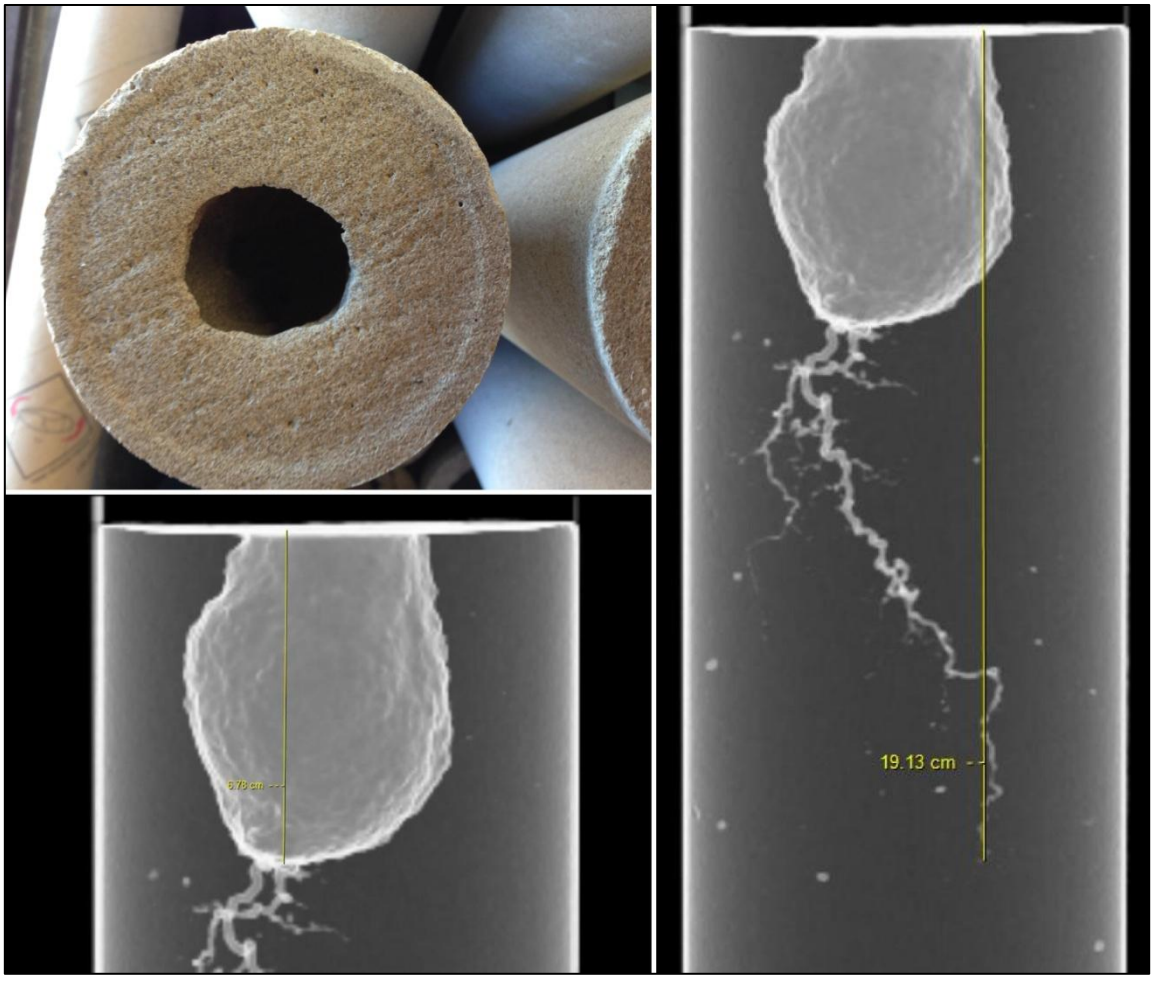

Fig. B.14 – Core 14

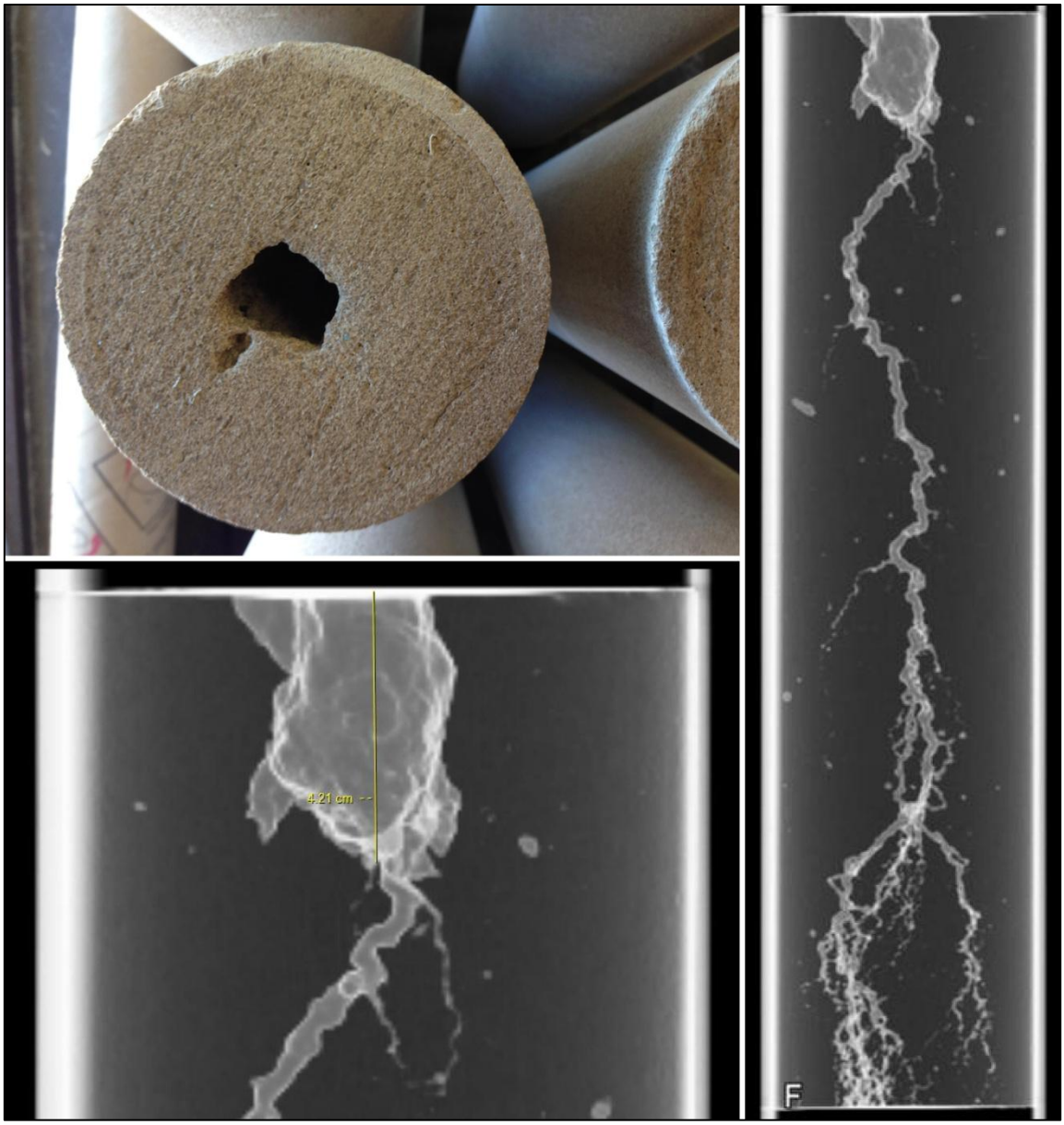

Fig. B.15 – Core 15

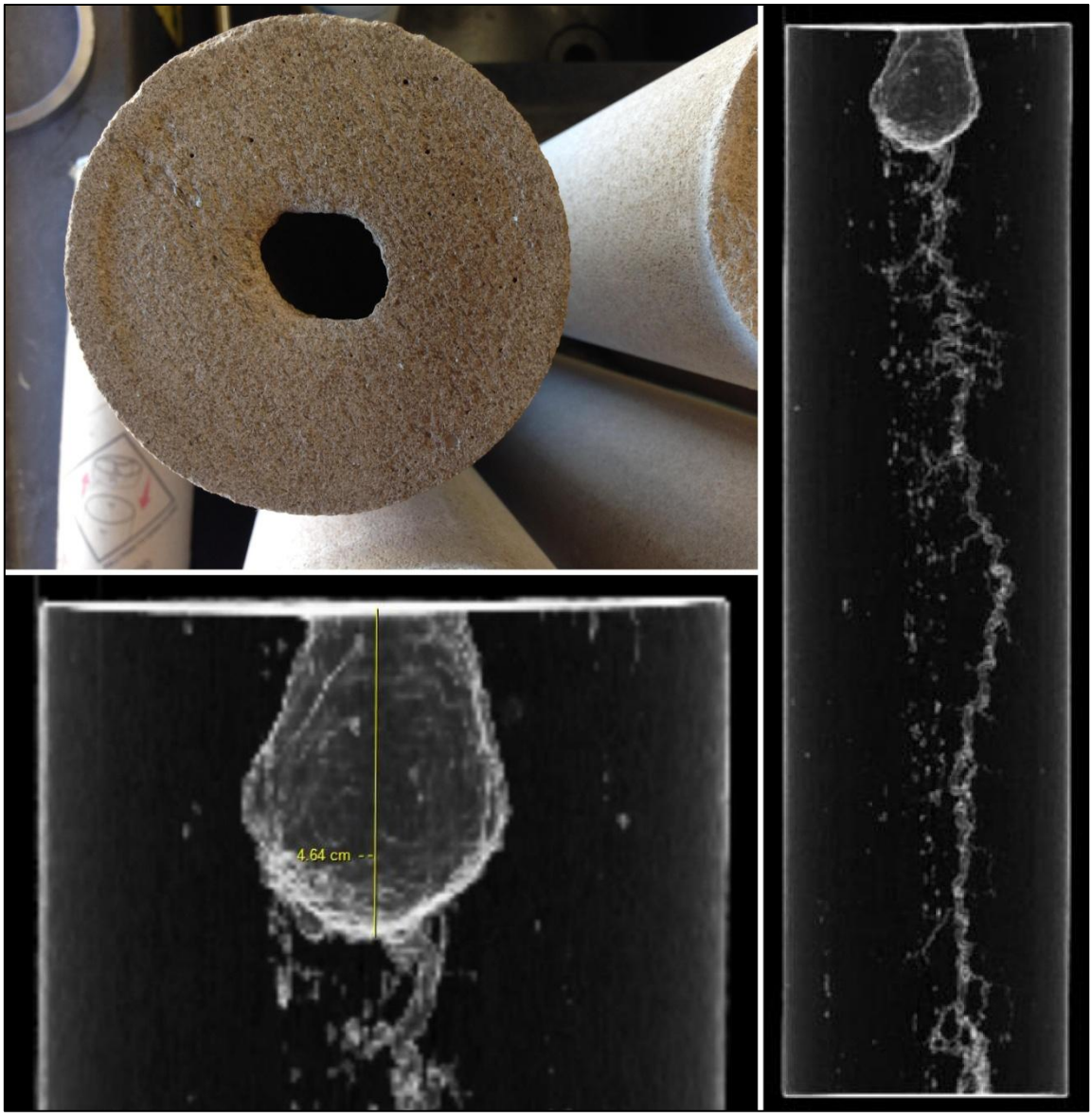

Fig. B.16 – Core 17